KfK 5230
September 1993

User and Reference Manual for the KfK Code INS

E. Daum
Institut für Materialforschung
Association KfK-Euratom

Kernforschungszentrum Karlsruhe

KERNFORSCHUNGSZENTRUM KARLSRUHE
Institut für Materialforschung
Association KfK-Euratom

KfK 5230

User and Reference Manual for the KfK Code INS

E. Daum

Diese Arbeit wurde im Rahmen der Zusammenarbeit auf dem Gebiet der Kernfusion zwischen dem Kernforschungszentrum Karlsruhe und Euratom durchgeführt.

Kernforschungszentrum Karlsruhe GmbH, Karlsruhe

Kernforschungszentrum Karlsruhe GmbH
Postfach 3640, 76021 Karlsruhe

ISSN 0303-4003

This work is dedicated to

Dr. S. Cierjacks,

the inventor of the t – H_2O neutron source concept,
who passed away on October 28, 1992. He was a vigorous
advocate of the t – H_2O concept and the center of
all activities in this field at KfK.

User and Reference Manual for the KfK Code INS

Abstract

The INS code (Intense Neutron Source) serves to calculate uncollided neutron flux contours, neutron flux volumes and spatial-dependent neutron flux spectra in the test cell of an intense neutron source, of the t-H_2O or d-Li concept. With the information of the neutron flux spectra the neutron irradiation damage like displacements per atom (DPA), H- and He-production rates and the generation of foreign elements by transmutations can be calculated for any element at any position in the test cell. This manual gives an introduction into the theory of neutron flux calculation of thick targets and neutron irradiation damage calculations. It is explained how the code is working and the handling of the input and output parameters. For each application of the several code modules an example is given. The results like contours, spectra, flux volumes and damage rates are summarized in tabular form and graphically. A big number of neutron flux spectra for the single beam (1-S) and double beam (2-S) case for the t – H_2O and d-Li case have been calculated. The most important ones, placed in the Z = 0 - plane, are plotted. Also equi-flux-contours of the (1-S) and (2-S) case for both source concepts have been calculated and plotted. In general, it has been found, that the t – H_2O spectra simulate much better the DEMO 1st wall spectrum than the d-Li spectra. This is evident when regarding the fraction of neutrons with an energy > 14 MeV, which is ($r \sim 2$ %) for the t – H_2O and ($r \sim 25$ %) for the d-Li concept. Furthermore it can be shown, that the (2-S) source provides bigger volumes for a flux limit, but no higher neutron fluxes, than the (1-S) source. The volumes and the spectral fluxes differ, comparing the t – H_2O and d-Li concept, only by a factor of 2. There are also given some quantitative expressions, calculating the approximate volumes in dependence of neutron flux (ϕ) or beam current (I), like $V \sim \phi^{const.}$ or $V \sim I^{const.}$. Damage and element transmutation data have been calculated for 23 isotopes and compared with the DEMO 1st wall values. These data are compared with results of other neutron sources and recent values of Doran and Greenwood.

Benutzer- und Referenzhandbuch zum KfK Programm INS

Kurzfassung

Das Programm INS (Intensive Neutron Quelle) dient der Berechnung von ungestörten Neutronenflußkonturen, Neutronenflußvolumen und Neutronenflußspektren, wie sie in der Testzelle einer intensiven Neutronquelle auftreten, die nach dem t-H_2O oder dem d-Li Prinzip arbeitet. Mit der spektralen Information kann die Strahlenschädigung durch Neutronen wie Verlagerungsschädigung (DPA), H- und He-Produktion und Fremdelementtransmutation für ein beliebiges Element an jeder beliebigen Stelle innerhalb der Testzelle berechnet werden. Dieses Handbuch gibt eine knappe Einführung in die Theorie der Neutronenflußberechnung an dicken Targets und in die Neutronenschädigungsrechnung. Hauptsächlich sind die Arbeitsweise des Programms und die Ein- und Ausgabeparameter beschrieben. Zur Anwendung der einzelnen Programmodule ist jeweils ein Beispiel angegeben. Die Ergebnisse, wie Konturen, Spektren, Flußvolumen und Neutronschädigungsraten, sind in tabellarischer Form und graphisch zusammengefaßt. Eine große Anzahl von Neutronflußspektren für den (1-S) und (2-S) Fall bei der t – H_2O und d-Li Quelle wurden berechnet. Die wichtigsten, in der Z = 0 - Ebene liegenden, Spektren sind abgebildet. Es wurden auch Äquiflußkonturen für den (1-S) und (2-S) Fall für beide Quellen Typen berechnet und abgebildet. Generell wird festgestellt, daß die t – H_2O Spektren wesentlich besser für die Simulation des DEMO-Erste-Wand-Spektrums geeignet sind als die d-Li Spektren. Dies wird durch den Anteil der Neutronen mit einer Energie > 14 MeV, der bei t – H_2O (r ~ 2 %) und bei d-Li bei (r ~ 25 %) liegt, verdeutlicht. Desweiteren gilt, daß die (2-S) Quelle nur größere Volumina für gegebene Flußlimits, nicht aber höhere Neutronflüße, als die (1-S) Quelle erzeugt. Volumen und spektrale Flüsse differieren zwischen t – H_2O und d-Li Quelle nur um einen Faktor 2. Es werden auch Formeln zur näherungsweisen Berechnung der Volumina in Abhängigkeit von Neutronfluß (ϕ) und Strahlstrom (I) der Form $V \sim \phi^{const.}$ bzw. $V \sim I^{const.}$ angegeben. Schädigungs- bzw. Elementtransmutationsdaten wurden für 23 Isotope berechnet und mit DEMO-Erste-Wand-Werten und anderen Neutronquellen bzw. früheren Werten von Doran und Greenwood verglichen.

Contents

1 Introduction 5

2 Theory 6

2.1 Neutron production reactions for the t-H_2O-source concept 6

2.2 Neutron production reactions for the d-Li-source concept 6

2.3 Method of flux- and spectra calculations 6

2.4 Method of neutron irradiation damage calculations 7

2.4.1 Neutron displacement damage 7

2.4.2 Element transmutation caused by neutron irradiation 8

2.4.3 Preparing neutron irradiation data 8

3 Structure of the code 9

3.1 General structure 9

3.2 Module CONVERT 12

3.3 Module SPECTRA 14

3.4 Module CONTOURS 18

3.5 Module DAMAGE 19

4 Data libraries 21

4.1 Reaction cross sections 21

4.1.1 Original H(t,n) data from M. Drosg 21

4.1.2 Original O(t,xn) data from M. Drosg 22

4.1.3 Original Li(d,xn) data from F.M. Mann 22

4.1.4 Double differential cross section, KfK data format 23

4.2 Displacement cross sections 23

4.3 Transmutation cross sections 24

5 Example runs 25

5.1 Data handling 25

5.1.1 H(t,n) Data 25

5.1.2 O(t,xn) Data 26

5.1.3 Li(d,xn) Data (Conversion) 26

5.1.4 Li(d,xn) Data (Interpolation) 26
5.2 Getting spectra 27
5.3 Getting volumes and contours 28
5.4 Getting damage parameters 30

6 Results **31**
6.1 Spectra data and plots 31
6.2 Contour data and plots 37
6.3 Minimum flux volumes 38
6.4 Neutron irradiation damage 42

7 Conclusion **60**

8 Recommendation **61**

9 Acknowledgement **61**

A Appendix **62**
A.1 Comparative plots of neutron flux spectra (1-S) 62
A.2 Comparative minimum flux contours (1-S) 68
A.3 Comparative plots of neutron flux spectra (2-S) 73
A.4 Comparative minimum flux contours (2-S) 91

References **102**

1 Introduction

Basis for the simulation calculations with INS are the two designs of a neutron source, the t-H_2O [1, 2, 3, 4] and the d-Li source [5, 6]. The designs are similar and therefore the results are easy to compare. The INS code calculates with the characteristic quantities of these neutron sources like beam current (I), kinetic energy of the tritons or deuterons, geometry of the target and test cell, the spectral neutron flux distribution in the test cell. Evaluations of the calculated neutron fluxes give information about the spectral energy distribution of the neutrons and about the integral neutron flux at any spatial point (contour plots for planes parallel to x-y-plane) and the flux volume (in cm^3) for a given minimum neutron flux limit. With the knowledge of the neutron flux spectrum, the irradiation damage displacement per atom (dpa) and element transmutation in atomic parts per million (appm) can be calculated, using suitable damage and transmutation cross sections [7]. The INS code uses external data libraries of the nuclear reaction cross sections for the H(t,n), O(t,xn) and Li(d,xn) reaction channels, which are given as neutron yields (H,O) and double differential cross sections (Li). Additional, data libraries for irradiation damage are used. The data libraries are provided by M. Drosg (H,O) [8, 9], F.M. Mann (Li) [10, 6] and L.R. Greenwood (Damage) [7]. At KfK, the INS code is installed on an IBM 3090-6 mainframe under TSO. The source code was written in FORTRAN (IBM-VS-FORTRAN-COMPILER). In the module SPECTRA, some graphical subroutines from the CERN-Program-Library HBOOK [11], HPLOT [12], HIGZ [13] and GKS [14] have been used. For execution of the code, a dataset (JCL) is submitted, which includes all system related parameters. The input parameters are read in from the FORTRAN code by the NAMELIST statement. The required input- or output-datasets are partially preallocated in the JCL. During the runtime, these datasets are recalled directly by the preallocated unit-number. The other datasets are allocated temporarily during runtime by the FORTRAN-OPEN-statement. The output of the results is stored in any case in a datafile. The contour-plots and spectra, given in the appendix, were made on a VERSATEC-plotter. To get the contour plots, the contour data have been processed with the interactive graphics editor GDDM [15] and the graphic format was changed to the GKS-format. Since every code installation is very specific, this handbook describes only the FORTRAN-source code and the used input- and output data and parameters. The JCL is described only basically and the preallocation of datasets is treated in more detail.

2 Theory

2.1 Neutron production reactions for the t-H_2O-source concept

Bombarding a 5 mm thick water-jet target with 21 MeV tritons (range in H_2O 1.96 mm [16]), several reaction channels for neutron production are open. The H(t,n) fraction is $^1H(t,n)^3He$ and the O(t,xn) fraction is

$^{16}O(t,n)^{18}F$,$^{16}O(t,n+^4He)^{14}N$,$^{16}O(t,n+p)^{17}O$,$^{16}O(t,n+d)^{16}O$,

$^{16}O(t,2n)^{17}F$,$^{16}O(t,2n+p)^{16}O$,$^{16}O(t,n+^3He)^{15}N$,$^{16}O(t,n+t)^{15}O$.

The H and O nuclei are available in the ratio 2:1, respectively, which has also been taken into account. The dependence from energy of the H(t,n) neutron yields is discussed in [3, 8]. This neutron production reaction emits neutrons only in a forward cone with an opening angle of 134 ° (kinematic collimation). The sharp cutoff at 14 MeV is also remarkable. The dependence of the O(t,xn) neutron yields from energy has been meassured by M.Drosg [1] [9]. The emitted neutrons have kinetic energies up to 21 MeV. The relative fraction of the O(t,xn) neutron production from the total neutron production in light water is about 5 %.

2.2 Neutron production reactions for the d-Li-source concept

Bombarding a thick Li-target with 35 MeV deuterons, the neutron production process is described by the reaction channels $^6Li(d,xn)$ and $^7Li(d,xn)$. The kinetic energy of the emitted neutrons is about 50 MeV at maximum. The used data are provided by F.M. Mann [2].

2.3 Method of flux- and spectra calculations

For the calculation of the energy dependent neutron flux ($d\phi/dE_n$), the following expression is used [3].

$$\frac{d\phi_i}{dE_n} = \frac{N}{e}\int_0^{E_i}\frac{dE_i}{\left|\frac{dE_i}{dx}\right|}\int_y\int_z\frac{If(y,z)}{r^2}\left(\frac{\partial^2\sigma}{\partial E_n\partial\Omega}\right)_i dydz$$

$$i = H(t,n), O(t,xn), Li(d,xn)$$

[1] Institute of Experimental Physics, University of Vienna

[2] Westinghouse Hanford Company, Richland

The used variables are atomic density of the target (N), electronic charge (e), energy of the incident particle (E_i), energy of the neutrons (E_n), double differential cross section ($(d^2\sigma/dE_n d\Omega)_i$), total beam current (I), normalized two-dimensional beam distribution (f(y,z)), distance between volume element in the target and volume element in the testcell (r) and the energy-dependent stopping power (dE_i/dx). This equation does not take into account the neutron scattering at target nuclei and the small loss of neutron intensity ($\leq 5\%$) in the target. A more exact treatment of the flux spectra and flux contours is described in the paragraphs 3.3 and 3.4, respectively.

2.4 Method of neutron irradiation damage calculations

The neutron irradiation damage in metals is basically devided into two parts, namely displacements of lattice atoms and transmutations of lattice atoms. These independent two effects are described briefly in the following two paragraphs.

2.4.1 Neutron displacement damage

For calculations of displacement damage, two effects have to be distinguished, namely the primary and the secondary damage. Both effects are treated in the SPECTER computer code [7], which uses neutron displacement damage-energy cross sections computed by the DISCS computer code [17]. The SPECTER code only needs the neutron energy spectrum to compute spectral-averaged displacements. The method of calculating the displacement rate (R) is

$$R = \int \sigma_D(E)\Phi(E)dE$$

where (E) is the energy of the incident neutron, (σ_D) is the displacement cross section and (Φ) is the neutron flux spectrum. The displacement cross section are calculated by DISCS with the expression

$$\sigma_D(E) = \sum_i \sigma_i(E) \int K(E,T)_i \nu(T)dT$$

where (σ_i) is the nuclear cross section, (i) indicates the different reaction channels, (T) is the energy of the primary recoil atom (PKA), ($K(E,T)_i$) gives the probability that a neutron with energy E makes a primary recoil atom with energy (T) and (ν) is the secondary displacement function, used in the Lindhard theory, which describes the production

of secondary recoil atoms as the primary recoil atom stops in the material. One point, which should be mentioned, is, that in DISCS it is assumed, that the angular distribution of the treated processes is isotropic. For higher neutron energies, this is an approximation, because small-angle-scattering is predominant [18]. Consequently, with increasing energies the displacement cross section values are overestimated. A further point is, that DISCS provides the displacement cross sections only for neutron energies from thermal energy up to 20 MeV. Above 20 MeV, the displacement cross sections are linearly extrapolated. This is a crude extrapolation, because the inelastic nuclear processes, which can give an important contribution, are not well known. This is especially a problem for displacement calculations of the d-Li source, because there are energies up to 50 MeV possible.

2.4.2 Element transmutation caused by neutron irradiation

Another important point of material damage is the element transmutaion induced by neutrons, which cause material activation. In this report, not the activation is the main point, but the production of hydrogen-gas and helium-gas, which is produced by the same process. The element transmutation cross sections are treated in the REAC computer coce [19]. The cross sections of H- and He-gas production for several materials are collected in the gas-production file [20]. This file was used at the SPECTER code to calculate the production rate G_i for H- and He-gas by

$$G_i = \int \sigma_{GAS_i}(E)\Phi(E)dE$$

$$i = H, He$$

where (E) is the neutron energy, (Φ) is the neutron flux spectrum and (σ_{GAS_i}) is the gas production cross section. The points, discussed for displacement cross sections, be also valid for gas production cross sections.

2.4.3 Preparing neutron irradiation data

Performing irradiation damage parameter it is convenient to use

$$\text{damage parameter} \sim \overline{\sigma}_{\text{SPAV}} * \phi_{\text{tot}}$$

where ($\overline{\sigma}_{SPAV}$) is the spectral averaged cross section and (ϕ_{tot}) is the integrated neutron flux. Therefore it is necessary to provide spectral averaged cross sections. The neutron flux

spectra, calculated by the INS-code, result in a relatively rough energy group structure, namely 50 energy groups which are 1 MeV wide and equidistant. The damage energy cross sections and the hydrogen and helium production cross sections are given with a very fine non-equidistant energy group structure, especially in the 0 - 1 MeV energy interval, where about 70 groups are present. Usually the first step is, to change the energy group structure from fine structure to rough structure, which is done by

$$\overline{\sigma(E_j)} = \frac{\sum_i \frac{1}{E_i}\Delta E_i \sigma(E_i)}{\sum_i \frac{1}{E_i}\Delta E_i} \qquad \text{for 0 - 1 MeV}$$

and

$$\overline{\sigma(E_j)} = \frac{\sum_i \Delta E_i \sigma(E_i)}{\sum_i \Delta E_i} \qquad \text{for 1 - 50 MeV}$$

That means, that in the 0 - 1 MeV energy group simply the common 1/E thermal weighting function is used. It should be mentioned, however, that this weighting function can only be an approximation to the real spectral behaviour. With the rough cross section data the spectral averaging of the cross sections is done by

$$\overline{\sigma}_{SPAV} = \frac{\sum_i \sigma_i \phi_i}{\sum_i \phi_i} = \frac{\sum \sigma_i \phi_i}{\phi_{tot}}$$

over the complete spectrum.

3 Structure of the code

3.1 General structure

The INS-code consists of 4 code modules, namely CONVERT, CONTOUR, SPECTRA and DAMAGE. The flowchart figures 1 and 2 give an overview about the dataflow in the INS-code. The rhombic boxes are input- or output data, the rectangular boxes symbolize the code modules. The dataflow goes strictly from top to bottom and from left hand side to right hand side.

Figure 1: Data flow chart of INS-Code for the t – H_2O - source

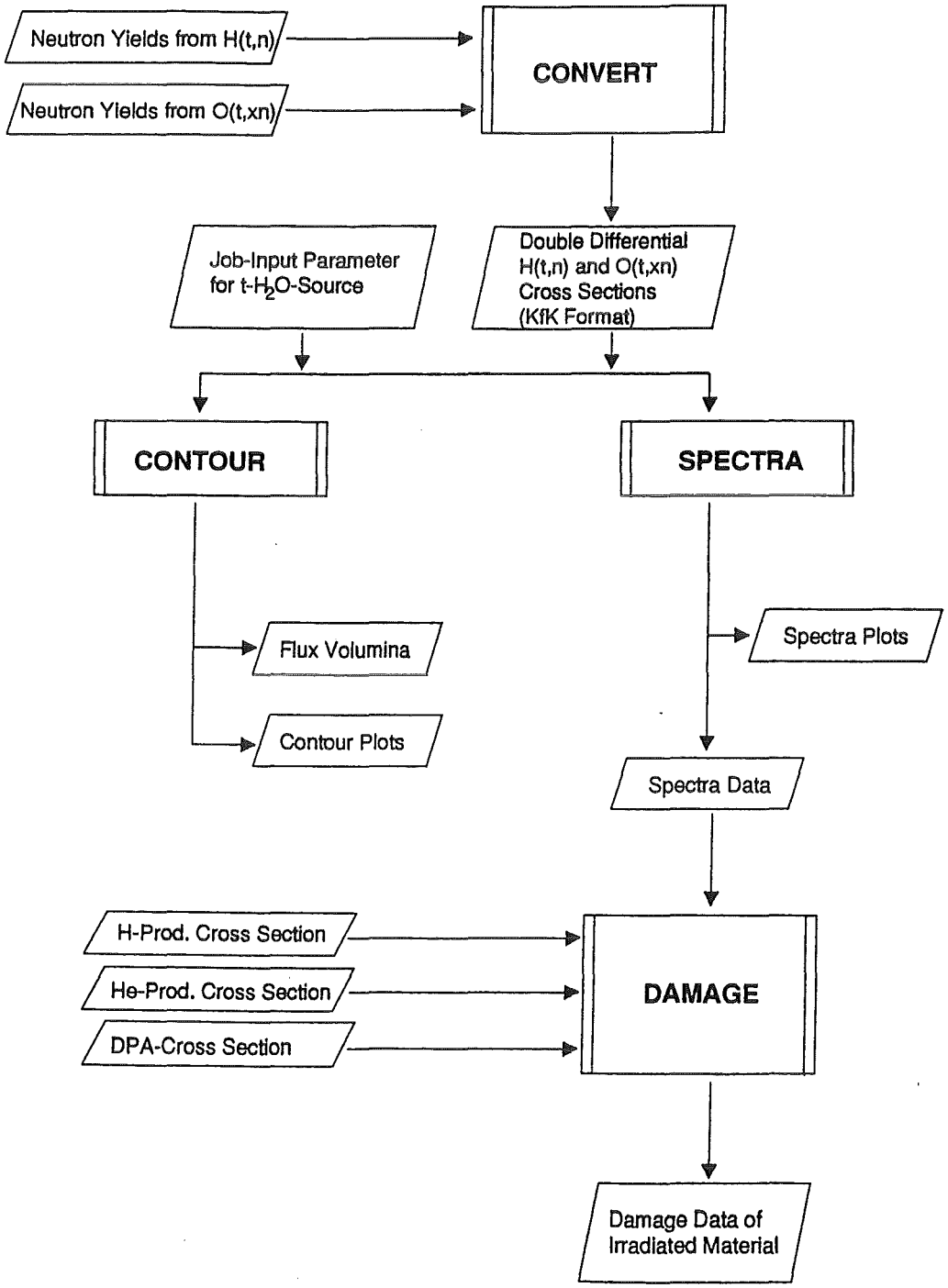

Figure 2: Data flow chart of INS-Code for the d-Li - source

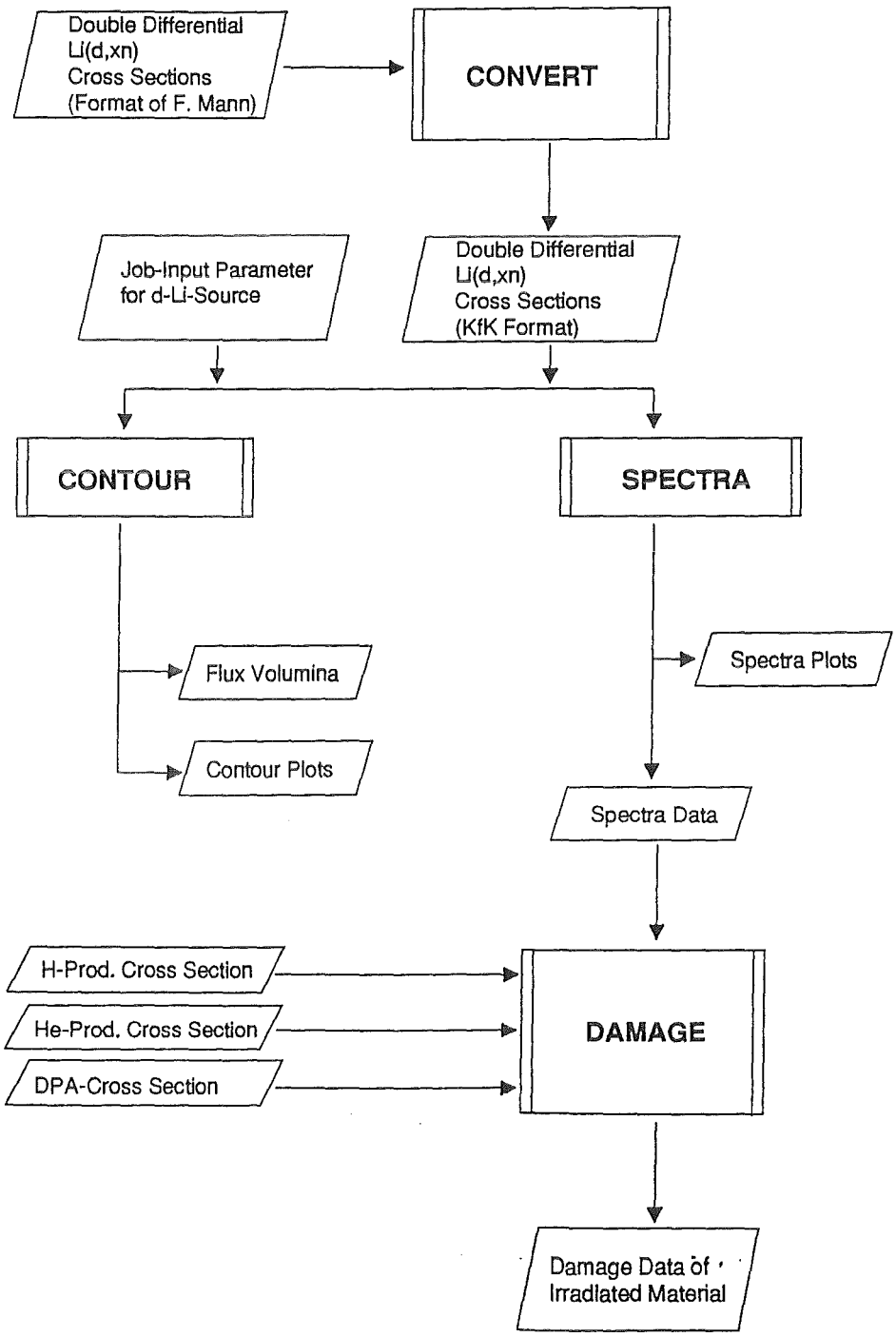

3.2 Module CONVERT

In the module CONVERT, the double differential nuclear cross sections for the reactions H(t,n), O(t,xn) and Li(d,xn) are provided.

The basic data for the t-H_2O-source are provided from M. Drosg [9, 21, 22]. For the H(t,n) reaction channel, the data exist already as double differential cross sections. The data are linearly interpolated in angular range from 1 °steps into 0.5 °steps and transformed into the KfK data format. The energy range from 3.0 to 21 MeV triton energy is divided into 60 equidistant energy intervals with 0.3 MeV width. The lower limit of 3.0 MeV is caused by the threshold energy of the H(t,n) reaction.

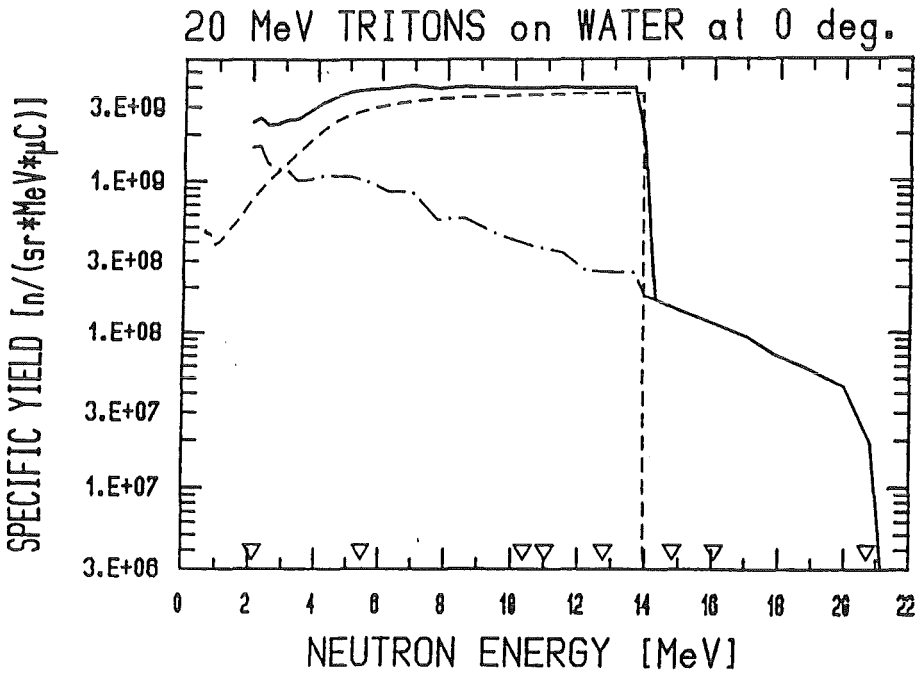

Figure 3: Neutron yield at 0 °for 20 MeV tritons stopped in light water. The yields from the processes H(t,n), O(t,xn) and the sum of both are plottet dashed, dashed dotted and solid, respectively.

For every energy interval, information about maximum emission angle of the neutrons, differential range of tritons in water in the energy interval, double differential cross sections and the kinetic energy of the emitted neutrons is stored. A more detailed description of the KfK data format and of the used data files is given in chapter 4.

For the O(t,xn) reaction channel, the data exist as differential thick target neutron yields at the angles 0 °, 15 °, 30 °, 45 °and 60 °[9, 21, 22]. Figure 3 shows the neutron yields for 0 °[9]. The data are linearly interpolated from the 15 °angle steps into 5 °steps, converted from differential neutron yields to double differential pseudo cross sections and transformed into KfK data format. Pseudo cross section means, that the cross sections are calcultaed as averaged cross sections over a thick water target.

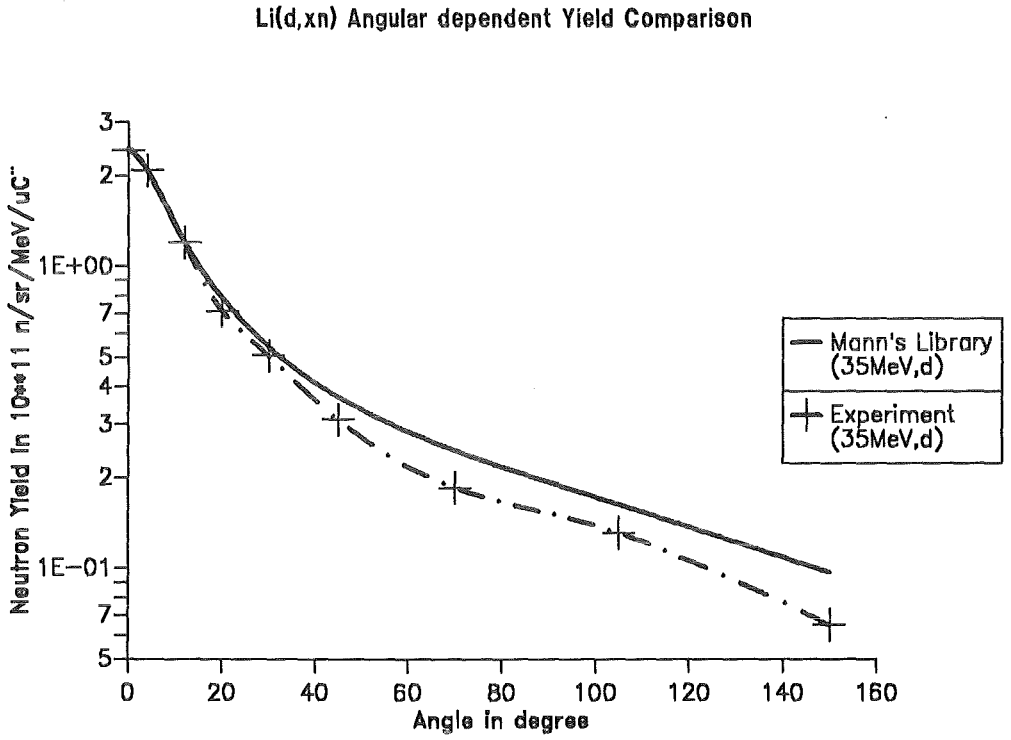

Figure 4: Neutron yield as a function for experimental and evaluated Li(d,xn) data.

The conversion factor (f) from yield (n/sr-MeV-μC) to pseudo cross section (mbarn/sr-MeV) is given by

$$f = \frac{\frac{tritons}{\mu C}}{\frac{target\ nucleus}{cm^2} * \frac{10^{-27} cm^2}{mbarn}}$$

$$f = \frac{\frac{e}{\mu C}}{\frac{N_A * R_{max}}{m_{Mol}(H_2O)} * \frac{10^{-27} cm^2}{mbarn}} = 2.438 * 10^{-8} \mu C * mbarn$$

The range (R_{max}) of 21 MeV tritons in water is 0.196 cm [16]. The data for the d-Li source are provided from F.M. Mann [10]. The data exist already as double differential cross sections. Therefore, the data are only interpolated from 5 °angle steps to 0.5 °angle steps and converted into KfK data format.

A comparison, see figure 4 , of the data from F.M. Mann and the experimental neutron yields [6], shows a different behaviour of the yields at angles $\geq$ 20 °. For that reason the cross section are scaled to match the experimental yields [6] . Now two datasets of double differential cross section are existing. One (ORIG) for the original data from F.M. Mann and one (REAL) for more realistic data. Both datasets are used during calculations.

3.3 Module SPECTRA

In the module SPECTRA, the neutron flux spectra are calculated. The used algorithm is valid, to calculate a flux spectrum at any spatial point in the test cell for one or two extended targets, rectangular in shape. The possible configurations are shown in figure 5 and figure 6.

For the 1-source case, the test cell is the part of the space with positive x-coordinate values. For the 2-source case, the test cell is limited by the planes, including the two symmetric to x-axe positioned targets. The 1-source case is computed as a special 2-source case, with the parameters SHIFT = 0 cm and $\vartheta = 180$ °. This means, that both targets are at same position and can be seen as only one target.

The contruction of the target is plotted in figure 7. The macroscopic target parameters are length (Tay), height (Taz) and width (d). The target is divided into a sufficient number of subelements. The subelement matrix at one layer in the target contains normally 48 elements (1-source) and 300 elements (2-source) with an area of $0.25^2 cm^2$. For each subelement (k), its contribution to the neutron flux at a choosen spatial point in the test cell is given by the expression

$$\left(\frac{d\phi}{dE_n}\right)_k = \frac{\xi}{N_t N_s} * \frac{\rho(element) N_A}{M_{mol}(element)} * \frac{10^{-27}\frac{cm^2}{mbarn}}{e} * \frac{I}{1000} * \left|\frac{dx}{dE}\right| dE * \frac{A}{\vec{r}^2} * \frac{\partial^2\sigma}{\partial E \partial\Omega}$$

where (ξ) is the stoichiometric factor for atomic abundance in chemical compounds ($\xi = 1$ for O and Li, $\xi = 2$ for H), (N_t) is the number of subelements in one target layer, (N_s) is number of sources, (ρ) is the density of target material, (M_{mol}) is the molar mass, (N_A) the Avogadro number, (I) the electric beam current in mA, (dx/dE) the differential range,

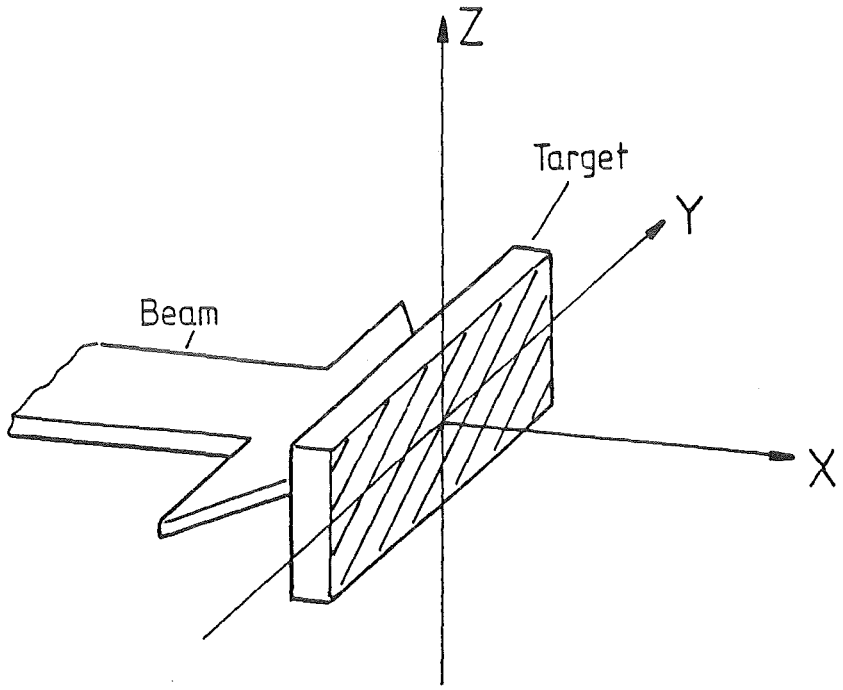

Figure 5: Single target (1-S) configuration.

Figure 6: Double target (2-S) configuration.

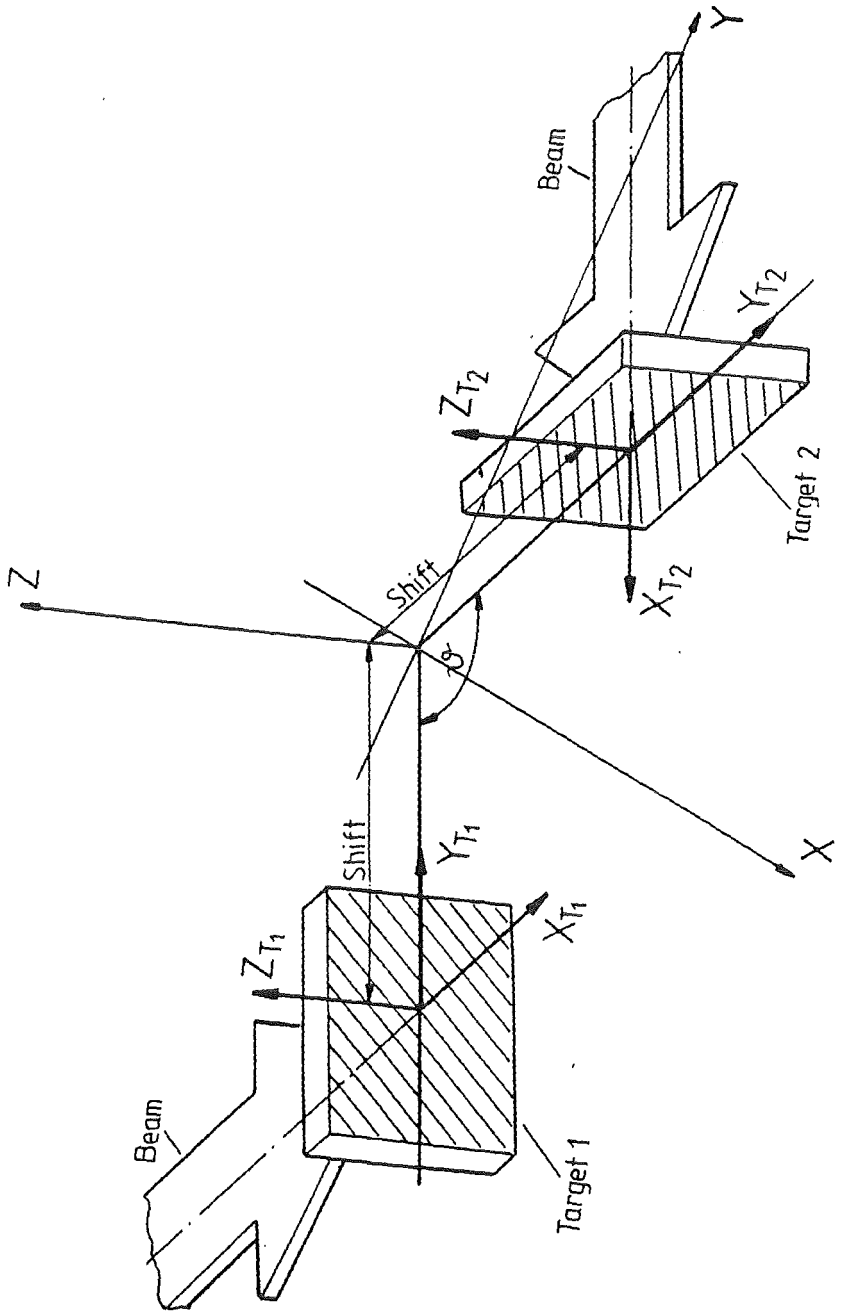

Figure 7: Target construction drawing as the target is used in the INS-code. The spatial points in the test cell and their coordinates are symbolized.

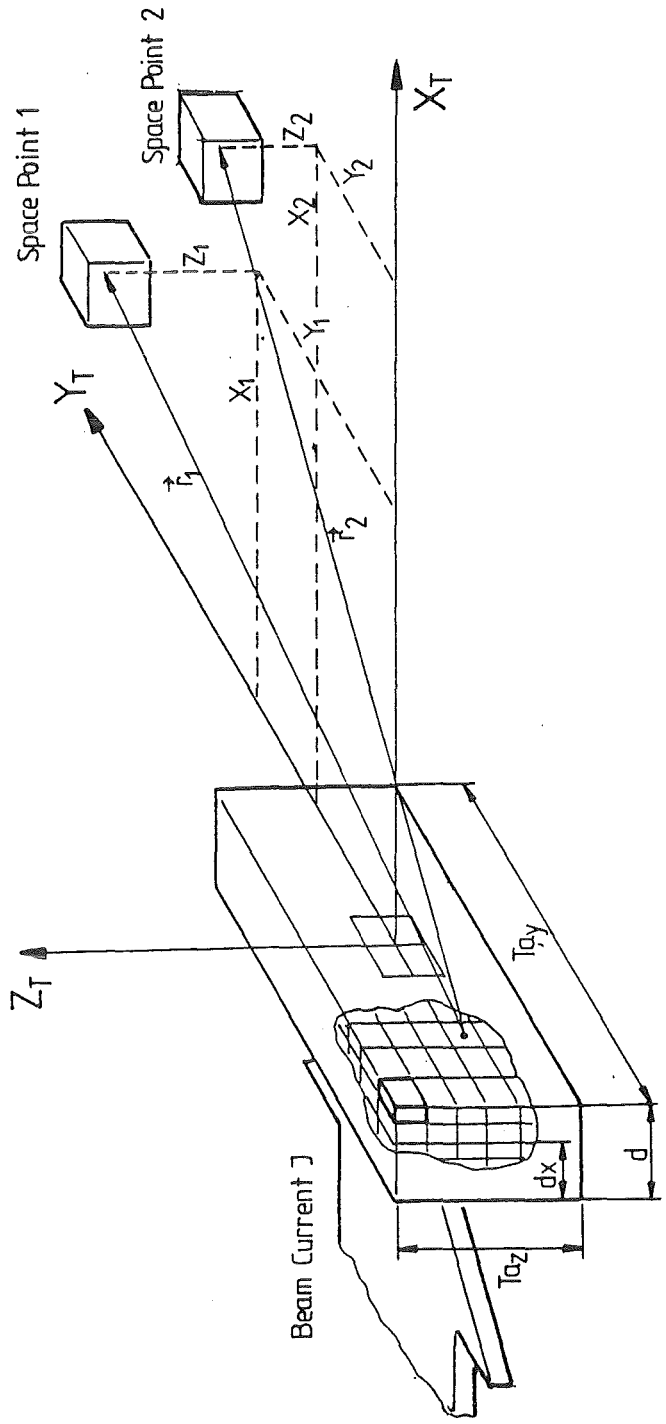

(dE) the energy loss in one layer in the target, (A = 1cm^2) the area element, ($\vec{r}$) the vector pointing from a target subelement to the spatial point in test cell and $\frac{\partial^2\sigma}{\partial E \partial\Omega}$ the double differential cross section.

In this step, the neutron flux is calculated in an empty test cell. For further calculations, like damage calculations, two options are available. First, to use the spectrum calculated at a spatial point in the empty test cell, or second, to use a spectrum which is calculated by a neutron transport code for a not empty test cell, e.g. filled with Fe, which is a topic for further investigations.

3.4 Module CONTOURS

In the module CONTOURS the volume for an integral neutron flux, higher than a given minimum limit, is calculated. The used algorithm is split into two parts, because of CPU-time problems. Using the same procedure analogous to spectrum calculation, the problem of volume calculation would be unsolvable. The first part calculates the integral neutron flux distribution in one quadrant of the x-y-plane for one line source. Line source means, that the source is only spread in beam direction, otherwise its a point source. Figure 8 shows a schematic drawing of this idea.

The meshwidth of the plane is about 0.25^{2}cm^2. That means, for each subelement in the x-y-plane the average flux contribution of each target piece of the line source as a point source is calculated and stored in a file as intermediate results. The used mathematical expression is

$$\phi_k = \sum_{E_n} \left(\frac{d\phi}{dE_n}\right)_k$$

for integral flux, while

$$\left(\frac{d\phi}{dE_n}\right)_k = \frac{\rho(element)N_A}{M_{mol}(element)} * \frac{10^{-27}\frac{cm^2}{mbarn}}{e} * \frac{I}{1000} * \left|\frac{dx}{dE}\right| dE * \frac{A}{\vec{r}^2} * \overline{\left(\frac{\partial^2\sigma}{\partial E \partial\Omega}\right)}$$

is the differential flux, averaged about one subelement k, and

$$\overline{\left(\frac{\partial^2\sigma}{\partial E \partial\Omega}\right)} = \frac{1}{n}\sum_{i=1}^{n} \frac{\partial^2\sigma}{\partial E \partial\Omega}$$

is the averaged cross section in an angle interval for one subelement k. The second part provides the volume for a minimum flux and a graphical plot of the contour lines, at planes parallel to the x-y-plane, for a given minimum flux and various z-coordinates. The

Figure 8: Schematic drawing of the x-y-plane with the dimensions in x- and y- direction and the variables to point out a plane subelement.

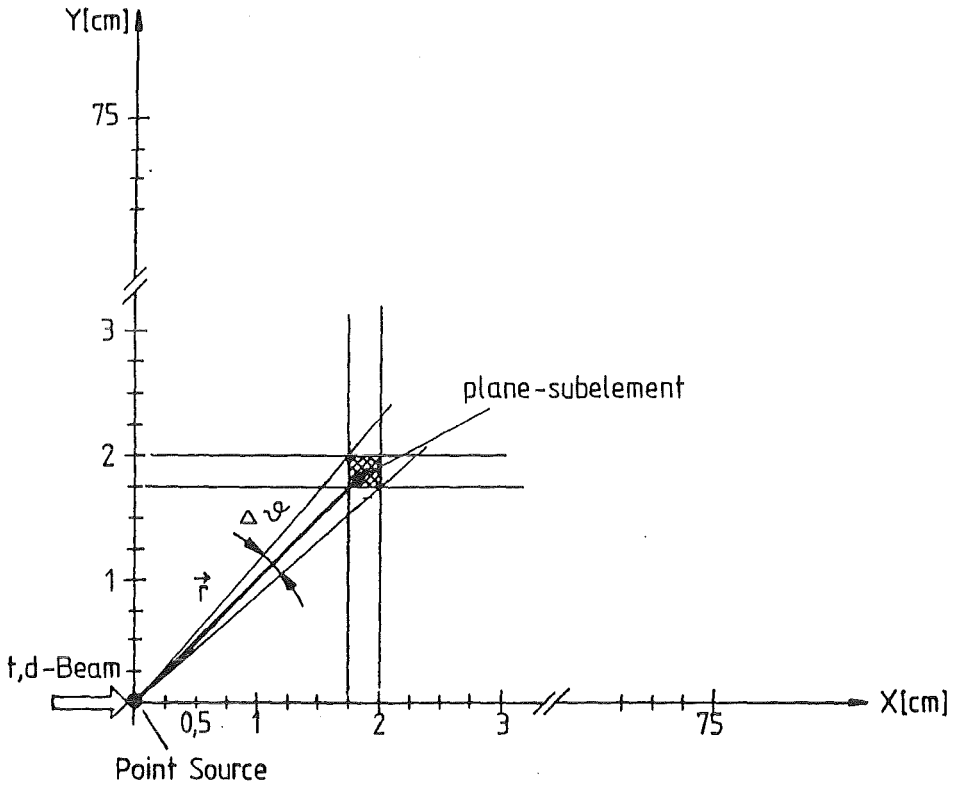

handling of the two targets, rectangular in shape, with various target areas and at various positions (SHIFT, ANGLE) is possible. In a first step, the integral flux contribution for each subelement in the x-y-plane for one spread source is calculated. This is easy to do by looking into the point source data. The second step is to calculate the transformation from target coordinates to world coordinate. For the one source case, both coordinate systems are the same, for the two source case, a tranformation matrix is used to move and rotate the sources. The third step is to extract the coordinate points for the contour lines and store the results in some files.

3.5 Module DAMAGE

In the module DAMAGE the irradiation damage parameters like H-, He- production rate and DPA for several medium weighted elements can be calculated. This is done in a first

step only for the simulation of an empty test-cell. That means, the neutron flux spectrum, calculated at any spatial point in the test-cell, is used to estimate the damage parameters at this spatial point, if there would be a differential small volume element of the material of interest. This is of course only an approximation to the real case, if the test cell is fullfilled with the material (e.g. a single element or a composite material or an alloy), because in the material, the neutron flux will be moderated and therefore the flux distribution becomes more and more thermalized. Such calculations need a treatment of the original source neutron flux by a neutron transport code (e.g. MCNP), which is a point for further investigations. In the present case, the three different program units HAPPM, HEAPPM and DPA are used to calculate H-, He-production rates (APPM/sec) and the displacement rate (DPA/sec), respectively. The mathematical expression to get the gas production rate in APPM/sec is

$$\frac{APPM_{H,He}}{sec} = \sum_i \sigma_i^{H,He} \phi_i 10^{-24} \frac{cm^2}{barn} 10^6$$

which can also expressed by

$$\frac{APPM_{H,He}}{sec} = \overline{\sigma}_{SPAV}^{H,He} \phi_{tot} 10^{-24} \frac{cm^2}{barn} 10^6$$

where $\sigma_i^{H,He}$ is the gas production cross section, $\sigma_{SPAV}^{H,He}$ is the spectral averaged gas production cross section, ϕ_i is the neutron flux, ϕ_{tot} is the integrated total neutron flux, 10^{-24}cm^2/barn is the conversion factor from cm^2 to barn and 10^6 gives the result in atomic parts per million (appm).

The mathematical expression to get the damage rate in DPA/sec is

$$\frac{DPA}{sec} = \sum_i \sigma_i^{DPA} \phi_i 10^{-24} \frac{cm^2}{barn} \frac{400}{ED}$$

which can also be expressed by

$$\frac{DPA}{sec} = \overline{\sigma}_{SPAV}^{DPA} \phi_{tot} 10^{-24} \frac{cm^2}{barn} \frac{400}{ED}$$

where σ_i^{DPA} is the damage cross section, σ_{SPAV}^{DPA} is the spectral averaged damage cross section, ϕ_i is the neutron flux, ϕ_{tot} is the integrated total neutron flux, 10^{-24}cm^2/barn is the conversion factor from cm^2 to barn and 400/ED converts keV-barn to barn where ED is the Lindhard cutoff energy which is the minimum energy to displace one atom from its lattice site.

But before the damage rate can be calculated, all spectra used in the calculations must have the same energy group structure. The changing of the energy group structure from fine non-equidistant to rough 1 MeV equidistant is done by two routines, EQBINDPA for displacement cross sections and EQBINGAS for gas production cross sections.

4 Data libraries

4.1 Reaction cross sections

In this section, the format of the used original datafiles and the KfK data format is described.

4.1.1 Original H(t,n) data from M. Drosg

The interesting information is the triton energy, e.g. 21 MeV, and the parameter in the laboratory system. In the energy range 3.0 - 21 MeV, for each 0.3 MeV triton energy interval, the following data block is used.

```
1NEUTRONS FROM THE REACTION 1H(t,n)3He with        water target

 INCIDENT LAB ENERGY   20.9997   INT. CROSS SECT.=   2.656E+02 MBARNS
 INTEGRAL YIELD with a 10 KeV SPREAD at 0 Deg=   2.395E+01 n/pC
 TOTAL ENERGY=  3752.4779 MOM OF PROJ=    86.0434

      LABORATORY SYSTEM          CENTER-OF-MASS 1.327E+01 KEV TARGET THICKNESS
 ANGLE     CROSS     ENERGY     ANGLE     CROSS     NEUTRONS/(sr*pC) for a 10
           SECTION                        SECTION   KeV NEUTRON ENERGY SPREAD
 DEGREE     MB/SR       MEV    DEGREE     MB/SR    at 0 D DUE TO ENERGY LOSS

   0.00   400.574    14.617      0.00    91.629          3.612E+01
   1.00   399.614    14.613      2.09    91.423          3.603E+01
   2.00   396.743    14.598      4.18    90.809          3.577E+01
   3.00   392.004    14.574      6.27    89.795          3.535E+01
   4.00   385.469    14.540      8.36    88.395          3.476E+01
   5.00   377.228    14.496     10.45    86.627          3.401E+01
                                  .
                                  .
                                  .
  64.00    35.360     1.662    140.84    16.476          3.188E+00
  65.00    36.422     1.413    144.04    16.686          3.284E+00
  66.00    39.558     1.154    147.68    16.949          3.567E+00
  67.00    53.955 8.504E-01    152.45    17.331          4.865E+00
   0.00     0.129 2.292E-02    180.00    18.976          1.164E-02
   1.00     0.129 2.293E-02    179.92    18.976          1.164E-02
   2.00     0.129 2.295E-02    179.84    18.976          1.166E-02
   3.00     0.130 2.299E-02    179.75    18.976          1.169E-02
   4.00     0.130 2.304E-02    179.67    18.976          1.173E-02
                                  .
                                  .
                                  .
  64.00     4.792 2.003E-01    167.34    18.532          4.321E-01
  65.00     6.708 2.355E-01    166.14    18.451          6.048E-01
  66.00    10.703 2.885E-01    164.49    18.332          9.651E-01
  67.00    26.013 3.915E-01    161.71    18.115          2.346E+00
```

4.1.2 Original O(t,xn) data from M. Drosg

These data are given in neutron yields (n/sr-MeV-μC). There are 5 spectra for the angles 0 °, 15 °, 30 °, 45 °and 60 °. Each spectra includes 24 yield values from 0 - 23 MeV in 1 MeV steps.

```
 DATA SPEKI/2.65E+9,
&           2.35E+9,1.33E+9,9.47E+8,9.43E+8,9.16E+8,7.63E+8,
&           6.94E+8,4.56E+8,3.53E+8,2.78E+8,2.33E+8,1.96E+8,
&           1.72E+8,1.58E+8,1.39E+8,1.27E+8,9.38E+7,7.10E+7,
&           5.19E+7,3.42E+7,1.71E+7,5.40E+5,0.0,
&           2.28E+9,
&           1.97E+9,1.32E+9,9.38E+8,9.37E+8,9.01E+8,7.38E+8,
&           5.40E+8,3.93E+8,3.02E+8,2.48E+8,2.07E+8,1.74E+8,
&           1.44E+8,1.09E+8,8.12E+7,6.12E+7,4.61E+7,3.46E+7,
&           2.44E+7,1.20E+7,2.55E+6,4.40E+5,0.0,
&           2.10E+9,
&           1.67E+9,1.10E+9,8.45E+8,7.63E+8,6.45E+8,5.00E+8,
&           3.91E+8,3.03E+8,2.37E+8,1.83E+8,1.44E+8,1.11E+8,
&           8.11E+7,5.82E+7,4.22E+7,3.24E+7,2.41E+7,1.73E+7,
&           8.80E+6,2.38E+5,0.0    ,0.0    ,0.0,
&           1.70E+9,
&           1.46E+9,8.95E+8,6.36E+8,4.79E+8,3.77E+8,2.84E+8,
&           2.16E+8,1.63E+8,1.24E+8,9.60E+7,7.20E+7,5.09E+7,
&           3.48E+7,2.64E+7,2.11E+7,1.72E+7,1.43E+7,1.08E+7,
&           3.42E+6,2.10E+5,0.0    ,0.0    ,0.0,
&           1.55E+9,
&           1.15E+9,5.38E+8,3.85E+8,2.94E+8,2.27E+8,1.72E+8,
&           1.19E+8,9.72E+7,7.45E+7,5.48E+7,4.01E+7,2.96E+7,
&           2.22E+7,1.61E+7,1.20E+7,8.82E+6,6.21E+6,3.97E+6,
&           5.90E+5,1.60E+5,0.0    ,0.0    ,0.0/
```

4.1.3 Original Li(d,xn) data from F.M. Mann

The first two lines in this data file are comment lines. In the third line, the number of various deuteron energy groups (40), the number of angle groups (35), the number of energy groups of the outgoing neutrons (50) and the stepwidth in the above named groups, $\Delta E_d = 1MeV$, $\Delta\vartheta = 5° = 0.08726$ rad , $\Delta E_n = 1MeV$ is given. The three following data blocks (line 4-8, line 9-13, line 14-20), are the explicitly typed values in the several groups, respectively. The information in the angle group is given in radian. In the following data blocks, the cross section values (mbarn) for the 50 1-MeV wide neutron energy intervals are written. First, all angle groups for one deuteron energy are counted, then the next deuteron energy is choosen.

```
test case
 1.0000000 1.0000000 1.0000000 1.0000000 0.5844322
       40          35          50   1.000000e+00   8.726605e-02   1.000000e+00
 0.5000000 1.5000000 2.5000000 3.5000000 4.5000000 5.5000000 6.5000000 7.5000000
 8.5000000 9.500000010.500000011.500000012.500000013.500000014.500000015.5000000
16.500000017.500000018.500000019.500000020.500000021.500000022.500000023.5000000
24.500000025.500000026.500000027.500000028.500000029.500000030.500000031.5000000
32.500000033.500000034.500000035.500000036.500000037.500000038.500000039.5000000
 0.         0.0872661 0.1745321 0.2617982 0.3490642 0.4363303 0.5235963 0.6108624
 0.6981284 0.7853945 0.8726605 0.9599266 1.0471926 1.1344587 1.2217247 1.3089908
 1.3962568 1.4835229 1.5707889 1.6580550 1.7453210 1.8325871 1.9198531 2.0071192
 2.0943852 2.1816513 2.2689173 2.3561834 2.4434494 2.5307155 2.6179815 2.7052476
 2.7925136 2.8797797 2.9670457 3.0543117
 0.         1.0000000 2.0000000 3.0000000 4.0000000 5.0000000 6.0000000 7.0000000
 8.0000000 9.000000010.000000011.000000012.000000013.000000014.000000015.0000000
16.000000017.000000018.000000019.000000020.000000021.000000022.000000023.0000000
24.000000025.000000026.000000027.000000028.000000029.000000030.000000031.0000000
32.000000033.000000034.000000035.000000036.000000037.000000038.000000039.0000000
```

```
40.000000041.000000042.000000043.000000044.000000045.000000046.000000047.0000000
48.000000049.000000050.0000000
0.          0.          0.          3.2360e-023.3760e-023.4840e-023.7800e-021.0059e-01
1.0615e-011.1057e-012.3861e-012.3861e-012.4117e-017.5862e-010.          0.
0.          0.          0.          0.          0.          0.          0.
0.          0.          0.          0.          0.          0.          0.
0.          0.          0.          0.          0.          0.          0.
0.          0.          0.          0.          0.          0.          0.
0.          0.
0.          0.          0.          0.          0.          6.6697e-027.3683e-027.8351e-02
8.3810e-022.2620e-012.3897e-012.4053e-015.0499e-015.2170e-015.2847e-011.6376e+00
0.          0.          0.          0.          0.          0.          0.
0.          0.          0.          0.          0.          0.          0.
0.          0.          0.          0.          0.          0.          0.
0.          0.          0.          0.          0.          0.          0.
0.          0.
                                      .
                                      .
                                      .
                                      .
```

4.1.4 Double differential cross section, KfK data format

For the KfK data format, an example with the H(t,n) double differential cross section is given. The used format is easy readable. For each 0.3 MeV interval, the following data block is used.

Description :

```
Number of triton-   Kinetic energy of
energy interval     trion in MeV
  Maximum emission    Maximum number      Differential        Interval
  angle               of groups           range               width in MeV
    Number of           Angle in            Number of
    group               degree              elements
      Number of           Cross section       Kinetic energy
      element             in mbarn            of neutron in MeV
```

```
1  ET =  3.30 MEV
 15.0   31   0.4000E-02  0.3
  1     0.0    2
      1   0.27885E+03   1.0080
      2   0.82402E+02   0.3262
  2     0.5    2
      1   0.27892E+03   1.0075
      2   0.82530E+02   0.3264
  3     1.0    2
      1   0.27900E+03   1.0070
      2   0.82658E+02   0.3266
                .
                .
                .
                .
 29    14.0    2
      1   0.41009E+03   0.7510
      2   0.23229E+03   0.4377
 30    14.5    2
      1   0.47040E+03   0.7225
      2   0.29381E+03   0.4556
 31    15.0    2
      1   0.53071E+03   0.6941
      2   0.35534E+03   0.4736
                .
                .
                .
```

4.2 Displacement cross sections

The displacement damage energy cross sections are listed for more than 40 elements in [7]. The energy group structure are 100 non-equidistant groups from thermal energies to

20 MeV. An extended version of the damage energy cross sections in a non-equidistant 130 group structure ranging from thermal energies to 50 MeV is provided from [23]. The extended data are converted to the 50 group structure and used for displacement rate calculations.

The energy grid for the 50 group structure is:

```
1.0000E+00 2.0000E+00 3.0000E+00 4.0000E+00 5.0000E+00 6.0000E+00 7.0000E+00
8.0000E+00 9.0000E+00 1.0000E+01 1.1000E+01 1.2000E+01 1.3000E+01 1.4000E+01
1.5000E+01 1.6000E+01 1.7000E+01 1.8000E+01 1.9000E+01 2.0000E+01 2.1000E+01
2.2000E+01 2.3000E+01 2.4000E+01 2.5000E+01 2.6000E+01 2.7000E+01 2.8000E+01
2.9000E+01 3.0000E+01 3.1000E+01 3.2000E+01 3.3000E+01 3.4000E+01 3.5000E+01
3.6000E+01 3.7000E+01 3.8000E+01 3.9000E+01 4.0000E+01 4.1000E+01 4.2000E+01
4.3000E+01 4.4000E+01 4.5000E+01 4.6000E+01 4.7000E+01 4.8000E+01 4.9000E+01
5.0000E+01
```

The values are in MeV and describe the upper energy group limits.

The data structure is:

```
Iron       1326        ED = 40.0 eV    TGAM = 395.0 eV
4.8964E+00 7.1966E+01 1.1215E+02 1.3900E+02 1.6253E+02 1.7976E+02 1.9148E+02
2.0069E+02 2.1234E+02 2.2569E+02 2.3760E+02 2.4741E+02 2.5852E+02 2.7135E+02
2.9027E+02 2.9320E+02 2.9273E+02 2.9765E+02 3.0726E+02 3.1636E+02 3.4842E+02
3.5293E+02 3.6038E+02 3.6783E+02 3.7527E+02 3.8076E+02 3.8429E+02 3.8781E+02
3.9134E+02 3.9479E+02 3.9816E+02 4.0154E+02 4.0491E+02 4.0801E+02 4.1084E+02
4.1366E+02 4.1649E+02 4.1766E+02 4.1717E+02 4.1668E+02 4.1619E+02 4.1690E+02
4.2002E+02 4.2434E+02 4.2866E+02 4.3298E+02 4.3724E+02 4.4137E+02 4.4543E+02
4.4950E+02
Carbon     1306        ED = 31.0 eV    TGAM = 671.0 eV
6.8573e+00 5.1011e+01 5.1274e+01 6.4937e+01 4.6863e+01 3.4961e+01 3.3700e+01
                                      .
                                      .
                                      .
                                      .
                                      .
                                      .
```

The unit of the numbers is keV*barn. The number at the right hand side of the element name is the material number of the element in the ENDF/B-V nuclear data library. The ED value is the Lindhard cutoff energy required to displace one atom and TGAM is the effective damage energy [7].

4.3 Transmutation cross sections

The transmutation cross sections lead directly to the H- and He-production cross section. For the important elements the data are evaluated from ENDF/B-V nuclear data file. The energy group structure there is 157 non-equidistant groups from thermal energies to 44 MeV. The data are changed to the 50 group structure and used for gas production rate calculations. The unit of the numbers is barn.

The data structure is:

```
Fe(n,Hydrogen)
1.4069E-07 3.7250E-04 4.0750E-03 1.1950E-02 2.1352E-02 3.4100E-02 5.0000E-02
6.6000E-02 8.1000E-02 9.4987E-02 1.0870E-01 1.2535E-01 1.3750E-01 1.4605E-01
1.7125E-01 1.9370E-01 2.1065E-01 2.2715E-01 2.4715E-01 2.6710E-01 2.7600E-01
2.7600E-01 2.7600E-01 2.7600E-01 2.7600E-01 2.7600E-01 2.7600E-01 2.7600E-01
2.7600E-01 2.7600E-01 2.7600E-01 2.7600E-01 2.7600E-01 2.7600E-01 2.7600E-01
2.7600E-01 2.7600E-01 2.7600E-01 2.7600E-01 2.7600E-01 2.7600E-01 2.7600E-01
2.7600E-01 2.7600E-01 2.7600E-01 2.7600E-01 2.7600E-01 2.7600E-01 2.7600E-01
2.7600E-01
                                        .
                                        .
                                        .
Fe(n,Helium)
0.0000E+00 0.0000E+00 0.0000E+00 3.5000E-05 2.6500E-04 1.5300E-03 4.9928E-03
1.0387E-02 1.6500E-02 2.2747E-02 2.9200E-02 3.4705E-02 3.8475E-02 4.0820E-02
4.4590E-02 5.0495E-02 5.7650E-02 6.4600E-02 7.1200E-02 7.6745E-02 7.9300E-02
7.9300E-02 7.9300E-02 7.9300E-02 7.9300E-02 7.9300E-02 7.9300E-02 7.9300E-02
7.9300E-02 7.9300E-02 7.9300E-02 7.9300E-02 7.9300E-02 7.9300E-02 7.9300E-02
7.9300E-02 7.9300E-02 7.9300E-02 7.9300E-02 7.9300E-02 7.9300E-02 7.9300E-02
7.9300E-02 7.9300E-02 7.9300E-02 7.9300E-02 7.9300E-02 7.9300E-02 7.9300E-02
7.9300E-02
                                        .
                                        .
                                        .
```

5 Example runs

First, a small overview about the used commands of the IBM-Job-Control-Language is given. The first card in the job is the jobcard (JOB), which includes the system need parameters and sets some parameters for the job. The //EXEC command executes a procedure i.e. FVCL to compile and link and FVG to run a FORTRAN program, or FVCLG for doing all three steps in one procedure. After the //C.SYSIN DD * , the FORTRAN source code is following. The //G.FT.... allocates a data file to the choosen FORTRAN I/O-unit number. The //* is the comment command in the JCL.

5.1 Data handling

5.1.1 H(t,n) Data

```
//XXXXXXX  JOB (XXXX,XXX,XXXXX),XXXXXX,NOTIFY=XXXXXX,
//         MSGCLASS=H,MSGLEVEL=(0,0),TIME=(0,30),REGION=4000K
//*
// EXEC FVCLG,PARM.C='SOURCE,NOVECTOR,SDUMP(ISN)'
//C.SYSIN DD *
      PROGRAM CONVHYD
*
* CONVERSION OF THE ORIGINAL H(T,N) DATA FROM M. DROSG, UNI VIENNA,
* IN THE KFK-DATA FORMAT AND AT THE SAME TIME,
* INTERPOLATION FROM 1 DEGREE TO 0.5 DEGREE ANGLE STEPS
*
                                        .
                                        .
                                        .
                     FORTRAN source code
                                        .
                                        .
                                        .
//G.FT10F001 DD DISP=SHR,DSN=INS.DATA.ORIGINAL.HTN
//G.FT11F001 DD DISP=SHR,DSN=INS.DATA.CROSS.HTN
```

The input unit is FORTRAN unit number 10. The output unit is FORTRAN unit number 11. Both units are already preallocated in the JCL.

5.1.2 O(t,xn) Data

```
//XXXXXXX  JOB (XXXX,XXX,XXXXX),XXXXXX,
//         MSGCLASS=H,MSGLEVEL=(0,0),
//         NOTIFY=XXXXXX,
//         REGION=5000K,TIME=(0,30)
//*
// EXEC FVCG,PARM.C='SOURCE,NOVECTOR,SDUMP(ISN)'
//C.SYSIN  DD *
      PROGRAM CONVOXY
*
* CONVERSION OF THE ORIGINAL O(T,XN) DATA FROM M. DROSG, UNI VIENNA,
* IN THE KFK-DATA FORMAT AND AT THE SAME TIME,
* INTERPOLATION FROM 15 DEGREE TO 5 DEGREE ANGLE STEPS
*
                                    .
                                    .
                                    .
                      FORTRAN source code
                                    .
                                    .
                                    .
//G.FT11F001 DD DISP=SHR,DSN=INS.DATA.CROSS.OTXN
```

The output unit is FORTRAN unit number 11, which is already preallocated in the JCL. The O(t,xn) yields are stored in the FORTRAN source code.

5.1.3 Li(d,xn) Data (Conversion)

```
//XXXXXXX  JOB (XXXX,XXX,XXXXX),XXXXXX,
//             NOTIFY=XXXXXX,
//             MSGLEVEL=(0,0),
//             MSGCLASS=H,
//             REGION=8000K,
//             TIME=(0,30)
//  EXEC  FVCLG,PARM.C='XREF'
//C.SYSIN    DD *
C
C   E.D. 28.10.1991
C - DESCRIPTION: PROGRAM TO CONVERT THE MANN DATA FROM  MANN'S
C                FORMAT TO KFK FORMAT
                                    .
                                    .
                                    .
                      FORTRAN source code
                                    .
                                    .
                                    .
//G.FT40F001 DD DISP=SHR,DSN=INS.DATA.ORIGINAL.DLI
//G.FT41F001 DD DISP=SHR,DSN=INS.DATA.CROSS.TEMP(ORIG)
/*
```

The input unit is FORTRAN unit number 40. The output unit is FORTRAN unit number 41 (temporary data file). Both units are already preallocated in the JCL.

5.1.4 Li(d,xn) Data (Interpolation)

```
//XXXXXXX  JOB (XXXX,XXX,XXXXX),XXXXXX,NOTIFY=XXXXXX,
//         MSGCLASS=H,MSGLEVEL=(0,0),TIME=(0,30),REGION=8000K
```

```
//*
//  EXEC FVCLG,PARM.C='SOURCE,NOVECTOR,SDUMP(ISN)'
//C.SYSIN DD *
      PROGRAM INTPOL
*
* PROGRAM TO INTERPOLATE THE D-LI DATA FROM FRED MANN
* FORM 5 DEGREE TO 0.5 DEGREE ANGLE STEPS
*
                                    .
                                    .
                                    .
                        FORTRAN source code
                                    .
                                    .
                                    .
//*G.FT10F001 DD DISP=SHR,DSN=INS.DATA.CROSS.TEMP(ORIG)
//*G.FT11F001 DD DISP=SHR,DSN=INS.DATA.CROSS.DLI(ORIG)
//*
//G.FT10F001 DD DISP=SHR,DSN=INS.DATA.CROSS.TEMP(REAL)
//G.FT11F001 DD DISP=SHR,DSN=INS.DATA.CROSS.DLI(REAL)
```

The input unit is FORTRAN unit number 10. The output unit is FORTRAN unit number 11. Both units are already preallocated in the JCL.

5.2 Getting spectra

```
//XXXXXXX  JOB (XXXX,XXX,XXXXX),XXXXXX,
//             NOTIFY=XXXXXX,
//             MSGLEVEL=(0,0),
//             MSGCLASS=H,
//             REGION=8000K,
//             TIME=(0,30)
//*****************************************************************
//*
//* CREATE A LOADMODULE FOR SPECTRA CALCULATIONS
//*
//*****************************************************************
//*
//FORT  EXEC  FVCL,PARM.C='SOURCE,NOVECTOR,SDUMP(ISN)',
//          PARM.L='LIST,SIZE=(7000K,100K)'
//C.SYSIN    DD *
      PROGRAM SPEC
C*********************************************************************
C**                                                                  *
C**   READ LAB CROSS SECTION AND ENERGY TO CALCULATE NEUTRON FLUX    *
C**   SPECTRA AT CERTAIN POINTS DEFINED IN A GLOBAL COORDINATE       *
C**   SYSTEM FOR ONE OR TWO T-H2O SOURCES                            *
C**   PROGRAM CONTAINS CALLS TO THE PROGRAM PACKAGES HBOOK, HPLOT    *
C**   AND HIGZ FROM CERN DD LIBRARY                                  *
C**                                                                  *
C*********************************************************************
C
                                    .
                                    .
                                    .
                                    .
//L.SYSLMOD  DD DISP=SHR,DSN=INS.LOAD(SPECTH2O)
//L.SYSLIB   DD DISP=SHR,DSN=SYS7.VSFORT
//           DD DISP=SHR,DSN=SYS2.FORTLIB
//           DD DISP=SHR,DSN=LOAD
//L.HPL      DD DISP=SHR,DSN=PLOTNODC.LOAD
//L.SYSIN    DD *
 INCLUDE HPL(BPIZGKS)
/*
//
```

The above job is used to create an executable load module. In this module, a lot of CERN-Graphics [11, 12, 13, 14] are used. Therefore,it was the more suitable way to create and keep a load module. When running for various spectra, only a new set of parameters is

included.

```
//XXXXXXX  JOB (XXXX,XXX,XXXXX),XXXXXX,
//             NOTIFY=XXXXXX,
//             MSGLEVEL=(0,0),
//             MSGCLASS=H,
//             REGION=8000K,
//             TIME=(00,30)
//*
//KING  EXEC FVG,NAME=SPECTH2O
//STEPLIB DD DISP=SHR,DSN=SYS7.VSLOAD
//        DD DISP=SHR,DSN=INS.LOAD
//**
//G.FT01F001 DD DISP=SHR,DSN=TSOSYS.GKSERR,LABEL=(,,,IN)
//G.FT02F001 DD DISP=SHR,DSN=TSOSYS.GKSFNT,LABEL=(,,,IN)
//G.FT03F001 DD DISP=NEW,DSN=&&GKSPAG,SPACE=(1024,(62,0)),
//            UNIT=SYSDA,DCB=(LRECL=1024,BLKSIZE=1024,RECFM=F)
//G.FT08F001 DD SYSOUT=*
//G.FT09F001 DD DISP=SHR,DSN=INS.DATA.CROSS.HTN
//G.FT10F001 DD DISP=SHR,DSN=INS.DATA.CROSS.OTXN
//G.SYSIN DD *
 &INPUT TAY=7.5, TAZ=2.5, TAELKA=0.25, CUR=834.,
        SPECST=1, SPECEN=2, NUMSOU=2,
        ANGLE= 90., SHIFT= 10., USER='XXXXXX',
      XPO= 10.0, 20.0
      YPO=  0.0,  0.0
      ZPO=  0.0,  0.0
 &END
/*
```

This job starts the spectra load module, named SPECTH2O for the t – H_2O case and SPECDLI for the d-Li case. Here, the cross section data files are allocated at FORTRAN units 9 and 10. The parameters, written between the statements &INPUT and &END, are input control parameter for the FORTRAN code. TAY and TAZ are the dimension of the extended target in y- or z-direction. TAELKA means the length of one side of a little subelement in the target. All measurements are given in cm. CUR is the electrical beam current in mA. SPECST and SPECEN marks the start and end position of the spetrum counter. In this case, only two spatial point are given, usually allowed are 600 defined spatial points. NUMSOU gives the number of used sources. ANGLE is the opening angle of the test cell limiting planes. USER is the user name prefix used to create output data file names in the FORTRAN code. XPO,YPO and ZPO are the spatial point coordinates in the world coordinate system. 600 coordinate triples are allowed to use at same time.

5.3 Getting volumes and contours

```
//XXXXXXX  JOB (XXXX,XXX,XXXXX),XXXX,
//             NOTIFY=XXXXXX,
//             MSGLEVEL=(1,1),
//             MSGCLASS=H,
//             REGION=8000K,
//             TIME=(3,00)
//  EXEC  FVCLG,PARM.C='NOVECTOR,SOURCE,SDUMP(ISN)'
//C.SYSIN    DD DISP=SHR,DSN=INS.FORT.TH2O(CPDATA)
//G.FT09F001 DD DISP=SHR,DSN=INS.CROSS.HTN
//G.FT10F001 DD DISP=SHR,DSN=INS.CROSS.OTXN
//G.FT11F001 DD DISP=SHR,DSN=INS.CONTOUR.DATA(DTH500)
```

```
//G.SYSIN DD *
 500.
/*
```

This job executes the FORTRAN program CPDATA, which prepares the flux distribution data for a point source in the required test cell, which is necessary for flux contour and flux volumes calculation for spread sources. The FORTRAN units 9 and 10 are the input units for the H(t,n) cross sections and the O(t,xn) pseudo cross sections. FORTRAN unit 11 is the output unit, where the point source flux distribution is stored in the dataset CONTOUR.DATA. The filename ABBCCC follows the convention A can be S for (1-S) and D for (2-S) case, BB can be TH for t – H_2O – source or LI for d-Li-source and CCC gives the beam current parameter in mA. After the SYSIN card the required beam current is written in mA.

```
//XXXXXXX  JOB (XXXX,XXX,XXXXX),XXXX,
//             NOTIFY=XXXXXX,
//             MSGLEVEL=(1,1),
//             MSGCLASS=H,
//             REGION=8000K,
//             TIME=(10,00)
//  EXEC  FVCLG,PARM.C='DC(A,B),SOURCE,NOVECTOR,SDUMP(ISN)'
//C.SYSIN    DD DISP=SHR,DSN=INS.FORT.TH20(CONTOUR)
//G.FT07F001 DD DISP=SHR,DSN=INS.OUT.TH20
//G.FT09F001 DD DISP=SHR,DSN=INS.CONTOUR.DATA(DTH500)
//G.FT11F001 DD DISP=SHR,DSN=INS.Z0
//G.FT22F001 DD DISP=SHR,DSN=INS.VOLUMINA.T75X25(DTH500)
//G.SYSIN    DD *
 &INPUT ZEB=  2.0, 0.0,
        ANGLE=  90.0, DISTAN= 10.0, TAY= 7.5, TAZ= 2.5,
        NUMSOU= 2, TYPE = 'DTH500',
        PLEVEL(1)=10.00E+14, PLEVEL(2)= 5.00E+14,
        PLEVEL(3)= 2.00E+14, PLEVEL(4)= 1.00E+14,
        PLEVEL(5)= 5.00E+13 &END
//* DEFINE PLANE WHERE CONTOURPLOT IS MADE. ZEB IN CM
//* DEFINE RECTANGULAR TARGET SHAPE TAY * TAZ IN CM**2
//* DEFINE CONTOUR LINE PRINTING LEVELS PLEVEL(1-5)
/*
```

This job executes the FORTRAN program CONTOUR. The input unit is unit 9, where the point source flux distribution data are read in. Unit 7 is an output unit, which was utilized during program development to perform cross checks with the calculated data. In FORTRAN unit 11, the calculated coordinate points for the required contour line are stored. In this case it is done for the Z = 0 cm plane. In unit 22 are the minimum flux volumes for the given flux limits stored as a table. One extension of the dataset name refers to the target dimensions. In this case the 25 mm * 75 mm target is calculated. The member name structure is explained above. Some job input parameters have already been explained. Additional new parameter is the ZEB parameter which represents the number of planes to be calculated plus one, followed by the z-coordinates of the planes separated

by comma. The PLEVEL parameter gives the minimum neutron flux limits in descending order.

5.4 Getting damage parameters

```
//XXXXXXX  JOB (XXXX,XXX,XXXXX),XXXX,
//             NOTIFY=XXXXXX,
//             MSGLEVEL=(0,0),
//             MSGCLASS=H,
//             REGION=8000K,
//             TIME=(0,30)
//  EXEC  FVCLG,PARM.C='SOURCE,NOVECTOR,SDUMP(ISN)'
//C.SYSIN    DD DISP=SHR,DSN=INS.FORT.MISC(EQBINGAS)
//*C.SYSIN    DD DISP=SHR,DSN=INS.FORT.MISC(EQBINDPA)
/*
```

This job is used to demonstrate how to convert the non-equidistant energy groups of the H- , He-production-cross sections and the DPA-cross sections to the 50, one MeV wide, equidistant energy groups. EQBINGAS gives an example how this is done for gas-production cross sections and EQBINDPA gives an example for the damage energy cross sections.

```
//XXXXXXX  JOB (XXXX,XXX,XXXXX),XXXX,
//             NOTIFY=XXXXXX,
//             MSGLEVEL=(0,0),
//             MSGCLASS=H,
//             REGION=8000K,
//             TIME=(0,30)
//  EXEC  FVCLG,PARM.C='SOURCE,NOVECTOR,SDUMP(ISN)'
//C.SYSIN    DD DISP=SHR,DSN=INS.FORT.MISC(DPA)
//G.FT22F001 DD DISP=SHR,DSN=INS.SPECTRA.OUTL.RLI100.T30X10
//G.FT23F001 DD DISP=SHR,DSN=INS.DAMAGE.CROSS(DPA)
//G.FT24F001 DD DISP=SHR,DSN=INS.OUT.DPA(RLI100)
//G.SYSIN    DD *
 &INPUT SPECNUM =  1, CROSSN = 4 &END
/*
```

```
//XXXXXXX  JOB (XXXX,XXX,XXXXX),XXXX,
//             NOTIFY=XXXXXX,
//             MSGLEVEL=(0,0),
//             MSGCLASS=H,
//             REGION=8000K,
//             TIME=(0,30)
//  EXEC  FVCLG,PARM.C='SOURCE,NOVECTOR,SDUMP(ISN)'
//C.SYSIN    DD DISP=SHR,DSN=INS.FORT.MISC(HAPPM)
//G.FT22F001 DD DISP=SHR,DSN=INS.SPECTRA.OUTL.STH170.T30X10
//G.FT23F001 DD DISP=SHR,DSN=INS.DAMAGE.CROSS(H15750)
//G.FT24F001 DD DISP=SHR,DSN=INS.OUT.HAPPM(STH170)
//G.SYSIN    DD *
 &INPUT SPECNUM =  82, CROSSN = 4, TIME = 1.2064E+08  &END
/*
```

```
//XXXXXXX  JOB (XXXX,XXX,XXXXX),XXXX,
//             NOTIFY=XXXXXX,
//             MSGLEVEL=(0,0),
//             MSGCLASS=H,
//             REGION=8000K,
```

```
//             TIME=(0,30)
//  EXEC  FVCLG,PARM.C='SOURCE,NOVECTOR,SDUMP(ISN)'
//C.SYSIN    DD DISP=SHR,DSN=INS.FORT.MISC(HEAPPM)
//G.FT22F001 DD DISP=SHR,DSN=INS.SPECTRA.OUTL.RLI100.T30X10
//G.FT23F001 DD DISP=SHR,DSN=INS.DAMAGE.CROSS(HE15750)
//G.FT24F001 DD DISP=SHR,DSN=INS.OUT.HEAPPM(RLI100)
//G.SYSIN    DD *
 &INPUT SPECNUM =  82, CROSSN = 4, TIME = 1.2064E+08  &END
/*
```

The three jobs above are used to calculate the H-, He- and DPA-rates. DPA calculates dpa/sec and HAPPM or HEAPPM calculates $APPM_H$/sec or $APPM_{He}$/sec , respectively. FORTRAN unit 22 allocates the neutron flux spectrum data input library, which is an output of the module SPECTRA. FORTRAN unit 23 allocates the damage cross sections library. In this library, the filenames are DPA for displacements, H15750 for H-production and HE15750 for He-production. FORTRAN unit 24 is used to store the results of the calculation. The INPUT parameter are SPECNUM = number of neutron flux spectra to process, CROSSN = number of element cross section data to process, and TIME is used to determine the total H-, He-production or displacements in $APPM_{H,He}$ or dpa, respectively.

6 Results

The results, produced with the INS-code, should give an overview about various parameters to characterize the two Intense Neutron Sources compared. Tables and graphical plots are used to show the results. Only a small set of all calculated results is presented in the appendix, since showing all plots falls beyond the framework of this manual.

6.1 Spectra data and plots

With the module SPECTRA, for the one source case (1-S) and the two source case (2-S), comparative flux spectra have been calculated. The comparison is made with the asumption, that both sources, t – H_2O and d-Li, use the same electrical power, namely 3.5 MW for (1-S) and 17.5 MW for (2-S). Therefore, the beam current of t – H_2O and d-Li differ by a factor of 1.67 . In table 1, the used parameters are listed.

	1-Source-Case	2-Source-Case
TAY	3.0 cm	7.5 cm
TAZ	1.0 cm	2.5 cm
TAELKA	0.25 cm	0.25 cm
Nt	48	300
NUMSOU	1	2
ANGLE	180.0 °	90.0 °
SHIFT	0.0 cm	10.0 cm
CUR (t – H_2O)	170.0 mA	834.0 mA
CUR (d – Li)	100.0 mA	500.0 mA

Table 1: Table of control parameters for module SPECTRA, used to calculate comparative flux spectra.

In the test cell a grid of 2cm * 2cm * 2cm is used to define the spatial points for the various spectra. Another number-limiting factor is the volume for a given minimum integrated flux of e.g. $5 * 10^{13}$n/sec/cm^2 at the t – H_2O source. That means, that in (1-S) case 82 spectra and in (2-S) case 562 spectra have been calculated. In the d-Li case, both cross section datafiles σ_{orig} and σ_{real} were used. A sample of the plots is given in appendix A.1 and A.3.

The difference in the spectral shape between the neutron flux spectra for d-Li source, calculated with σ_{orig} and σ_{real}, can be neglected. Therefore only the d-Li flux spectra calculated by σ_{orig} are compared with the t – H_2O flux spectra. In figure 9 and figure 11, a comparison with the calculated flux spectra (1-S) , (2-S) and the DEMO 1st. wall spectrum [24] is made.

For the 1-S case with the small target (3cm^2), the integral value at position (0,0,0) is by a factor of 3 bigger than the DEMO value. At position (10,0,0), the integral value is decreased by a factor of 20 (t – H_2O) and 10 (d-Li). The integral flux of d-li is always higher as the t – H_2O value. This is caused by a not neglectible part of neutrons with energies greater than 14 MeV. To quantify this part, a ratio $r = \frac{\text{neutron flux}(E_n > 14\text{MeV})}{\text{total neutron flux}}$ is defined. The integral flux and the belonging ratio for all compared positions are listed in table 2. The fraction values for all spectra are plotted for (1-S) case in figure 10.

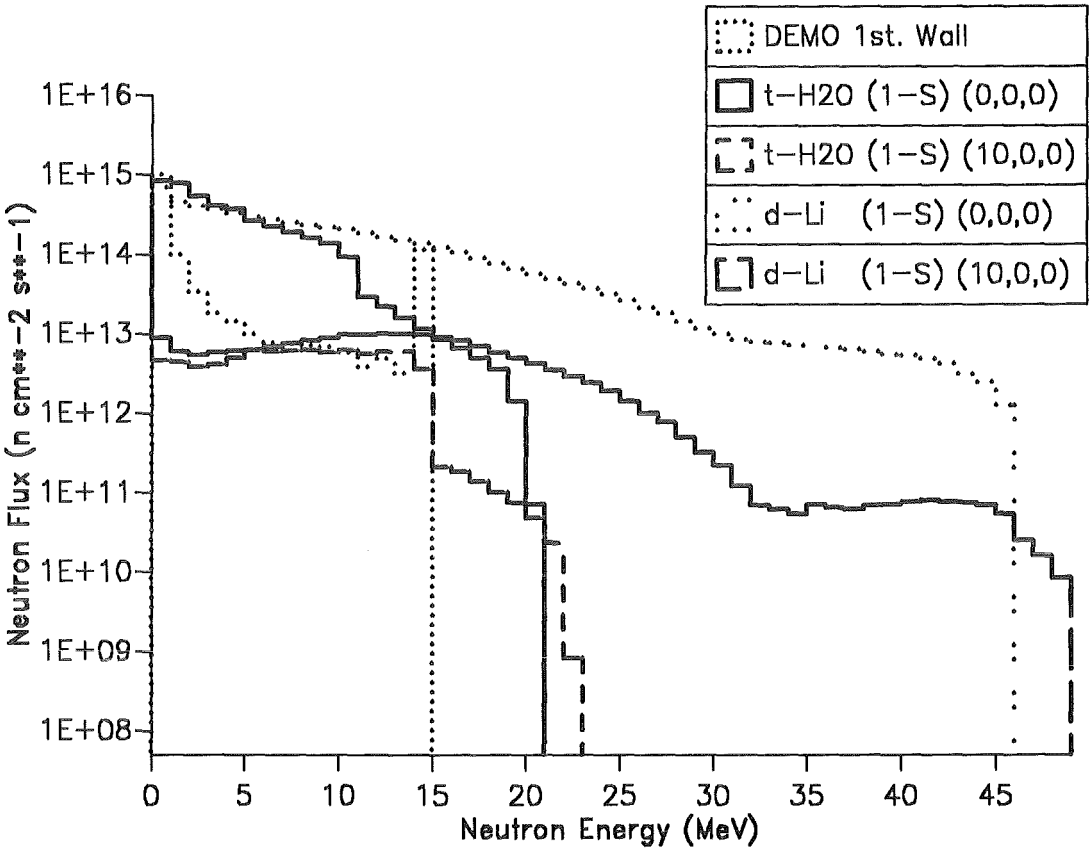

Figure 9: Neutron flux comparison 1-S case with DEMO 1st. wall

This allows an overview about the different behaviour of the spectra. The average value of (r) for all computed (1-S) spectra is for $t - H_2O$, $r = 2$ % , and for d-Li , $r = 25$ %. This shows that the $t - H_2O$ spectra fit much better to the DEMO 1st. wall spectrum than the d-Li spectra.

At the (2-S) case with the big target ($20cm^2$), the same calculations have been performed. The compared positions are (14,0,0) and (22,0,0). The (14,0,0) is choosen, because it is the intersection point of the x-axes of the source-coordinate systems. The (22,0,0) point is choosen, because the integral flux of $t - H_2O$ is approximately $10^{14} n/cm^2/s$. The compared spectra are plotted in figure 11 and the integral values and ratios (r) are listed in table 2. The values (r) of all 562 computed spectra in (2-S) case are plotted in figure 12. The average values of (r) are $r = 1.7$ % for $t - H_2O$ and $r = 22.2$ % for d-Li. A more general comparison of the flux spectra calculated by INS-code with earlier calculations is described in table 3.

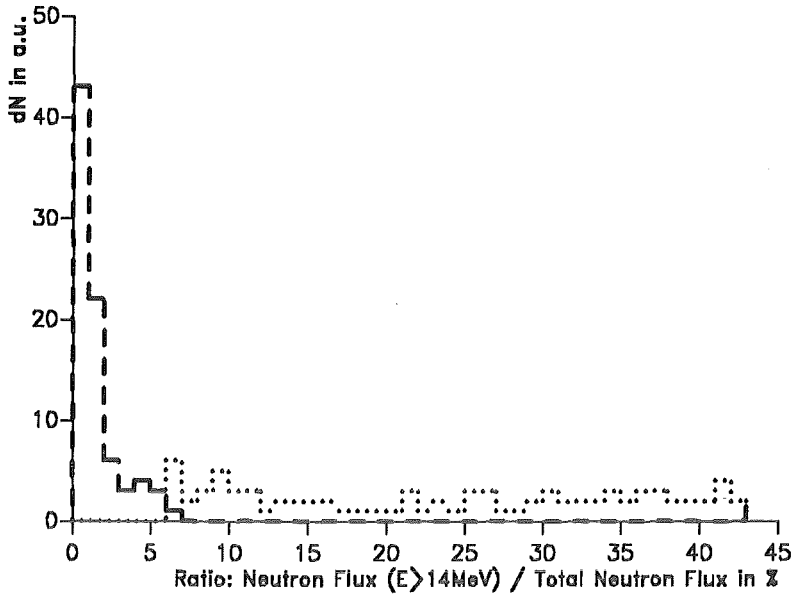

Figure 10: Fraction (r) for all computed 82 flux spectra in (1-S) case. The dashed line is the t – H_2O and the dotted line is the d-Li source.

Description	Integral flux $n/cm^2/s$	Ratio r %
DEMO 1st. wall	$1.41 * 10^{15}$	0.1
(1-S), t – H_2O, (0,0,0)	$4.09 * 10^{15}$	0.9
(1-S), t – H_2O, (10,0,0)	$8.01 * 10^{13}$	5.4
(1-S), d-Li, (0,0,0)	$5.25 * 10^{15}$	21.9
(1-S), d-Li, (10,0,0)	$1.74 * 10^{14}$	43.0
(2-S), t – H_2O, (14,0,0)	$6.48 * 10^{14}$	3.1
(2-S), t – H_2O, (22,0,0)	$1.91 * 10^{14}$	1.6
(2-S), d-Li, (14,0,0)	$1.44 * 10^{15}$	35.7
(2-S), d-Li, (22,0,0)	$3.11 * 10^{14}$	33.4

Table 2: Table of integral and (r) values of the spectra compared with the DEMO 1st. wall spectrum.

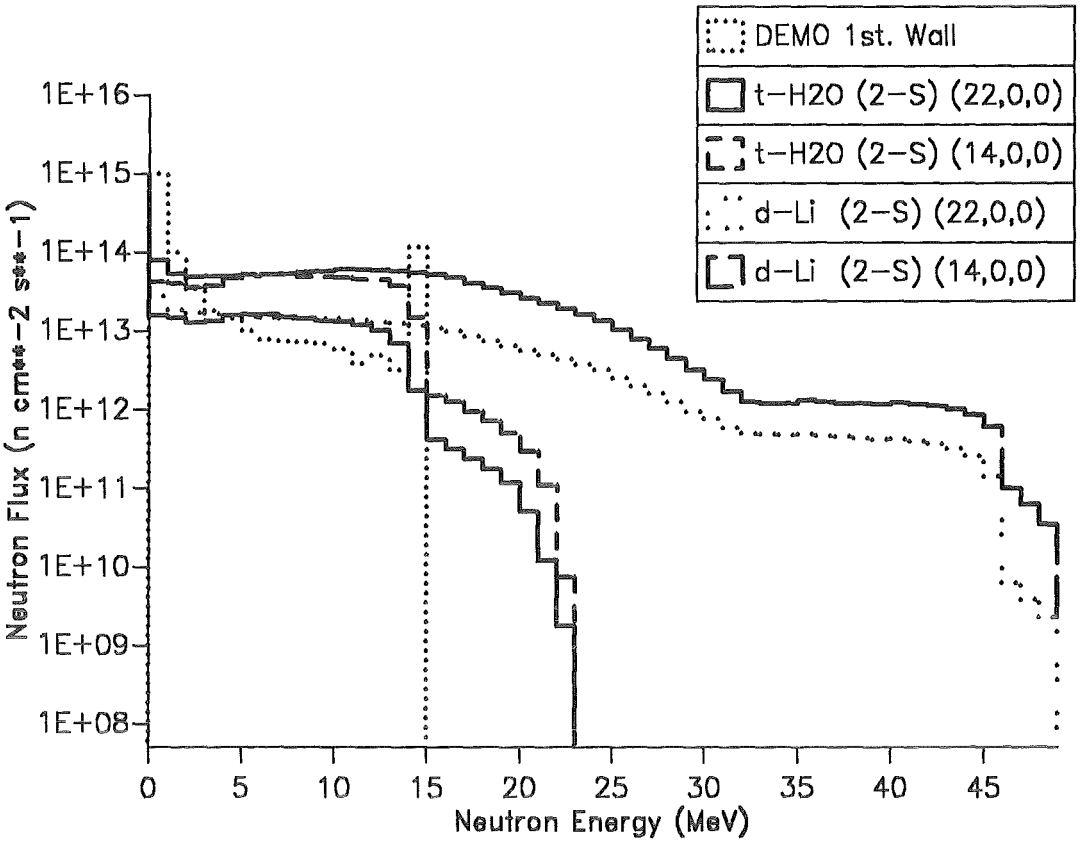

Figure 11: Neutron flux comparison (2-S) case with DEMO 1st. wall

Spectrum	Reference	Code used	Total flux $n/cm^2/s$	Fraction r %
DEMO 1st. wall	[24]	?	$1.41 * 10^{15}$	0.1
d-Li, (1-S), (0,0,0)	This manual	INS, KfK	$5.25 * 10^{15}$	22
d-Li, (1-S), (4,0,0)	This manual	INS, KfK	$6.57 * 10^{14}$	40
t – H_2O, (1-S), (0,0,0)	This manual	INS, KfK	$4.09 * 10^{15}$	1
t – H_2O, (1-S), (4,0,0)	This manual	INS, KfK	$3.84 * 10^{14}$	3
d-Li, 2 * 250 mA, at 90 °, (8.5,0,0)	[25]	FMITSP (Mann)	$5.45 * 10^{14}$	$E_n > 15MeV$ 37
d-Li, 2 * 250 mA, at 90 °, (14,0,0)	[25]	FMITSP (Mann)	$5.27 * 10^{14}$	$E_n > 15MeV$ 49
d-Li, (2-S), (8,0,0)	This manual	INS, KfK	$1.11 * 10^{15}$	28
d-Li, (2-S), (14,0,0)	This manual	INS, KfK	$1.19 * 10^{15}$	39
t – H_2O, (2-S), (8,0,0)	This manual	INS, KfK	$6.88 * 10^{14}$	1
t – H_2O, (2-S), (14,0,0)	This manual	INS, KfK	$6.54 * 10^{14}$	3
d-Li, (2-S), (8,8,0), Max. flux position	This manual	INS, KfK	$6.84 * 10^{15}$	18
t – H_2O, (2-S), (8,8,0), Max. flux position	This manual	INS, KfK	$4.41 * 10^{15}$	1

Table 3: Table of more general comparison of neutron flux spectra.

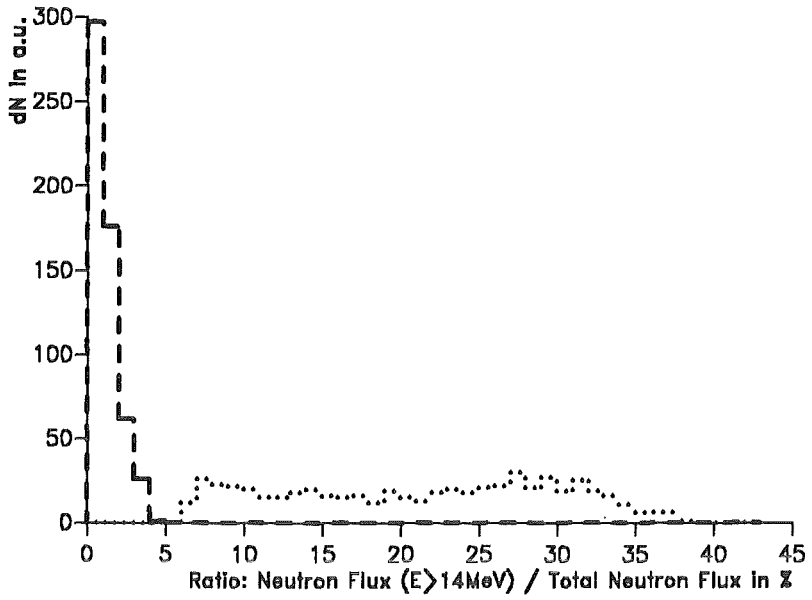

Figure 12: Ratios (r) for all computed 562 flux spectra in (2-S) case. The dashed line is the t – H_2O and the dotted line is the d-Li source.

The one source and two source comparisons show once more, that the t – H_2O spectra are fitting much better to the DEMO spectrum shape. The average r = 1.7 % can be considered as ideal. The t – H_2O shape differs only at very low energies ($E_n < 1MeV$) and at the high energy region ($E_n > 14MeV$). It is obvious, that the best fit of d-Li is not as good as the worst case of t – H_2O. A more general comparison with results from [25] shows for d-Li an increased total flux by a factor of two. This factor can be understood if the used target shape and target area are not the same like in the INS-code. At comparable positions, the t – H_2O flux lacks only by a factor less than 2 as against d-Li. At the maximum flux position the t – H_2O has an advantage in total flux by 50 %. This is aproximately a factor of 5 higher than the DEMO flux, which represents suitable conditions for end-of-life-testing of fusion materials, but as shown in chapter 6.2, only in a small volume.

6.2 Contour data and plots

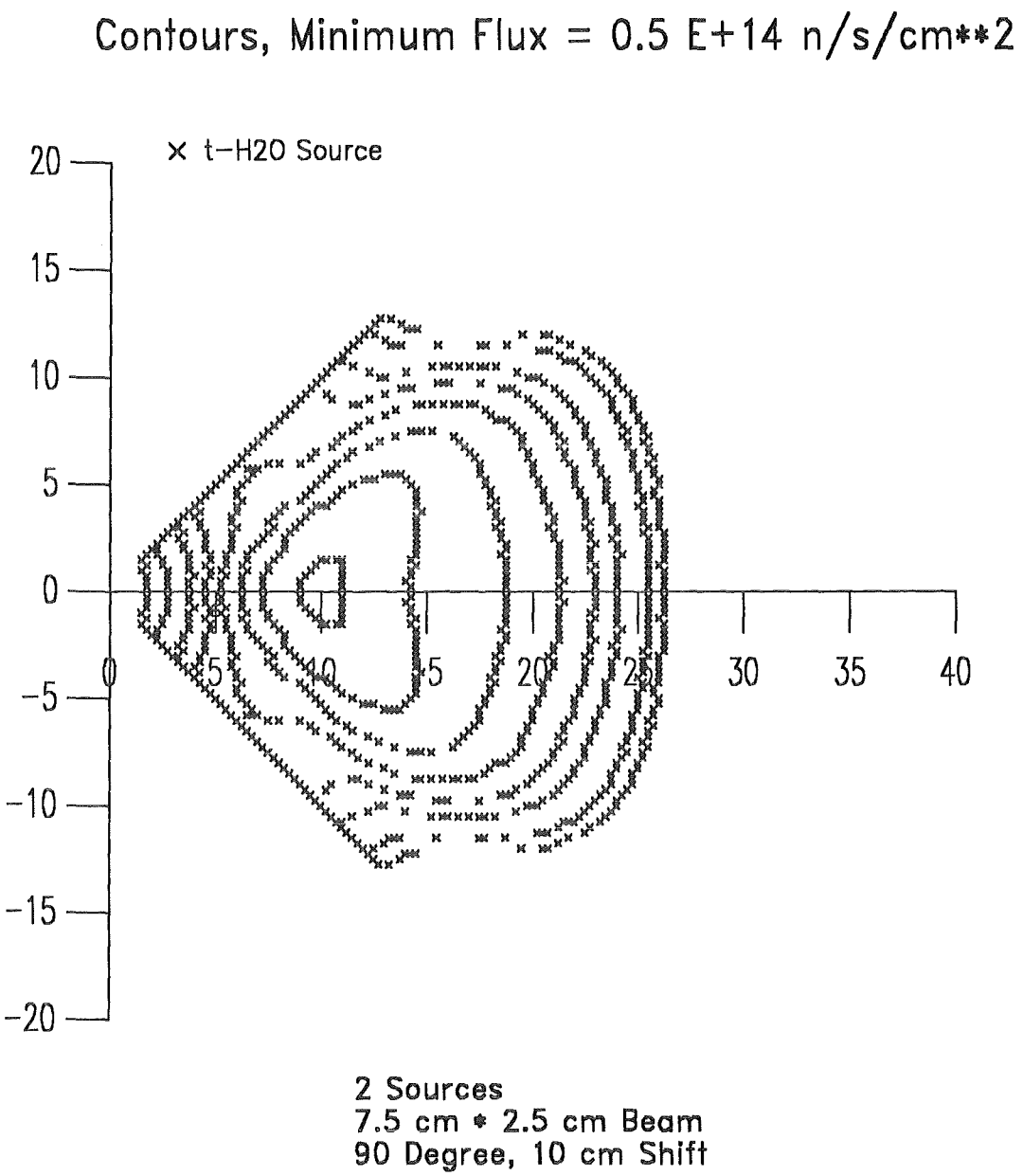

Figure 13: Figure of the minimum flux contour lines for the (2-S) $t-H_2O$ case. Shown are the contour lines going from outside to inside for z = 0 cm, z = 3 cm and z = 5,6,7,8,9,10 cm.

The contour plots have been calculated for the cases (1-S) and (2-S) at various z-coordinates in 1 cm steps, from z = 0 cm up to the z-coordinate where the neutron flux of the $t-H_2O$ source decreases below the $5 * 10^{13} n/sec/cm^2$. The figures for all relevant cases are listed in the appendix. The minimum neutron flux levels are $10^{15}, 5 * 10^{14}, 2 * 10^{14}, 10^{14}$ and

$5 * 10^{13}$n/sec/cm^2. An overview about the behaviour of the contour lines for the (2-S) t – H_2O case at various z-coordinates is shown in figure 13 for the minimum neutron flux of $5 * 10^{13}$n/sec/cm^2. This picture gives a feeling about the shape of the volume for a neutron flux of at least $\phi_n \geq 5 * 10^{13}$n/sec/cm^2 . From z = 0 cm to z = 3 cm there is only a slow variation of the contourlines but from z = 6 cm to z = 10 cm it is a very rapid variation and the contour lines quickly disappear.

6.3 Minimum flux volumes

While calculating the flux contour coordinates, the flux volumes with a neutron flux greater than the required limit, have been simultaneously calculated. For the (1-S) and the (2-S) case the volumes are listed in dependence of beam power and flux level limit in table 4.

Source	Beam Power in MW	ϕ_{min} in n/sec/cm^2	Volume in cm^3 d-Li	Volume in cm^3 t – H_2O
(1-S)	3.5	$1 * 10^{15}$	2.5	6.4
		$5 * 10^{14}$	28.2	19.3
		$2 * 10^{14}$	133.8	75.8
		$1 * 10^{14}$	405.3	208.7
		$5 * 10^{13}$	1204.1	561.6
(2-S)	17.5	$1 * 10^{15}$	24.0	48.9
		$5 * 10^{14}$	454.0	184.0
		$2 * 10^{14}$	1997.8	1024.1
		$1 * 10^{14}$	5047.9	2540.1
		$5 * 10^{13}$	12711.2	6087.6

Table 4: Table of minimum flux volumes at specific flux level limits for (1-S) and (2-S) source case.

In general, the volumes differ, compared at equal beam power, at the (1-S) and (2-S) case by a factor of two. That means, that the t – H_2O source has in both cases a factor of 2 lower volume in comparison to the d-Li source.

To characterize further properties of the neutron sources, the flux volumes versus the beam current are plotted.

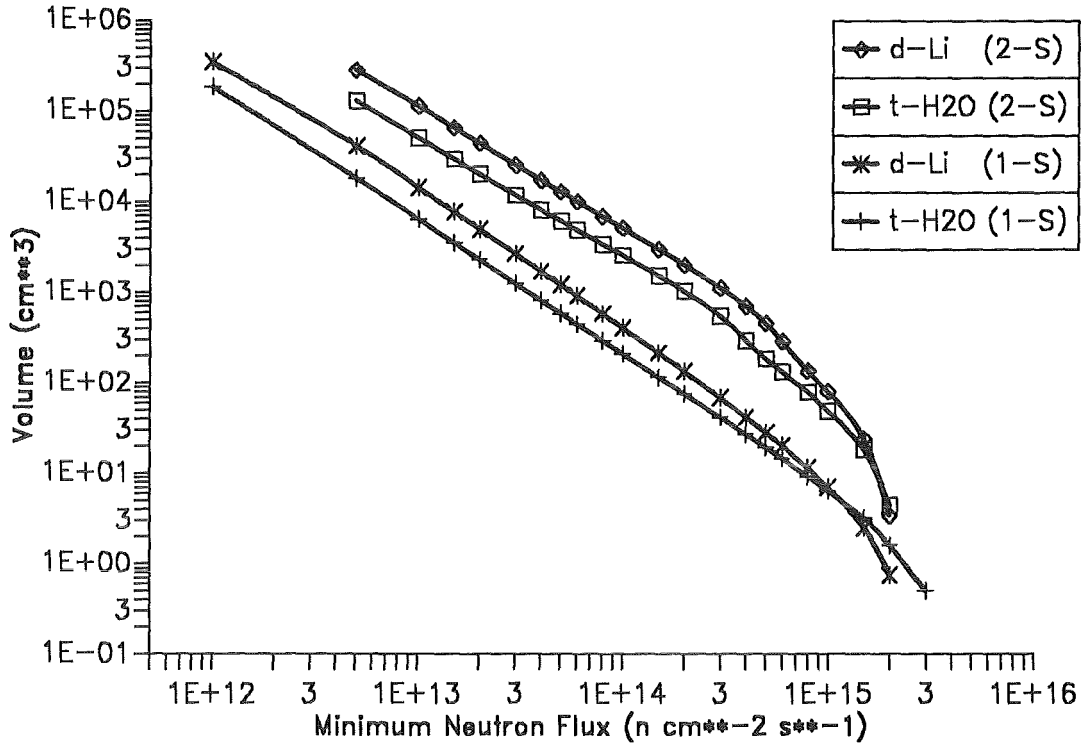

Figure 14: Figure of the minimum flux volumes plotted versus the neutron flux for the (1-S) and (2-S) case.

In figure 14 one can see, that by the logarithmic scale V $\sim \phi$ is valid in the flux range from 10^{12}n/sec/cm^2 to $3 * 10^{14}$n/sec/cm^2. This yealds to

$$V = \frac{5.7 * 10^{22}}{\phi^{1.46}} \qquad for \quad (1-S)$$

and to

$$V = \frac{3.14 * 10^{21}}{\phi^{1.297}} \qquad for \quad (2-S)$$

The unit of V in cm^3 and ϕ is given in n/sec/ cm^2 . For large neutron fluxes, the approximation V $\sim \phi$ is no more valid, because the target geometry becomes an important factor. This effect decreases the flux volumes more than proportional.

In a plot of flux volume versus beam current in a logarithmic scale also a proportionality can be recognized. This yields to

$$V \sim I^{1.47} \qquad for \quad (1-S)$$

and to

$$V \sim I^{1.42} \quad to \quad V \sim I^{1.93} \qquad for \quad (2-S)$$

for V in cm^3 while I is in mA.

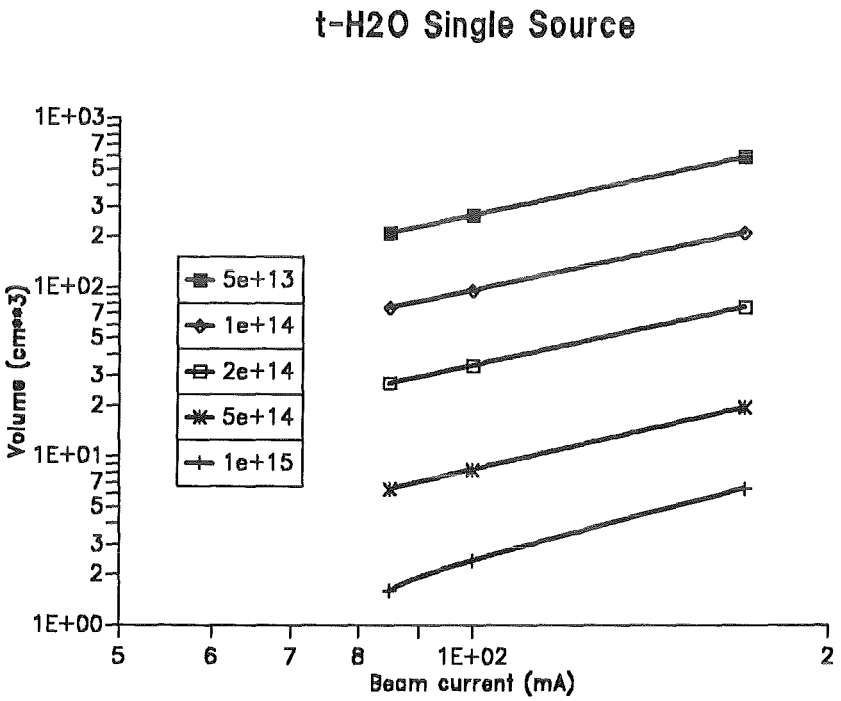

Figure 15: Figure of the minimum flux volumes plotted versus the beam current for the (1-S) case.

Hence the exponent for the (2-S) case is greater than that for the (1-S) case, the flux volume for (2-S) increases faster than for (1-S). This can be understood by analyzing the growth of flux volumes in the (2-S) case. In figure 17 a symbolized drawing shows, how the contourlines for a high flux value are developping by changing the beam current parameter.

The beam current values are $I_1 < I_2 < I_3$. For I_1 and I_2 the contour lines behave each like a single source. For I_3 , the contour lines got in contact and in that moment, the flux volumes grew faster than for single source case. This effect leads to the bigger exponent in the double source case.

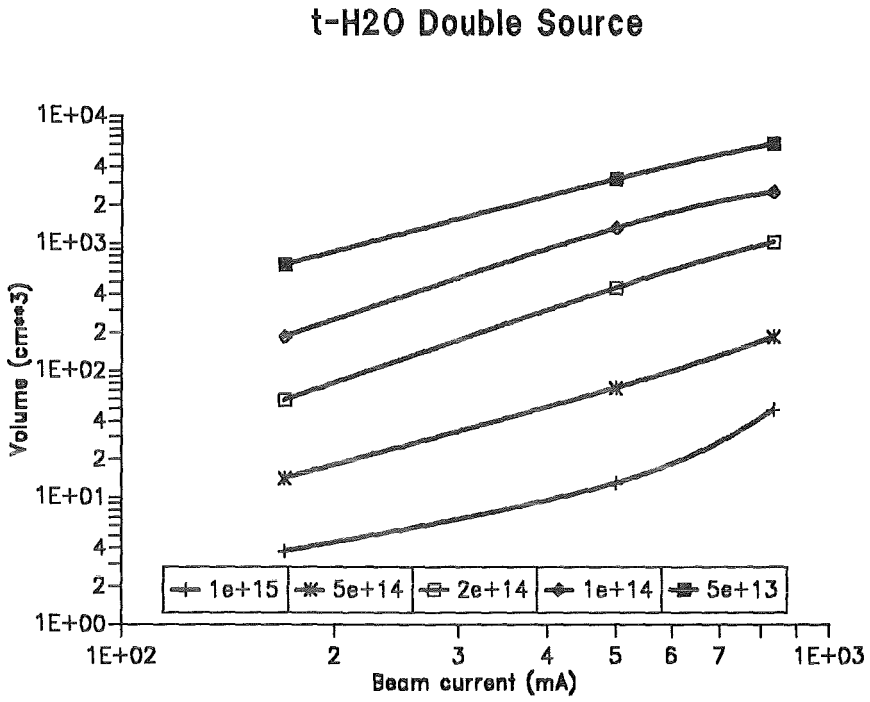

Figure 16: Figure of the minimum flux volumes plotted versus the beam current for the (2-S) case.

ϕ_{min} in n/sec/cm^2	Volume in cm^3 (2-S)	Volume in cm^3 (1-S)
$1 * 10^{15}$	3.8	6.4
$5 * 10^{14}$	14.1	19.3
$2 * 10^{14}$	58.1	75.8
$1 * 10^{14}$	184.1	208.7
$5 * 10^{13}$	677.8	561.6

Table 5: Comparison of the minimum flux volumes of (1-S) and (2-S) case for the t – H_2O source at 3.5 MW beam power.

In a further comparison it is inquired, how the minimum flux volumes behave, if the cases (1-S) and (2-S) are compared for the t – H_2O source at equal beam power. The beam power choosen was 3.5 MW which corresponds to a beam current of 170 mA. In both

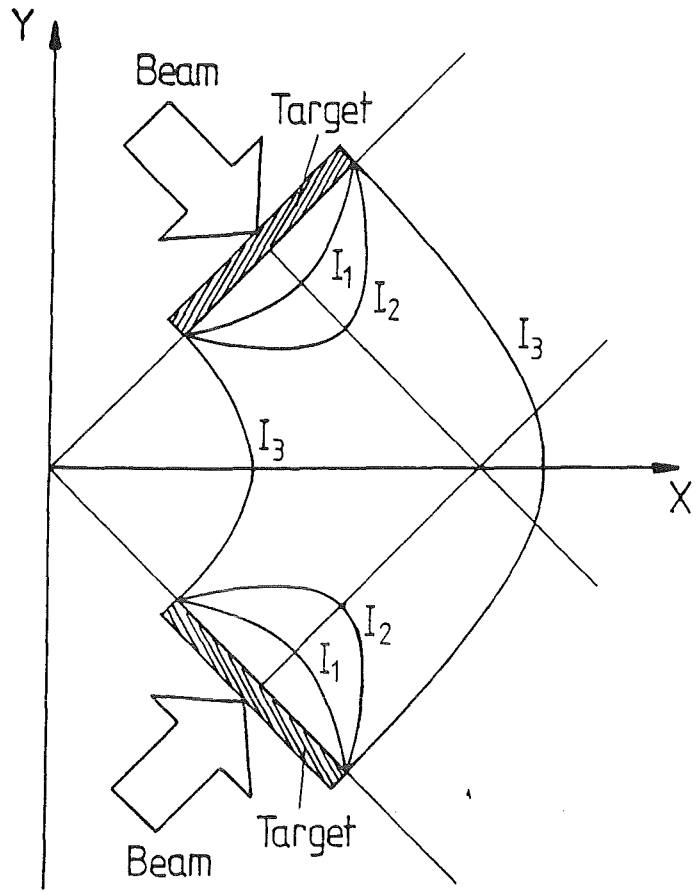

Figure 17: Schematic drawing of the development of high flux contour lines for the (2-S) case with the beam current I as a parameter.

cases the same target size of $3cm^2$ was used. Only the position and number of the targets are different. The minimum flux volumes values are listed in table 5.

The result is, that the (1-S) source has volume advantages at higher fluxes. Only at fluxes lower than $10^{14}n/s/cm^2$ the (2-S) source becomes advantageous.

6.4 Neutron irradiation damage

Characterizing the neutron irradiation damage is important, because this information leads to a understanding, how an irradiated material will be damaged. One the other hand, a comparison of the d-Li- or $t-H_2O$-source with other neutron irradiation facilities is possible. A comparison of the damage data with the data obtained from the DEMO 1st. wall spectrum is also important.

Before presenting the damage results, some words about the spectral averaging process should be mentioned. The DEMO spectrum and the damage energy cross sections are used as an example. Normally, the DISCS code, which calculates the damage energy cross sections, is running in a very fine energy group structure (100 bins). Also the DEMO spectrum is given in a very fine energy group structure (GAM II). While calculating the spectral averaged damage energy cross sections, the whole information of the spectral behaviour in the 0 - 1 MeV region can be used. Rebinnig of the fine energy group structure of the cross section data to the 50 energy group structure requires a spectral weighting factor in the energy region 0 - 1 MeV. The factor 1/E, used for nuclear fission spectra, is used for the fusion spectra, too. How this factor fits to the fusion spectra is shown in table 6 for the two important elements Fe and C.

	C	Fe
DEMO (100)	31	69
DEMO (50)	16	47

Table 6: Spectral averaged damage energy cross sections (keV * barn) for fine (100) and rough (50) energy group structure.

The uncertainty, produced by spectral averaging of the rough spectra data, can be determined to be a factor of $\sim$ 2. This shows, that the spectral behaviour of the DEMO spectrum at low energies cannot be simply treated like a thermal spectrum and it would be better to fix the problems at low energies by calculating spectral averaged values in future in the fine energy group structure.

The isotopes, where damage data have been calculated, are listed with some attributes in table 7. Some of this isotopes are also published in [26].

Isotope	Ref. Mat.	ED (eV)	DPA/sec		$APPM_H$/sec		$APPM_{He}$/sec	
			$t - H_2O$	d-Li	$t - H_2O$	d-Li	$t - H_2O$	d-Li
^{6}Li	1303	10	*		*	*	*	*
^{7}Li	1272	10	*				*	*
^{9}Be	1304	31	*		*	*	*	*
^{10}B	1305	25	*		*	*	*	*
^{11}B	1160	25	*		*	*	*	*
^{12}C	1306	31	*	*	*	*	*	*
^{14}N	1275	30	*		*	*	*	*
^{16}O	1276	30	*					
^{17}O	1307						*	*
^{19}F	1309	30	*		*	*	*	*
Mg	1312	25	*					
^{27}Al	1313	27	*		*	*	*	*
^{28}Si	1314	25	*	*	*	*	*	*
Ti	1322	40	*		*	*	*	*
V	1323	40	*	*	*	*	*	*
Cr	1324	40	*	*	*	*	*	*
Mn	1325	40	*		*	*	*	*
Fe	1326	40	*	*	*	*	*	*
Co	1327	40	*		*	*	*	*
Ni	1328	40	*	*	*	*	*	*
Cu	1329	40	*	*	*	*	*	*
Nb	1189	40	*	*				
^{104}W	1130	90	*	*				

Table 7: List of calculated isotopes.

Some of the isotopes listed in table 7 are used to calculate the gas concentration to damage ratios. This results are listed in tables 8 - 19. The empty boxes in the tables are due to lack of DPA-cross section data, not available for energies greater than 20 MeV. This means, that for the d-Li source the DPA/sec and consequently also the gas/DPA ratios could not

be calculated.

Material			^{6}Li	^{9}Be	^{10}B	^{11}B
DEMO 1st Wall			$3.9 * 10^{-4}$	$2.1 * 10^{-7}$	$1.4 * 10^{-3}$	$3.0 * 10^{-7}$
(1-S)	d-Li	(0,0,0)				
		(4,0,0)				
	$t - H_2O$	(0,0,0)	$2.6 * 10^{-4}$	$1.4 * 10^{-6}$	$1.2 * 10^{-3}$	$1.9 * 10^{-6}$
		(4,0,0)	$7.8 * 10^{-6}$	$1.3 * 10^{-7}$	$3.4 * 10^{-5}$	$1.9 * 10^{-7}$
(2-S)	d-Li	(8,0,0)				
		(14,0,0)				
		(8,8,0)				
	$t - H_2O$	(8,0,0)	$2.4 * 10^{-5}$	$2.3 * 10^{-7}$	$1.1 * 10^{-4}$	$3.4 * 10^{-7}$
		(14,0,0)	$1.4 * 10^{-5}$	$2.2 * 10^{-7}$	$5.9 * 10^{-5}$	$3.3 * 10^{-7}$
		(8,8,0)	$3.4 * 10^{-4}$	$1.4 * 10^{-6}$	$1.5 * 10^{-3}$	$2.0 * 10^{-6}$

Table 8: Displacement rates in DPA/sec.

Material			^{12}C	^{14}N	^{19}F	^{27}Al
DEMO 1st Wall			$2.9 * 10^{-7}$	$3.6 * 10^{-7}$	$6.3 * 10^{-7}$	$7.9 * 10^{-7}$
(1-S)	d-Li	(0,0,0)	$2.7 * 10^{-6}$			
		(4,0,0)	$3.4 * 10^{-7}$			
	$t - H_2O$	(0,0,0)	$2.0 * 10^{-6}$	$2.6 * 10^{-6}$	$4.7 * 10^{-6}$	$6.1 * 10^{-6}$
		(4,0,0)	$1.9 * 10^{-7}$	$2.8 * 10^{-7}$	$5.0 * 10^{-7}$	$7.6 * 10^{-7}$
(2-S)	d-Li	(8,0,0)	$5.7 * 10^{-7}$			
		(14,0,0)	$6.2 * 10^{-7}$			
		(8,8,0)	$3.5 * 10^{-6}$			
	$t - H_2O$	(8,0,0)	$3.4 * 10^{-7}$	$4.7 * 10^{-7}$	$8.5 * 10^{-7}$	$1.2 * 10^{-6}$
		(14,0,0)	$3.2 * 10^{-7}$	$4.7 * 10^{-7}$	$8.4 * 10^{-7}$	$1.3 * 10^{-6}$
		(8,8,0)	$2.1 * 10^{-6}$	$2.7 * 10^{-6}$	$4.8 * 10^{-6}$	$6.3 * 10^{-6}$

Table 9: Displacement rates in DPA/sec.

Material			^{28}Si	Ti	V	Mn
DEMO 1st Wall			$8.9 * 10^{-7}$	$6.5 * 10^{-7}$	$7.1 * 10^{-7}$	$7.1 * 10^{-7}$
(1-S)	d-Li	(0,0,0)	$1.1 * 10^{-5}$		$9.8 * 10^{-6}$	
		(4,0,0)	$1.7 * 10^{-6}$		$1.5 * 10^{-6}$	
	$t - H_2O$	(0,0,0)	$6.8 * 10^{-6}$	$4.9 * 10^{-6}$	$5.2 * 10^{-6}$	$5.0 * 10^{-6}$
		(4,0,0)	$8.8 * 10^{-7}$	$6.7 * 10^{-7}$	$7.1 * 10^{-7}$	$6.9 * 10^{-7}$
(2-S)	d-Li	(8,0,0)	$2.6 * 10^{-6}$		$2.2 * 10^{-6}$	
		(14,0,0)	$3.0 * 10^{-6}$		$2.7 * 10^{-6}$	
		(8,8,0)	$1.4 * 10^{-5}$		$1.2 * 10^{-5}$	
	$t - H_2O$	(8,0,0)	$1.4 * 10^{-6}$	$1.1 * 10^{-6}$	$1.1 * 10^{-6}$	$1.1 * 10^{-6}$
		(14,0,0)	$1.5 * 10^{-6}$	$1.1 * 10^{-6}$	$1.2 * 10^{-6}$	$1.2 * 10^{-6}$
		(8,8,0)	$7.0 * 10^{-6}$	$5.1 * 10^{-6}$	$5.3 * 10^{-6}$	$5.1 * 10^{-6}$

Table 10: Displacement rates in DPA/sec.

Material			Fe	Co	Ni	Cu
DEMO 1st Wall			$6.6 * 10^{-7}$	$7.8 * 10^{-7}$	$7.1 * 10^{-7}$	$6.6 * 10^{-7}$
(1-S)	d-Li	(0,0,0)	$9.5 * 10^{-6}$		$1.0 * 10^{-5}$	$9.5 * 10^{-6}$
		(4,0,0)	$1.5 * 10^{-6}$		$1.6 * 10^{-6}$	$1.5 * 10^{-6}$
	$t - H_2O$	(0,0,0)	$4.8 * 10^{-6}$	$4.6 * 10^{-6}$	$5.0 * 10^{-6}$	$4.5 * 10^{-6}$
		(4,0,0)	$7.1 * 10^{-7}$	$6.8 * 10^{-7}$	$7.8 * 10^{-7}$	$7.1 * 10^{-7}$
(2-S)	d-Li	(8,0,0)	$2.2 * 10^{-6}$		$2.3 * 10^{-6}$	$2.2 * 10^{-6}$
		(14,0,0)	$2.7 * 10^{-6}$		$2.9 * 10^{-6}$	$2.8 * 10^{-6}$
		(8,8,0)	$1.2 * 10^{-5}$		$1.2 * 10^{-5}$	$1.1 * 10^{-5}$
	$t - H_2O$	(8,0,0)	$1.1 * 10^{-6}$	$1.0 * 10^{-6}$	$1.2 * 10^{-6}$	$1.1 * 10^{-6}$
		(14,0,0)	$1.2 * 10^{-6}$	$1.1 * 10^{-6}$	$1.3 * 10^{-6}$	$1.2 * 10^{-6}$
		(8,8,0)	$4.9 * 10^{-6}$	$4.7 * 10^{-6}$	$5.1 * 10^{-6}$	$4.7 * 10^{-6}$

Table 11: Displacement rates in DPA/sec

Material			^{6}Li	^{9}Be	^{10}B	^{11}B
DEMO 1st Wall			$3.6 * 10^{-2}$	$8.1 * 10^{-2}$	$7.9 * 10^{-3}$	1.20
(1-S)	d-Li	(0,0,0)				
		(4,0,0)				
	$t - H_2O$	(0,0,0)	$3.1 * 10^{-1}$	$2.2 * 10^{-2}$	$5.9 * 10^{-2}$	$7.9 * 10^{-2}$
		(4,0,0)	2.31	$4.1 * 10^{-2}$	4.12	$3.8 * 10^{-1}$
(2-S)	d-Li	(8,0,0)				
		(14,0,0)				
		(8,8,0)				
	$t - H_2O$	(8,0,0)	$9.8 * 10^{-1}$	$3.0 * 10^{-2}$	1.73	$1.7 * 10^{-1}$
		(14,0,0)	$5.1 * 10^{-1}$	$4.3 * 10^{-2}$	3.90	$3.6 * 10^{-1}$
		(8,8,0)	$2.4 * 10^{-1}$	$2.2 * 10^{-2}$	$4.9 * 10^{-1}$	$8.0 * 10^{-2}$

Table 12: H-Gas to DPA ratios in $APPM_H/DPA$

Material			^{12}C	^{14}N	^{19}F	^{27}Al
DEMO 1st Wall			$1.0 * 10^{-1}$	722.22	25.40	43.04
(1-S)	d-Li	(0,0,0)	4.06			
		(4,0,0)	7.22			
	$t - H_2O$	(0,0,0)	$1.4 * 10^{-1}$	130.77	9.15	16.39
		(4,0,0)	$2.1 * 10^{-1}$	153.57	30.0	40.79
(2-S)	d-Li	(8,0,0)	1.28			
		(14,0,0)	1.53			
		(8,8,0)	$9.1 * 10^{-1}$			
	$t - H_2O$	(8,0,0)	$1.7 * 10^{-1}$	134.04	20.0	30.83
		(14,0,0)	$2.2 * 10^{-1}$	153.19	28.57	40.0
		(8,8,0)	$1.3 * 10^{-1}$	148.15	9.58	17.46

Table 13: H-Gas to DPA ratios in $APPM_H/DPA$

Material			^{28}Si	Ti	V	Mn
DEMO 1st Wall			60.67	29.67	18.31	12.25
(1-S)	d-Li	(0,0,0)	73.51		18.64	
		(4,0,0)	95.56		25.61	
	t – H_2O	(0,0,0)	30.88	10.82	4.62	4.93
		(4,0,0)	65.91	23.88	15.49	11.45
(2-S)	d-Li	(8,0,0)	80.77		21.33	
		(14,0,0)	95.39		25.37	
		(8,8,0)	66.61		16.67	
	t – H_2O	(8,0,0)	51.43	17.27	10.91	8.45
		(14,0,0)	64.0	23.64	15.33	10.83
		(8,8,0)	31.43	11.18	5.47	5.29

Table 14: H-Gas to DPA ratios in $APPM_H/DPA$

Material			Fe	Co	Ni	Cu
DEMO 1st Wall			37.70	20.51	169.01	53.03
(1-S)	d-Li	(0,0,0)	44.31		194.56	50.50
		(4,0,0)	54.22		213.19	58.68
	t – H_2O	(0,0,0)	20.96	8.04	147.14	31.11
		(4,0,0)	36.80	17.65	179.49	52.11
(2-S)	d-Li	(8,0,0)	48.45		202.26	54.54
		(14,0,0)	53.96		212.66	58.41
		(8,8,0)	40.96		191.67	48.22
	t – H_2O	(8,0,0)	30.21	13.86	162.83	41.82
		(14,0,0)	36.67	18.18	176.92	51.67
		(8,8,0)	21.59	8.44	146.65	31.26

Table 15: H-Gas to DPA ratios in $APPM_H/DPA$

Material			^{6}Li	^{9}Be	^{10}B	^{11}B
DEMO 1st Wall			492.82	1095.24	351.57	13.33
(1-S)	d-Li	(0,0,0)				
		(4,0,0)				
	t – H_2O	(0,0,0)	620.0	1642.85	341.92	2.89
		(4,0,0)	521.79	2769.23	357.06	17.37
(2-S)	d-Li	(8,0,0)				
		(14,0,0)				
		(8,8,0)				
	t – H_2O	(8,0,0)	632.08	2434.78	348.27	9.71
		(14,0,0)	602.50	2772.72	355.93	16.36
		(8,8,0)	138.27	1685.71	352.47	3.57

Table 16: He-Gas to DPA ratios in $APPM_{He}/DPA$

Material			^{12}C	^{14}N	^{19}F	^{27}Al
DEMO 1st Wall			379.31	123.89	152.38	21.52
(1-S)	d-Li	(0,0,0)	448.21			
		(4,0,0)	925.78			
	t – H_2O	(0,0,0)	91.60	184.62	131.91	8.03
		(4,0,0)	442.11	189.29	307.0	24.76
(2-S)	d-Li	(8,0,0)	692.81			
		(14,0,0)	916.94			
		(8,8,0)	457.14			
	t – H_2O	(8,0,0)	263.82	193.62	235.29	17.81
		(14,0,0)	437.50	189.36	309.52	23.85
		(8,8,0)	104.76	177.18	133.33	8.73

Table 17: He-Gas to DPA ratios in $APPM_{He}/DPA$

Material			^{28}Si	Ti	V	Mn
DEMO 1st Wall			28.09	6.78	4.08	6.70
(1-S)	d-Li	(0,0,0)	36.32		5.69	
		(4,0,0)	46.34		8.23	
	$t - H_2O$	(0,0,0)	16.18	2.16	$6.5 * 10^{-1}$	2.02
		(4,0,0)	37.0	4.84	2.25	5.94
(2-S)	d-Li	(8,0,0)	38.46		6.67	
		(14,0,0)	46.67		8.15	
		(8,8,0)	33.57		4.92	
	$t - H_2O$	(8,0,0)	28.71	3.45	1.45	4.09
		(14,0,0)	36.24	4.91	2.17	5.63
		(8,8,0)	16.86	2.24	$7.4 * 10^{-1}$	2.22

Table 18: He-Gas to DPA ratios in $APPM_{He}/DPA$

Material			Fe	Co	Ni	Cu
DEMO 1st Wall			9.25	5.26	32.39	10.15
(1-S)	d-Li	(0,0,0)	11.04		34.89	12.74
		(4,0,0)	14.30		39.81	16.19
	$t - H_2O$	(0,0,0)	3.47	2.09	22.54	3.78
		(4,0,0)	8.37	5.59	37.18	9.15
(2-S)	d-Li	(8,0,0)	12.27		37.39	14.55
		(14,0,0)	14.07		39.66	16.10
		(8,8,0)	9.97		34.17	11.48
	$t - H_2O$	(8,0,0)	6.25	4.20	31.67	6.68
		(14,0,0)	8.33	5.73	37.69	9.17
		(8,8,0)	3.75	2.34	23.53	4.13

Table 19: He-Gas to DPA ratios in $APPM_{He}/DPA$

	t – H_2O (1-S)		d-Li (1-S)	
	(0,0,0)	(4,0,0)	(0,0,0)	(4,0,0)
$\frac{DPA/sec}{DPA/sec_{DEMO}}$	7.2	1.8	13.8	2.1
$\frac{APPM_H/sec}{APPM_H/sec_{DEMO}}$	1.9	0.9	16.6	3.4
$\frac{APPM_{He}/sec}{APPM_{He}/sec_{DEMO}}$	2.7	1.0	19.4	3.9
$\frac{APPM_H/DPA}{APPM_H/DPA_{DEMO}}$	0.3	0.5	1.2	1.6
$\frac{APPM_{He}/DPA}{APPM_{He}/DPA_{DEMO}}$	0.4	0.6	1.4	1.9

Table 20: Overview of the (1-S) case about the damage parameters for the isotopes starting at carbon normalized to the damage of the DEMO 1st wall spectrum.

	t – H_2O (2-S)			d-Li (2-S)		
	(8,0,0)	(14,0,0)	(8,8,0)	(8,0,0)	(14,0,0)	(8,8,0)
$\frac{DPA/sec}{DPA/sec_{DEMO}}$	1.5	1.7	7.4	3.2	3.8	16.8
$\frac{APPM_H/sec}{APPM_H/sec_{DEMO}}$	1.0	1.5	2.3	4.6	6.1	21.1
$\frac{APPM_{He}/sec}{APPM_{He}/sec_{DEMO}}$	1.1	1.6	3.0	5.3	7.0	24.7
$\frac{APPM_H/DPA}{APPM_H/DPA_{DEMO}}$	0.7	0.9	0.3	1.4	1.6	1.3
$\frac{APPM_{He}/DPA}{APPM_{He}/DPA_{DEMO}}$	0.7	0.9	0.4	1.7	1.8	1.5

Table 21: Overview of the (2-S) case about the damage parameters for the isotopes starting at carbon normalized to the damage of the DEMO 1st wall spectrum.

$APPM_{He}$/DPA - Comparison: INS/Greenwood/Doran									
	DEMO			d-Li (0,0,0)			t – H_2O (0,0,0)		
C	379	290	240	448	625	522	92	84	97
Si	28	27	17	36	33	19	16	16	6
V	4	3	4	6	5	8	0.7	1	0.7
Fe	9	8.7	9	11	9.5	12	3.5	3.4	4
Ni	32	31		35	35		23	23	
Cu	10	5.1		13	7.5		4	2.8	
W		0.9	3.3		5	14		0.2	0.7

Table 22: Comparison of the $APPM_{He}$/DPA values of DEMO and (1-S) spectrum at (0,0,0) for INS, Greenwood and Doran. The values are listed in the 1. , 2. and 3. column, respectively, at each spectrum.

$APPM_{He}$/DPA - Comparison: INS/Greenwood/Doran									
	DEMO			d-Li (4,0,0)			t – H_2O (4,0,0)		
C	379	290	240	926	1039	924	442	421	454
Si	28	27	17	46	43	27	37	36	19
V	4	3	4	8	6	12	2.3	1.8	2.6
Fe	9	8.7	9	14	12	15	8	8.1	9
Ni	32	31		40	40		37	38	
Cu	10	5.1		16	9.5		9	6.6	
W		0.9	3.3		6.3	20		0.3	1.7

Table 23: Comparison of the $APPM_{He}$/DPA values of DEMO and (1-S) spectrum at (4,0,0) for INS, Greenwood and Doran. The values are listed in the 1. , 2. and 3. column, respectively, at each spectrum.

Figure 18: In this figure the DPA-rates in DPA/sec versus the different isotopes are plottet. Parameters are the different neutron spectra used.

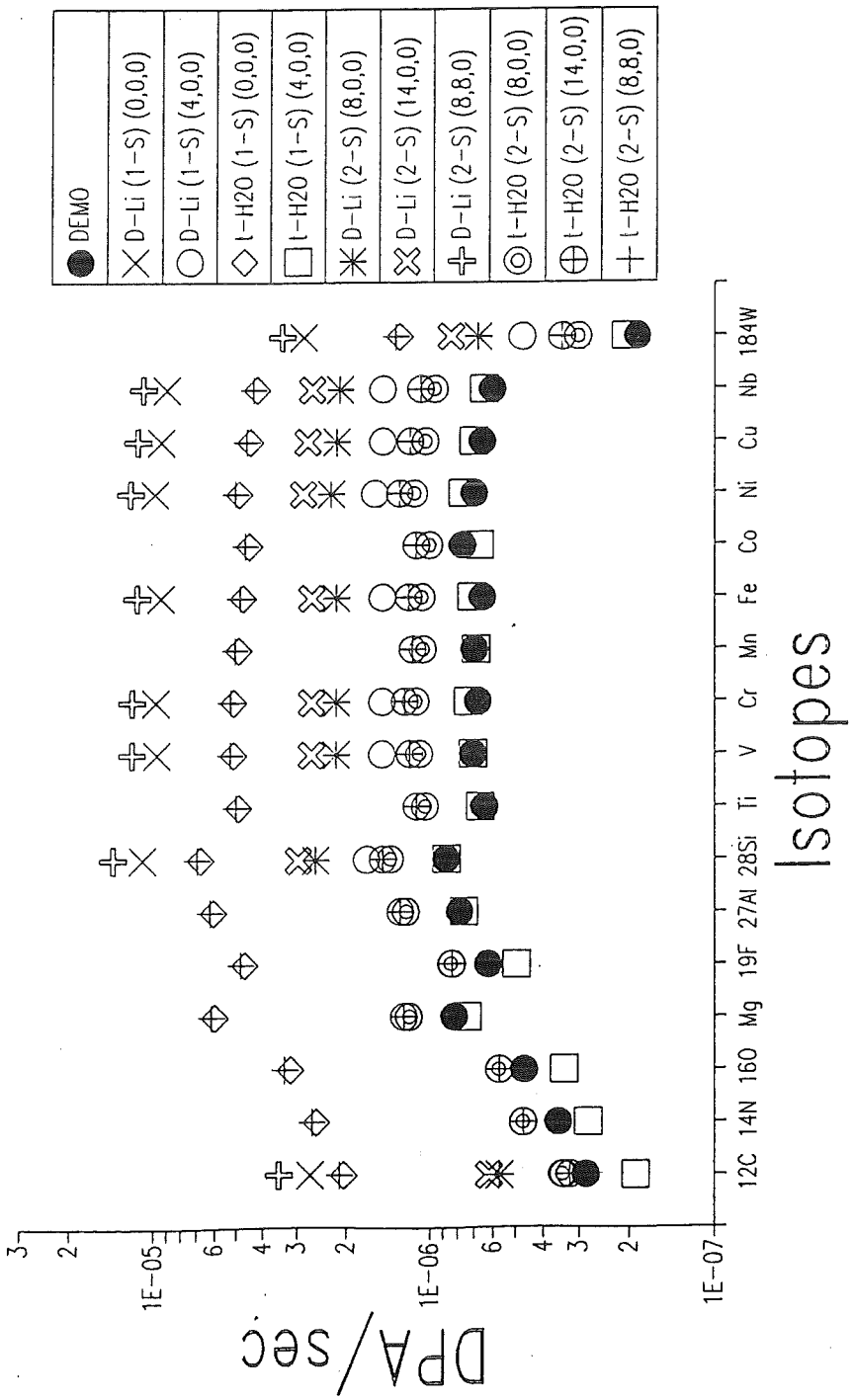

Figure 20: In this figure the helium-rates in $APPM_{He}$/sec versus the different isotopes are plottet. Parameters are the different neutron spectra used.

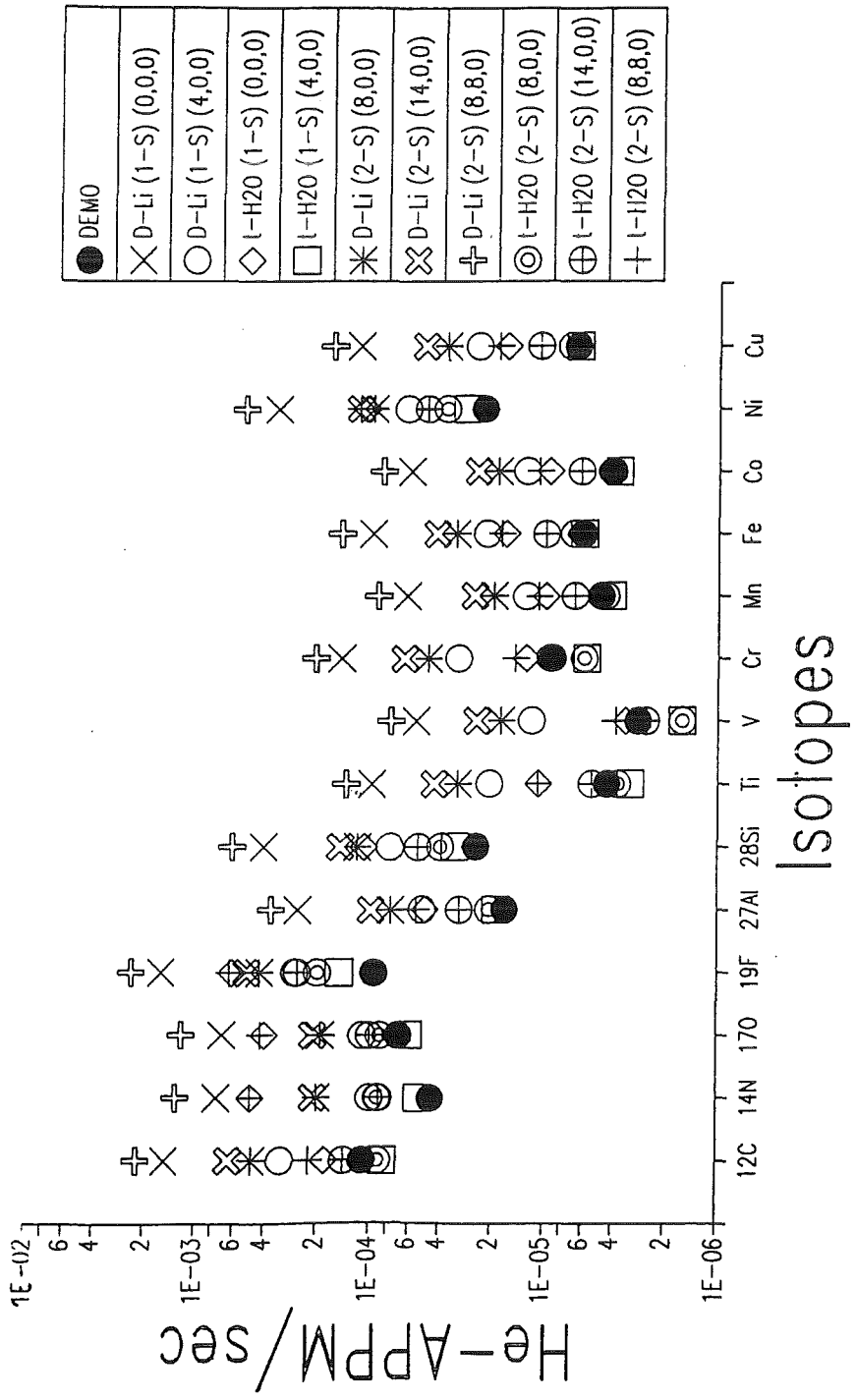

Figure 19: In this figure the hydrogen-rates in $APPM_H$/sec versus the different isotopes are plottet. Parameters are the different neutron spectra used.

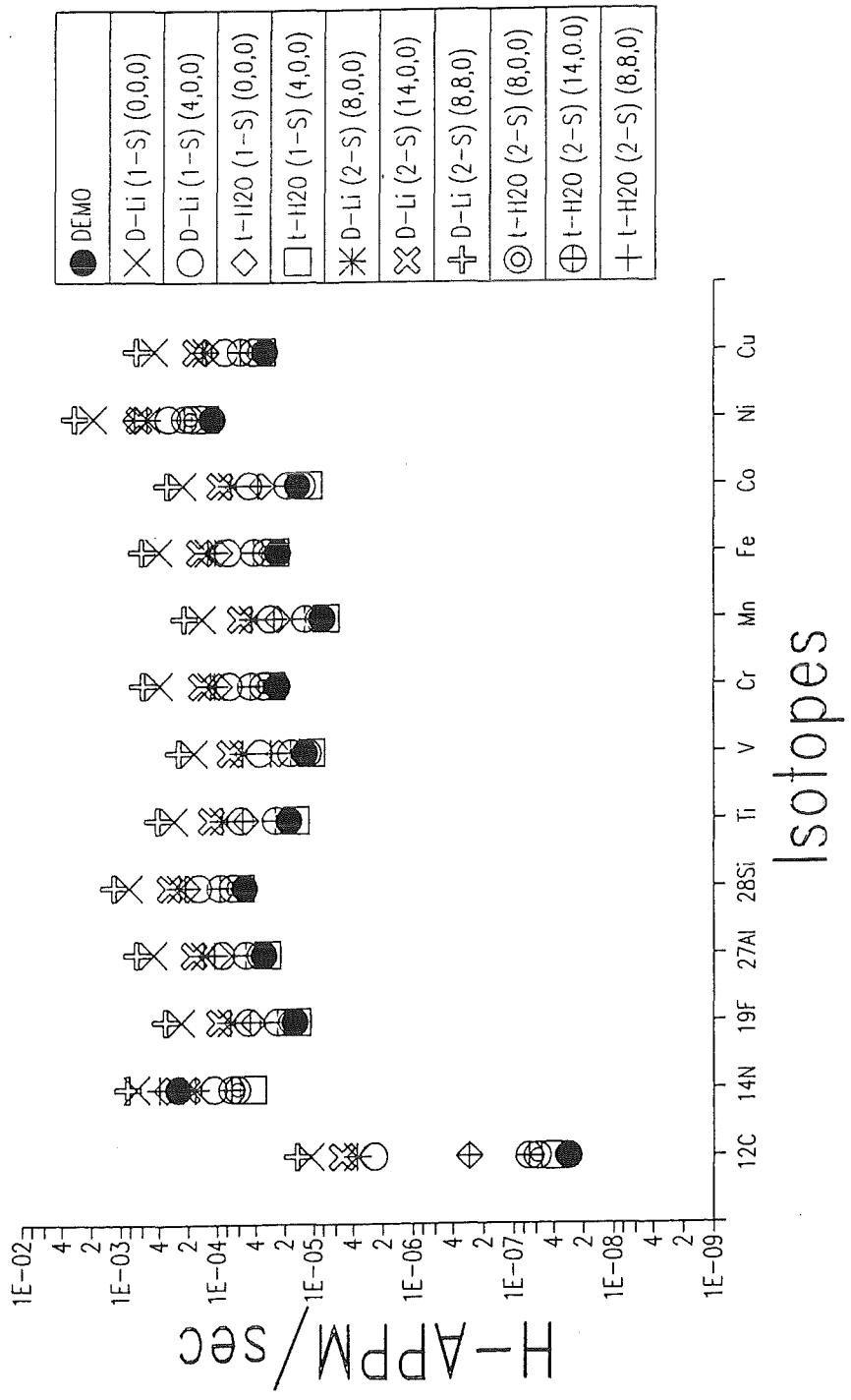

Figure 21: In this figure the hydrogen to DPA ratios in $APPM_H/DPA$ versus the different isotopes are plottet. Parameters are the different neutron spectra used.

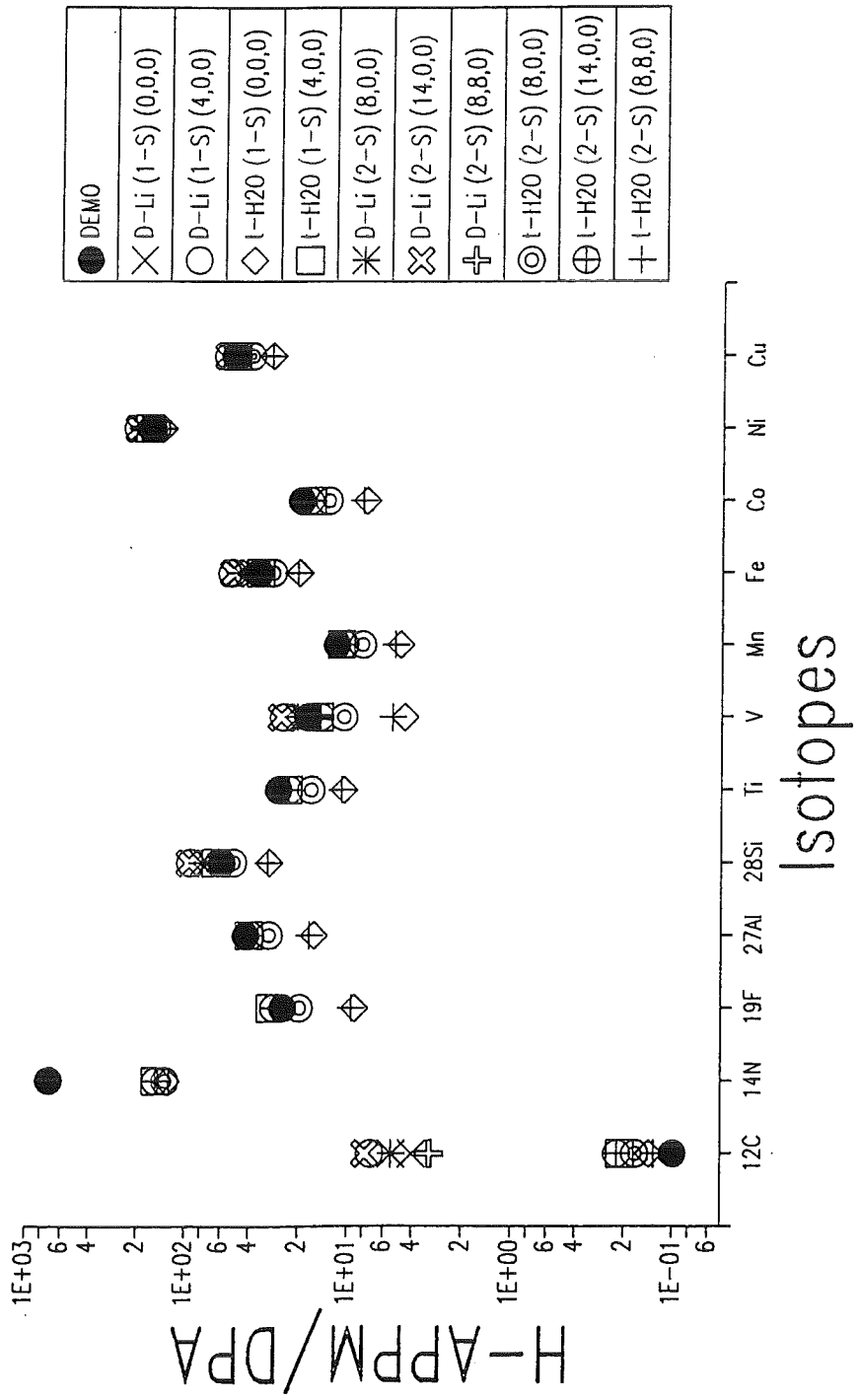

Figure 22: In this figure the helium to DPA ratios in $APPM_{He}/DPA$ versus the different isotopes are plottet. Parameters are the different neutron spectra used.

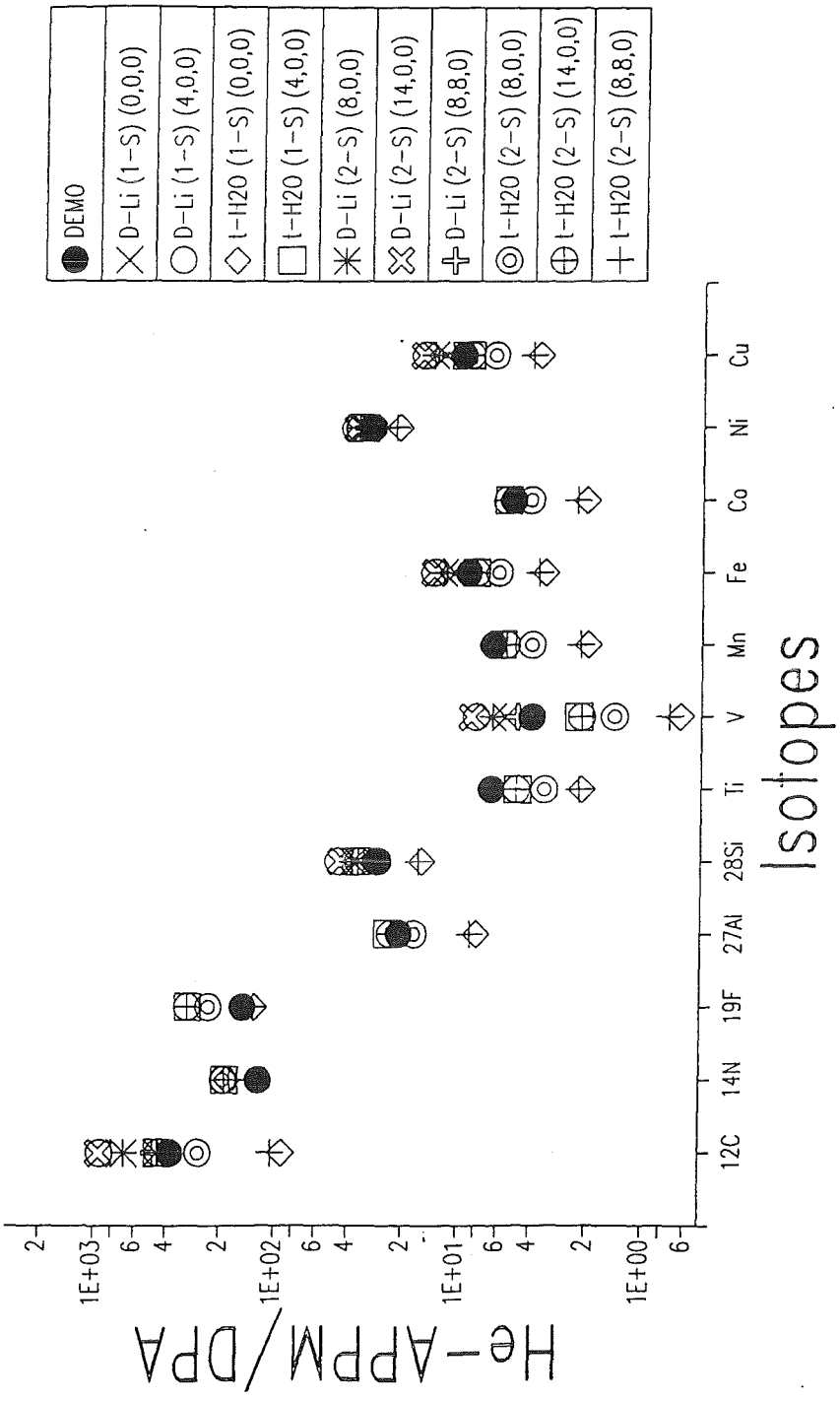

Figure 23: Comparison of the weekly DPA and helium production rates in iron for various irradiation facillities. The line marked fusion assumes 1 -10 MW/m^2 wall loading. The fusion bullet marks the DEMO 1st wall spectrum, which is equal to 2.5 MW/m^2 wall loading. The other bullets marking the t – H_2O and d-Li source with its one (1-S) and two source (2-S) case.

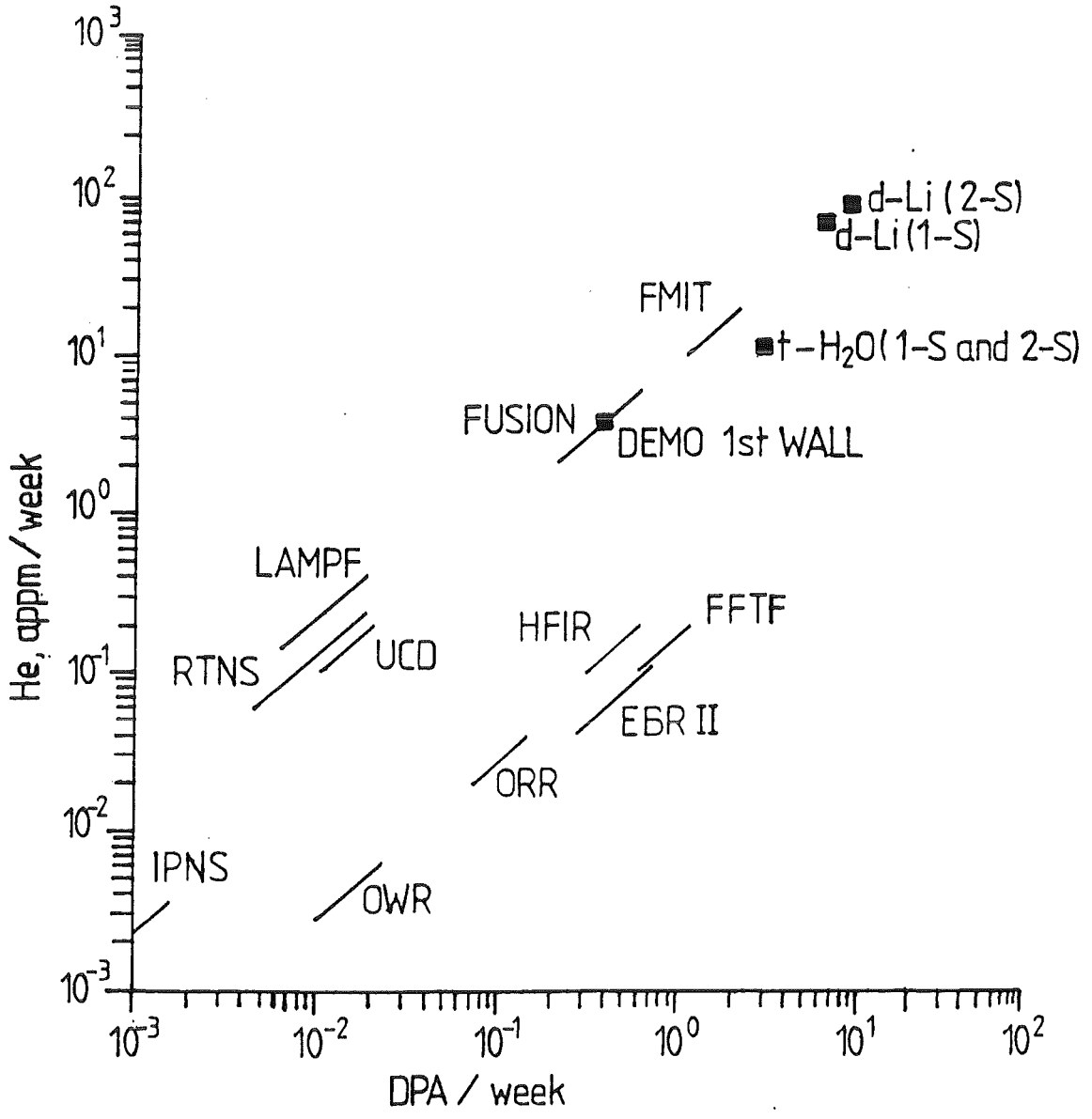

Looking on the tables 8 - 19, it is possible to get a feeling, how the several spectra and the different isotopes produce DPA's and H-, He-gas. Plotting the production rates like figure 18 (DPA/sec), figure 19 ($APPM_H$/sec) and figure 20 ($APPM_{He}$/sec), one can see, that the data points for a choosen neutron spectrum (e.g. DEMO) have a similar behaviour like the data points of the other neutron spectra. That means, that for isotopes, starting at carbon, basically a linear factor is the difference. This factors, normalized to the DEMO-spectrum, is given for the (1-S) case of d-Li and $t-H_2O$ in table 20. For the (2-S) cases, the results are listed in table 21. In the (1-S) and (2-S) case for the $t-H_2O$ source, the DPA, H- and He-production is always higher or equal to the DEMO-spectrum, but the ratios gas to DPA, normalized to the DEMO gas to DPA ratio, are always less than 1, which is also listed in the tables 20 and 21. This is caused by a relatively low gas-production rate. This low gas-production rate can be understood, looking on the gas production cross section data [20], which show a negative Q-value for the nuclear reactions of about 3 - 5 MeV. Therefore a big part of the $t-H_2O$ neutron spectrum producing DPA gives no contribution to the gas production. This is also true for the DEMO spectrum, but for the DEMO spectrum shows a very high peak in the neutron spectrum at 14 MeV neutron energy, which leads in DEMO case to a somewhat higher gas production rate than for the $t-H_2O$ case. For the d-Li neutron spectrum, the situation is different, because this spectra have neutrons up to 50 Mev neutron energy. Therefore, the effect of the Q-value at the gas production cross sections is unimportant and negligible. The gas to DPA ratios, normalized to the DEMO gas to DPA ratios, tables 20 and 21 and figures 21 and 22, are significantly higher than for the $t-H_2O$ ratios and they are always larger than 1. A further comparison of gas to DPA ratios between data of INS, Greenwood and Doran [27], shows a basic agreement of the data. The results are listed in tables 22 and 23. A final comparison of the He-gas production versus the DPA-production, see figure 23, of the INS neutron sources, the DEMO 1st wall and other neutron irradiation facillities [7, 28], gives an overview about the performance of the high energy high intensity neutron sources. As a reference point the DEMO 1st wall symbol (2.5 MW/m^2 wall loading) can be used. The $t-H_2O$ source is for a maximum neutron flux position which regard to the DPA production one order of magnitude larger than DEMO; and with respect to the He-gas production a factor 3-4 larger than DEMO. In contrast to the $t-H_2O$ source the d-Li source is in DPA- and He-production more than one order of magnitude larger than DEMO.

7 Conclusion

With the INS-code, a tool for characterizing neutron sources based on the d-Li or $t-H_2O$ concept is developed. It is the first time that a complete treatment of the $t-H_2O$ neutron source is presented. Two neutron-generating reactions are included, the H(t,n) fraction and the O(t,xn) fraction; which is one order of magnitude lower in neutron production yield than the H(t,n) fraction. With this data and the d-Li neutron production cross sections, two source concepts, the (1-S) and (2-S) case, are designed.

An important point is the comparison of the neutron flux spectra with the fusion conditions. This yields to result, that the $t-H_2O$ neutron flux spectra fit much better with the DEMO 1st wall spectrum than the d-Li neutron flux spectra. The fraction of neutrons with energy > 14 MeV is by more than a factor of 10 lower for the $t-H_2O$ source than for the d-Li source. The maximum fraction of high energetic neutrons (E>14 MeV) at the d-Li source is about 1/3 of the total neutron flux.

The neutron flux in the interesting energy region 0 - 14 MeV is in general a factor of 2 lower for the $t-H_2O$ source when compared with the d-Li source. This factor of 2 is also valid for the flux volumes. With a flux $\phi > 10^{14} \frac{n}{s\ cm^2}$ the $t-H_2O$ source provides a usable flux volume of 0.2 liter (1-S) and 2.5 liter (2-S). The dependence of the achievable irradiation volumes from type (single beam or dual beam configuration) and beam current can be described by the expressions $V = 5.7 * 10^{22} * \phi^{-1.46}$ (1-S) and $V \sim I^{1.47}$ (1-S). For the (2-S) case there are very little different exponents, dependent on the target ant test cell geometry.

A comparison of the (1-S) and the (2-S) case of the $t-H_2O$ concept shows for $\phi > 10^{14} \frac{n}{s\ cm^2}$ an advantage in the flux volume for the (1-S) case.

Regarding the damage and transmutation calculations the $t-H_2O$ concept has a disadvantage in the production rates against the d-Li concept. But the higher producting rates of the d-Li are caused by the high energy tail in the neutron flux spectra together with the linear extrapolation to energies > 20 MeV of the related damage and transmutation cross sections. This is also the reason for the lower gas production rate in the $t-H_2O$ source, which leads to GAS/DPA ratios < 1, normalized to the DEMO 1st wall GAS/DPA ratio. For the d-Li case, this ratios are always bigger than 1 and a factor 2-4 bigger than for the $t-H_2O$ case. A general comparison of the damage and gas production data for important elements show a consistency with recent data from Doran and Greenwood.

8 Recommendation

It is recommended to do further investigations in the field of evaluation of accelerator based intense neutron sources. A main point in the futur will be, to know how the spectral neutron flux behave in a not empty test cell, e.g. filled up with strucural materials. This task can be done by calculating the neutron flux distribution in the test cell of the $t - H_2O$ or d-Li neutron source with a neutron transport code, e.g. MCNP. This leads to information about the moderation and thermalisation of the known neutron flux distribution in an empty test cell (uncollided). Furthermore the values for damage and element transmutation (gas production) of the collided neutron spectra are of importance. This step will lead to a more realistic picture about the possibilities to irradiate materials in the test cell of accelarator based intense neutron sources.

9 Acknowledgement

The author would like to thank Dr. Y. Hino [3], for many suggestions about running the early programs, which are the roots of the INS code, Dr. M. Drosg [4], for preparing the $t - H_2O$ neutron yield data, and S. Kelzenberg [5], for doing some code development.

[3] Electrotechnical Laboratory, 114 Umezono, Ibaraki, Japan

[4] Institute of Experimental Physics, University of Vienna, Austria

[5] KfK Karlsruhe, Institute of Material Research I, Germany

A Appendix

A.1 Comparative plots of neutron flux spectra (1-S)

Coordinates (cm)			Total flux (n/s/cm^2)		Fraction r (%)	
X	Y	Z	t-H	d-Li	t-H	d-li
0	0	0	$4.09 * 10^{15}$	$5.25 * 10^{15}$	0.9	19.1
2	0	0	$9.39 * 10^{14}$	$1.41 * 10^{14}$	2.1	31.3
4	0	0	$3.84 * 10^{14}$	$6.57 * 10^{14}$	3.2	34.7
6	0	0	$2.00 * 10^{14}$	$3.82 * 10^{14}$	4.1	36.0
8	0	0	$1.21 * 10^{14}$	$2.49 * 10^{14}$	4.9	36.8
10	0	0	$8.01 * 10^{13}$	$1.74 * 10^{14}$	5.4	37.3
12	0	0	$5.70 * 10^{13}$	$1.28 * 10^{14}$	5.8	37.5
14	0	0	$4.25 * 10^{13}$	$9.89 * 10^{13}$	6.0	37.6
0	2	0	$3.31 * 10^{14}$	$8.56 * 10^{14}$	1.0	8.8
2	2	0	$3.46 * 10^{14}$	$5.09 * 10^{14}$	1.0	21.7
4	2	0	$2.06 * 10^{14}$	$3.16 * 10^{14}$	1.4	27.6
6	2	0	$1.34 * 10^{14}$	$2.14 * 10^{14}$	1.9	31.0
8	2	0	$9.24 * 10^{13}$	$1.53 * 10^{14}$	2.4	33.0
10	2	0	$6.63 * 10^{13}$	$1.17 * 10^{14}$	3.0	34.2
12	2	0	$4.95 * 10^{13}$	$9.13 * 10^{13}$	3.5	35.0
0	4	0	$4.87 * 10^{13}$	$1.22 * 10^{14}$	1.0	6.4
2	4	0	$7.43 * 10^{13}$	$1.20 * 10^{14}$	0.7	9.8
4	4	0	$6.24 * 10^{13}$	$1.07 * 10^{14}$	1.0	14.7
6	4	0	$5.43 * 10^{13}$	$8.84 * 10^{13}$	0.9	19.8
8	4	0	$4.79 * 10^{13}$	$7.24 * 10^{13}$	1.0	23.9
10	4	0	$4.07 * 10^{13}$	$5.98 * 10^{13}$	1.0	26.9
2	6	0	$2.17 * 10^{13}$	$5.04 * 10^{13}$	0.9	7.6
4	6	0	$3.20 * 10^{13}$	$4.86 * 10^{13}$	0.6	10.3
0	0	1	$5.13 * 10^{14}$	$1.27 * 10^{15}$	1.0	8.6
2	0	1	$5.06 * 10^{14}$	$7.47 * 10^{14}$	1.0	23.2
4	0	1	$2.96 * 10^{14}$	$4.33 * 10^{14}$	1.3	30.4
6	0	1	$1.75 * 10^{14}$	$2.85 * 10^{14}$	2.0	33.3
8	0	1	$1.11 * 10^{14}$	$1.99 * 10^{14}$	3.3	35.0
10	0	1	$7.58 * 10^{13}$	$1.46 * 10^{14}$	4.3	36.2
12	0	1	$5.49 * 10^{13}$	$1.11 * 10^{14}$	5.0	36.9

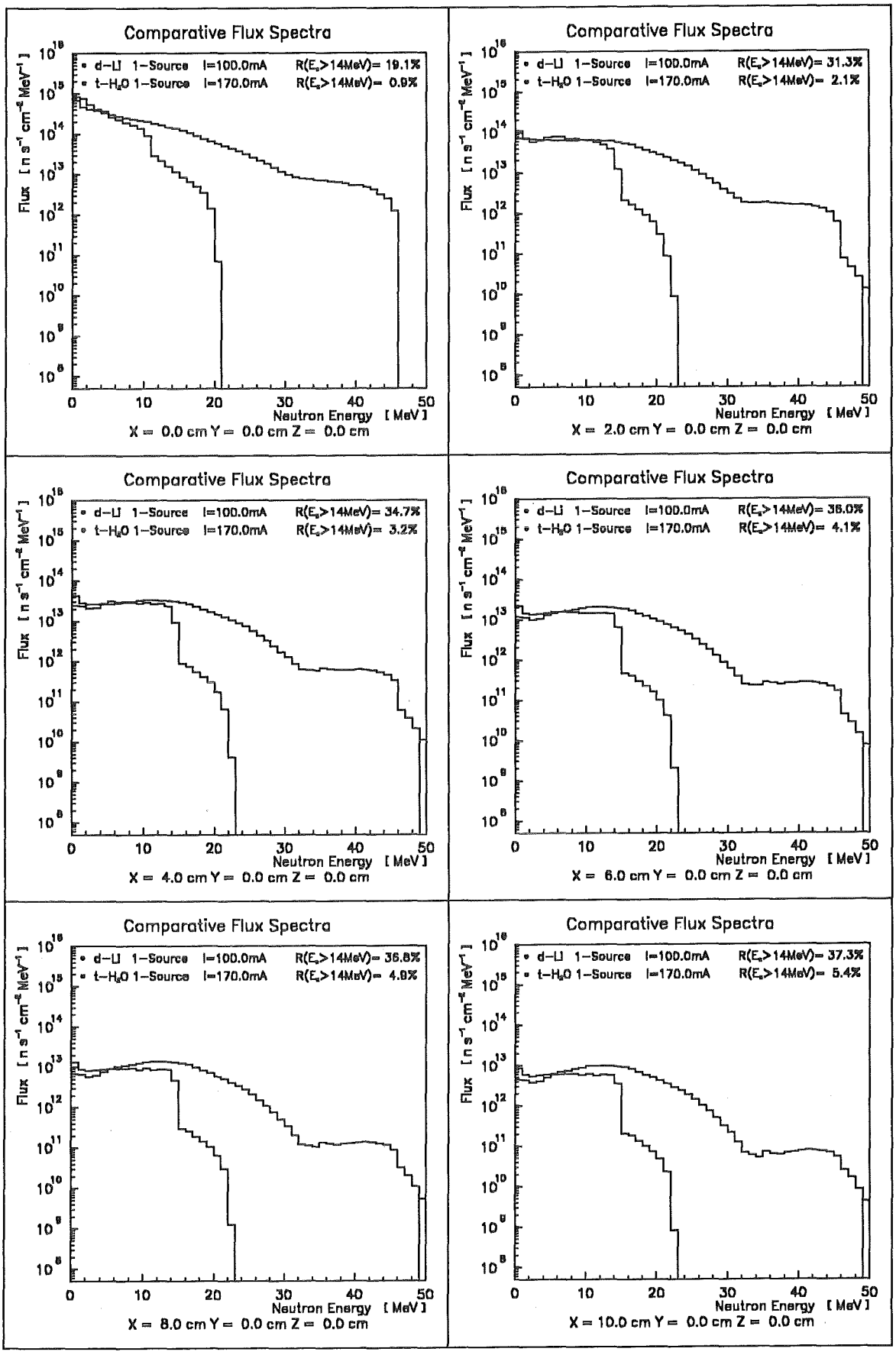
Comparative Flux Spectra
d-Li 1-Source I=100.0mA R(En>14MeV)= 19.1%
t-H2O 1-Source I=170.0mA R(En>14MeV)= 0.9%
Flux [n s-1 cm-2 MeV-1]
Neutron Energy [MeV]
X = 0.0 cm Y = 0.0 cm Z = 0.0 cm
Comparative Flux Spectra
d-Li 1-Source I=100.0mA R(En>14MeV)= 31.3%
t-H2O 1-Source I=170.0mA R(En>14MeV)= 2.1%
Flux [n s-1 cm-2 MeV-1]
Neutron Energy [MeV]
X = 2.0 cm Y = 0.0 cm Z = 0.0 cm
Comparative Flux Spectra
d-Li 1-Source I=100.0mA R(En>14MeV)= 34.7%
t-H2O 1-Source I=170.0mA R(En>14MeV)= 3.2%
Flux [n s-1 cm-2 MeV-1]
Neutron Energy [MeV]
X = 4.0 cm Y = 0.0 cm Z = 0.0 cm
Comparative Flux Spectra
d-Li 1-Source I=100.0mA R(En>14MeV)= 36.0%
t-H2O 1-Source I=170.0mA R(En>14MeV)= 4.1%
Flux [n s-1 cm-2 MeV-1]
Neutron Energy [MeV]
X = 6.0 cm Y = 0.0 cm Z = 0.0 cm
Comparative Flux Spectra
d-Li 1-Source I=100.0mA R(En>14MeV)= 36.8%
t-H2O 1-Source I=170.0mA R(En>14MeV)= 4.8%
Flux [n s-1 cm-2 MeV-1]
Neutron Energy [MeV]
X = 8.0 cm Y = 0.0 cm Z = 0.0 cm
Comparative Flux Spectra
d-Li 1-Source I=100.0mA R(En>14MeV)= 37.3%
t-H2O 1-Source I=170.0mA R(En>14MeV)= 5.4%
Flux [n s-1 cm-2 MeV-1]
Neutron Energy [MeV]
X = 10.0 cm Y = 0.0 cm Z = 0.0 cm

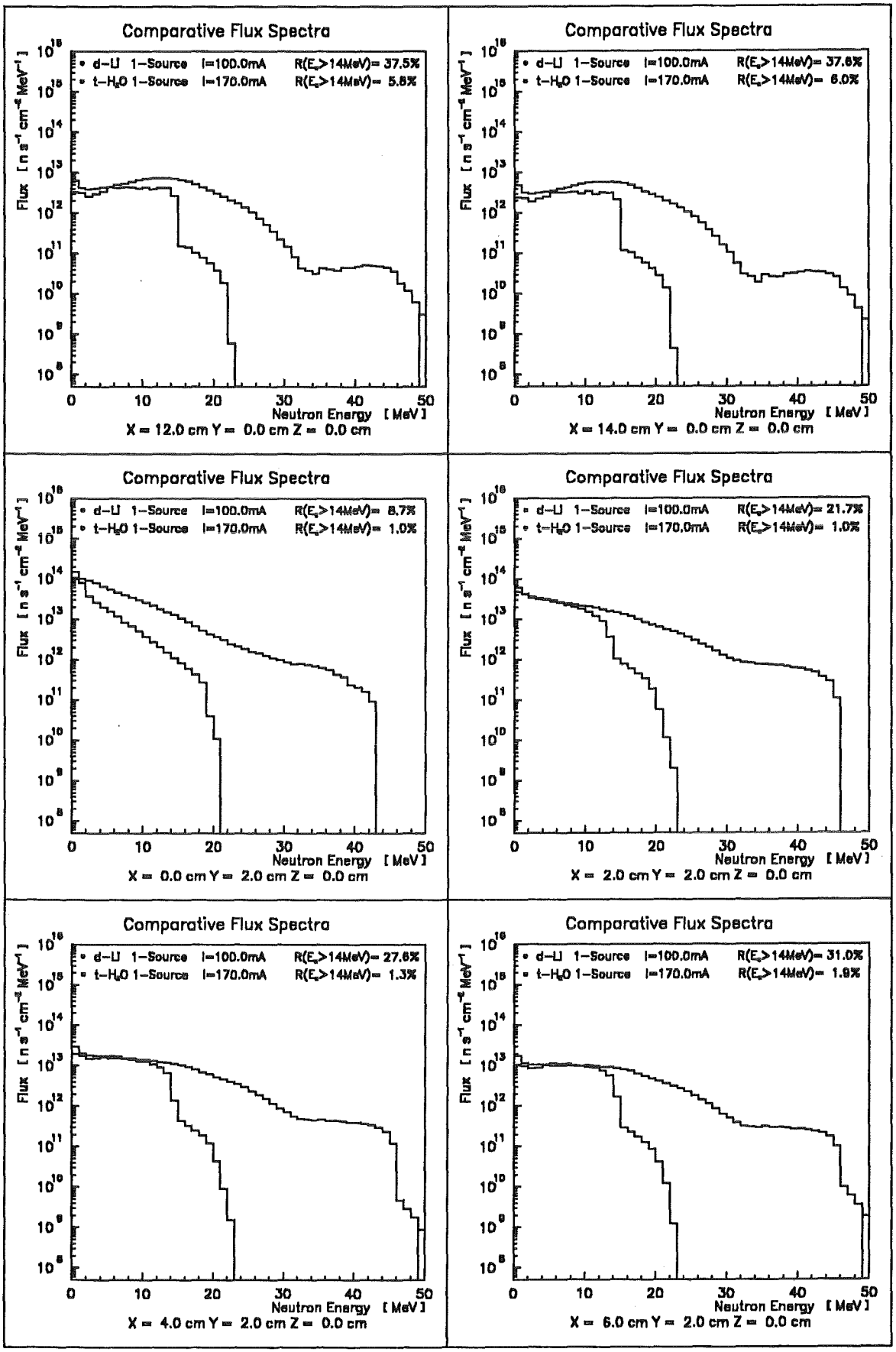
Comparative Flux Spectra
d-Li 1-Source I=100.0mA R(E>14MeV)= 37.5%
t-H2O 1-Source I=170.0mA R(E>14MeV)= 5.8%
Flux [n s-1 cm-2 MeV-1]
Neutron Energy [MeV]
X = 12.0 cm Y = 0.0 cm Z = 0.0 cm
Comparative Flux Spectra
d-Li 1-Source I=100.0mA R(E>14MeV)= 37.6%
t-H2O 1-Source I=170.0mA R(E>14MeV)= 6.0%
Flux [n s-1 cm-2 MeV-1]
Neutron Energy [MeV]
X = 14.0 cm Y = 0.0 cm Z = 0.0 cm
Comparative Flux Spectra
d-Li 1-Source I=100.0mA R(E>14MeV)= 8.7%
t-H2O 1-Source I=170.0mA R(E>14MeV)= 1.0%
Flux [n s-1 cm-2 MeV-1]
Neutron Energy [MeV]
X = 0.0 cm Y = 2.0 cm Z = 0.0 cm
Comparative Flux Spectra
d-Li 1-Source I=100.0mA R(E>14MeV)= 21.7%
t-H2O 1-Source I=170.0mA R(E>14MeV)= 1.0%
Flux [n s-1 cm-2 MeV-1]
Neutron Energy [MeV]
X = 2.0 cm Y = 2.0 cm Z = 0.0 cm
Comparative Flux Spectra
d-Li 1-Source I=100.0mA R(E>14MeV)= 27.6%
t-H2O 1-Source I=170.0mA R(E>14MeV)= 1.3%
Flux [n s-1 cm-2 MeV-1]
Neutron Energy [MeV]
X = 4.0 cm Y = 2.0 cm Z = 0.0 cm
Comparative Flux Spectra
d-Li 1-Source I=100.0mA R(E>14MeV)= 31.0%
t-H2O 1-Source I=170.0mA R(E>14MeV)= 1.9%
Flux [n s-1 cm-2 MeV-1]
Neutron Energy [MeV]
X = 6.0 cm Y = 2.0 cm Z = 0.0 cm

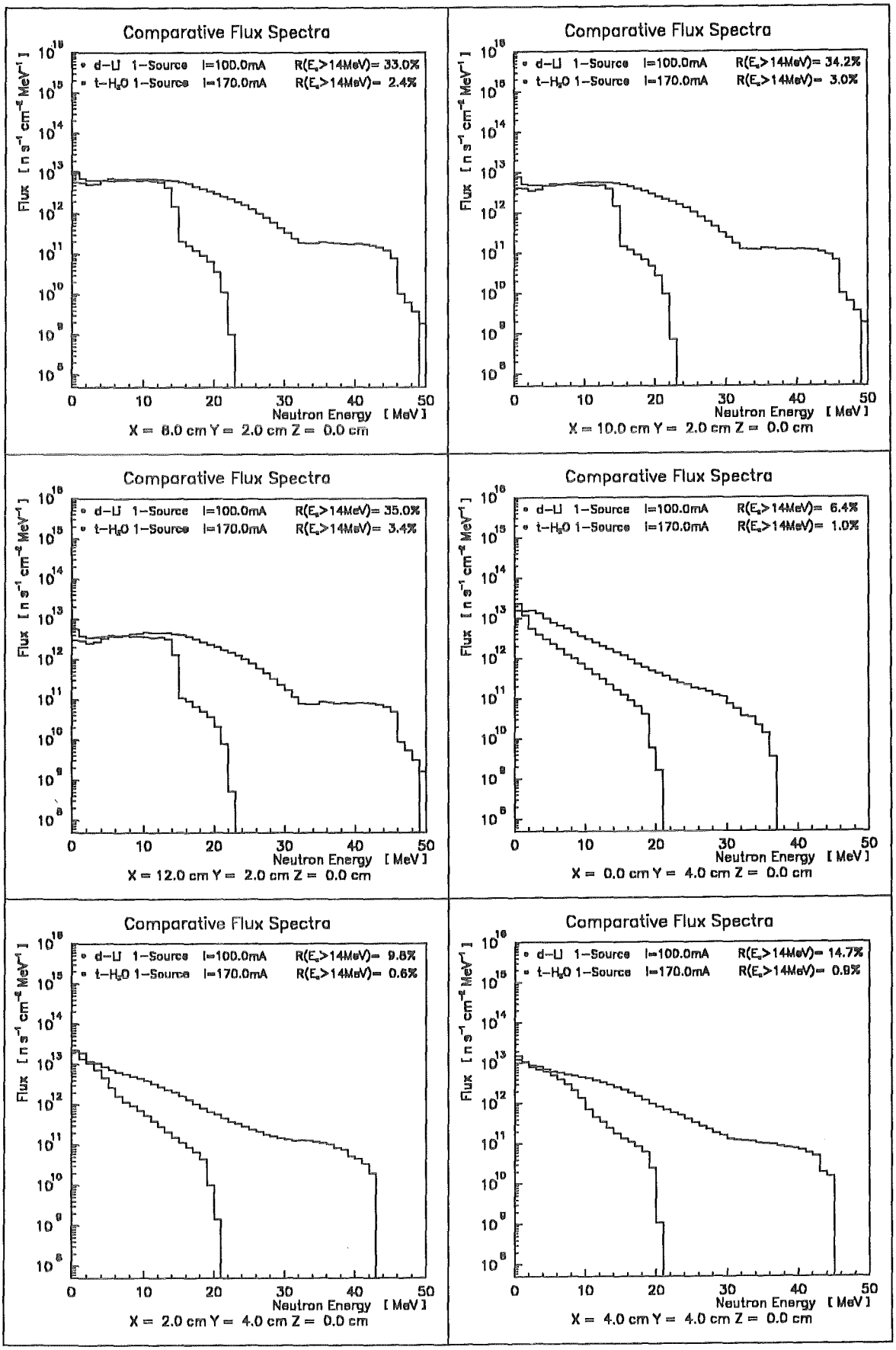
Comparative Flux Spectra
d-Li 1-Source I=100.0mA R(En>14MeV)= 33.0%
t-H2O 1-Source I=170.0mA R(En>14MeV)= 2.4%
Flux [n s-1 cm-2 MeV-1]
Neutron Energy [MeV]
X = 8.0 cm Y = 2.0 cm Z = 0.0 cm
Comparative Flux Spectra
d-Li 1-Source I=100.0mA R(En>14MeV)= 34.2%
t-H2O 1-Source I=170.0mA R(En>14MeV)= 3.0%
Flux [n s-1 cm-2 MeV-1]
Neutron Energy [MeV]
X = 10.0 cm Y = 2.0 cm Z = 0.0 cm
Comparative Flux Spectra
d-Li 1-Source I=100.0mA R(En>14MeV)= 35.0%
t-H2O 1-Source I=170.0mA R(En>14MeV)= 3.4%
Flux [n s-1 cm-2 MeV-1]
Neutron Energy [MeV]
X = 12.0 cm Y = 2.0 cm Z = 0.0 cm
Comparative Flux Spectra
d-Li 1-Source I=100.0mA R(En>14MeV)= 6.4%
t-H2O 1-Source I=170.0mA R(En>14MeV)= 1.0%
Flux [n s-1 cm-2 MeV-1]
Neutron Energy [MeV]
X = 0.0 cm Y = 4.0 cm Z = 0.0 cm
Comparative Flux Spectra
d-Li 1-Source I=100.0mA R(En>14MeV)= 9.8%
t-H2O 1-Source I=170.0mA R(En>14MeV)= 0.6%
Flux [n s-1 cm-2 MeV-1]
Neutron Energy [MeV]
X = 2.0 cm Y = 4.0 cm Z = 0.0 cm
Comparative Flux Spectra
d-Li 1-Source I=100.0mA R(En>14MeV)= 14.7%
t-H2O 1-Source I=170.0mA R(En>14MeV)= 0.9%
Flux [n s-1 cm-2 MeV-1]
Neutron Energy [MeV]
X = 4.0 cm Y = 4.0 cm Z = 0.0 cm

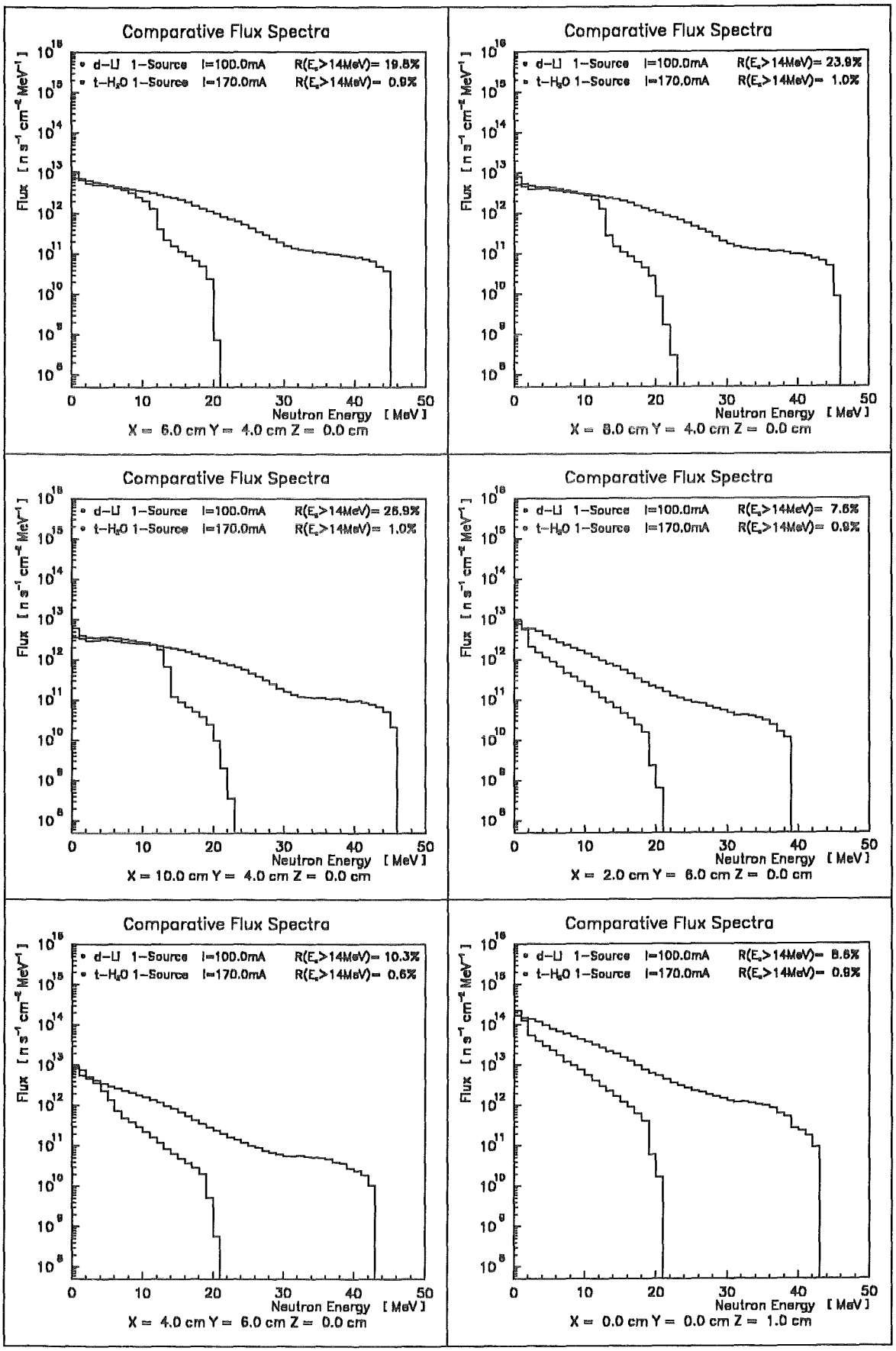
Comparative Flux Spectra
d-Li 1-Source I=100.0mA R(En>14MeV)= 19.8%
t-H2O 1-Source I=170.0mA R(En>14MeV)= 0.9%
Flux [n s-1 cm-2 MeV-1]
Neutron Energy [MeV]
X = 6.0 cm Y = 4.0 cm Z = 0.0 cm
Comparative Flux Spectra
d-Li 1-Source I=100.0mA R(En>14MeV)= 23.9%
t-H2O 1-Source I=170.0mA R(En>14MeV)= 1.0%
Flux [n s-1 cm-2 MeV-1]
Neutron Energy [MeV]
X = 8.0 cm Y = 4.0 cm Z = 0.0 cm
Comparative Flux Spectra
d-Li 1-Source I=100.0mA R(En>14MeV)= 26.9%
t-H2O 1-Source I=170.0mA R(En>14MeV)= 1.0%
Flux [n s-1 cm-2 MeV-1]
Neutron Energy [MeV]
X = 10.0 cm Y = 4.0 cm Z = 0.0 cm
Comparative Flux Spectra
d-Li 1-Source I=100.0mA R(En>14MeV)= 7.6%
t-H2O 1-Source I=170.0mA R(En>14MeV)= 0.9%
Flux [n s-1 cm-2 MeV-1]
Neutron Energy [MeV]
X = 2.0 cm Y = 6.0 cm Z = 0.0 cm
Comparative Flux Spectra
d-Li 1-Source I=100.0mA R(En>14MeV)= 10.3%
t-H2O 1-Source I=170.0mA R(En>14MeV)= 0.6%
Flux [n s-1 cm-2 MeV-1]
Neutron Energy [MeV]
X = 4.0 cm Y = 6.0 cm Z = 0.0 cm
Comparative Flux Spectra
d-Li 1-Source I=100.0mA R(En>14MeV)= 8.6%
t-H2O 1-Source I=170.0mA R(En>14MeV)= 0.9%
Flux [n s-1 cm-2 MeV-1]
Neutron Energy [MeV]
X = 0.0 cm Y = 0.0 cm Z = 1.0 cm

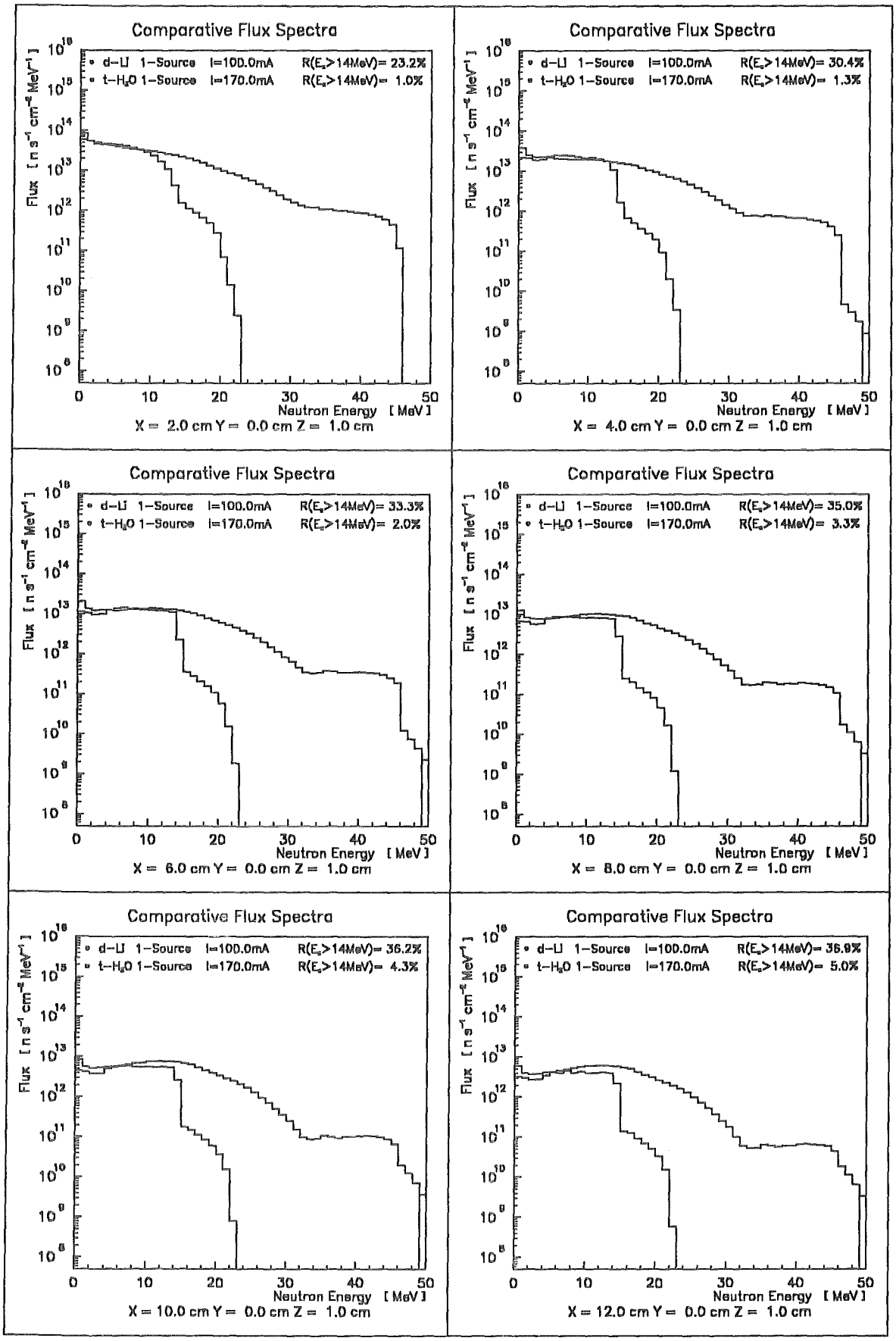
Comparative Flux Spectra
d–Li 1–Source I=100.0mA R(E>14MeV)= 23.2%
t–H2O 1–Source I=170.0mA R(E>14MeV)= 1.0%
Flux [n s-1 cm-2 MeV-1]
Neutron Energy [MeV]
X = 2.0 cm Y = 0.0 cm Z = 1.0 cm
Comparative Flux Spectra
d–Li 1–Source I=100.0mA R(E>14MeV)= 30.4%
t–H2O 1–Source I=170.0mA R(E>14MeV)= 1.3%
Flux [n s-1 cm-2 MeV-1]
Neutron Energy [MeV]
X = 4.0 cm Y = 0.0 cm Z = 1.0 cm
Comparative Flux Spectra
d–Li 1–Source I=100.0mA R(E>14MeV)= 33.3%
t–H2O 1–Source I=170.0mA R(E>14MeV)= 2.0%
Flux [n s-1 cm-2 MeV-1]
Neutron Energy [MeV]
X = 6.0 cm Y = 0.0 cm Z = 1.0 cm
Comparative Flux Spectra
d–Li 1–Source I=100.0mA R(E>14MeV)= 35.0%
t–H2O 1–Source I=170.0mA R(E>14MeV)= 3.3%
Flux [n s-1 cm-2 MeV-1]
Neutron Energy [MeV]
X = 8.0 cm Y = 0.0 cm Z = 1.0 cm
Comparative Flux Spectra
d–Li 1–Source I=100.0mA R(E>14MeV)= 36.2%
t–H2O 1–Source I=170.0mA R(E>14MeV)= 4.3%
Flux [n s-1 cm-2 MeV-1]
Neutron Energy [MeV]
X = 10.0 cm Y = 0.0 cm Z = 1.0 cm
Comparative Flux Spectra
d–Li 1–Source I=100.0mA R(E>14MeV)= 36.9%
t–H2O 1–Source I=170.0mA R(E>14MeV)= 5.0%
Flux [n s-1 cm-2 MeV-1]
Neutron Energy [MeV]
X = 12.0 cm Y = 0.0 cm Z = 1.0 cm

A.2 Comparative minimum flux contours (1-S)

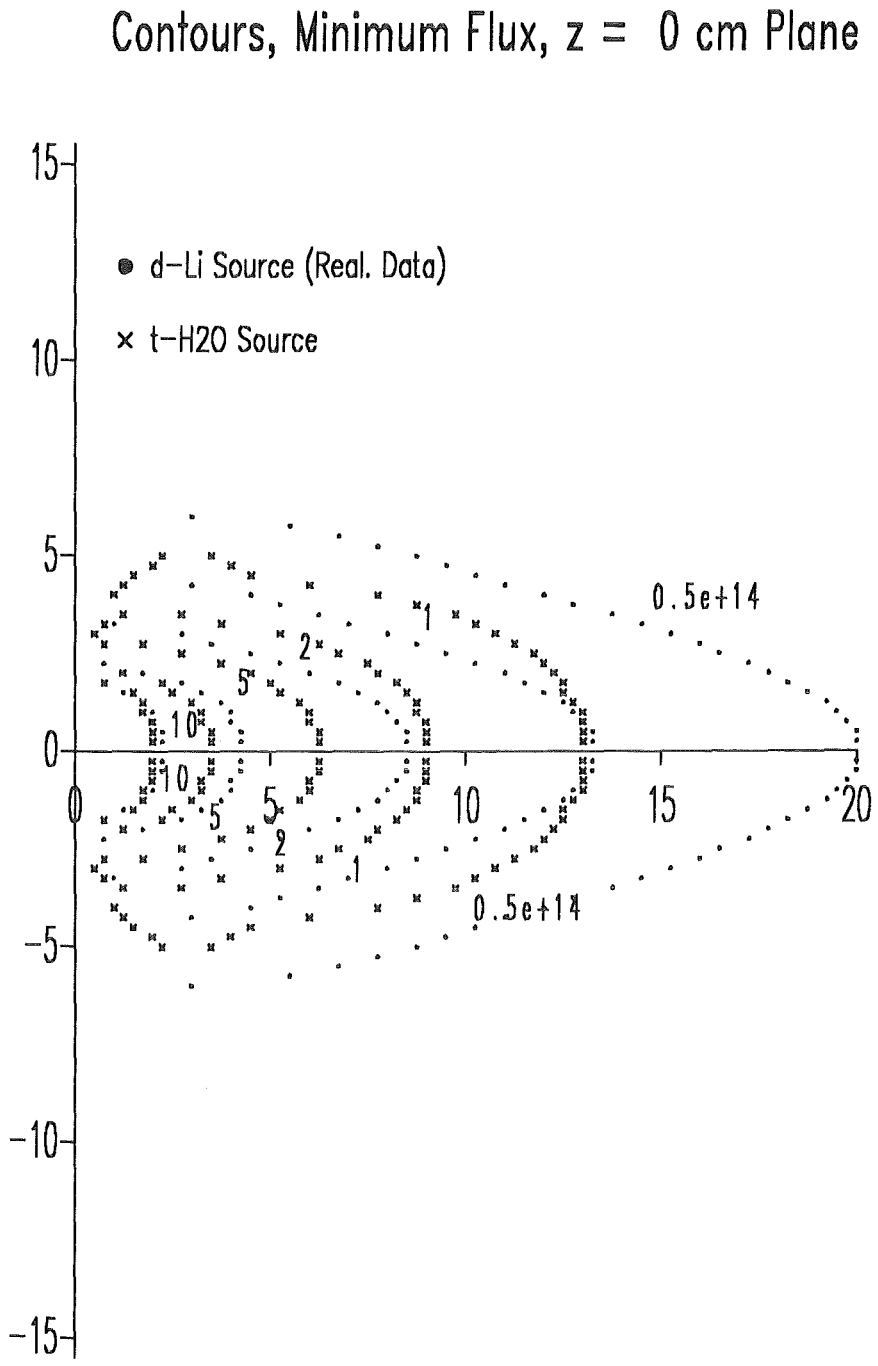

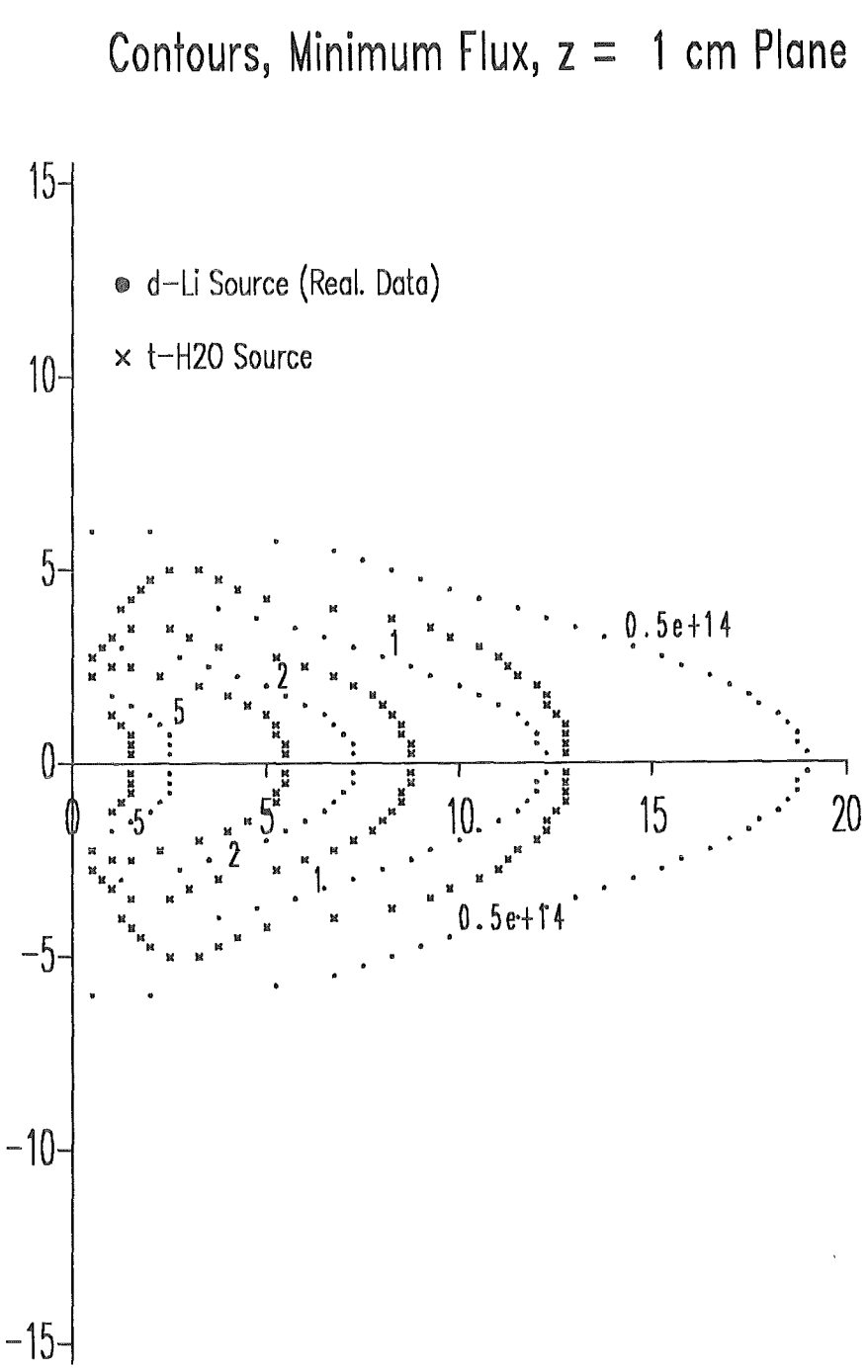

Single Source, 3.0 cm * 1.0 cm Beam

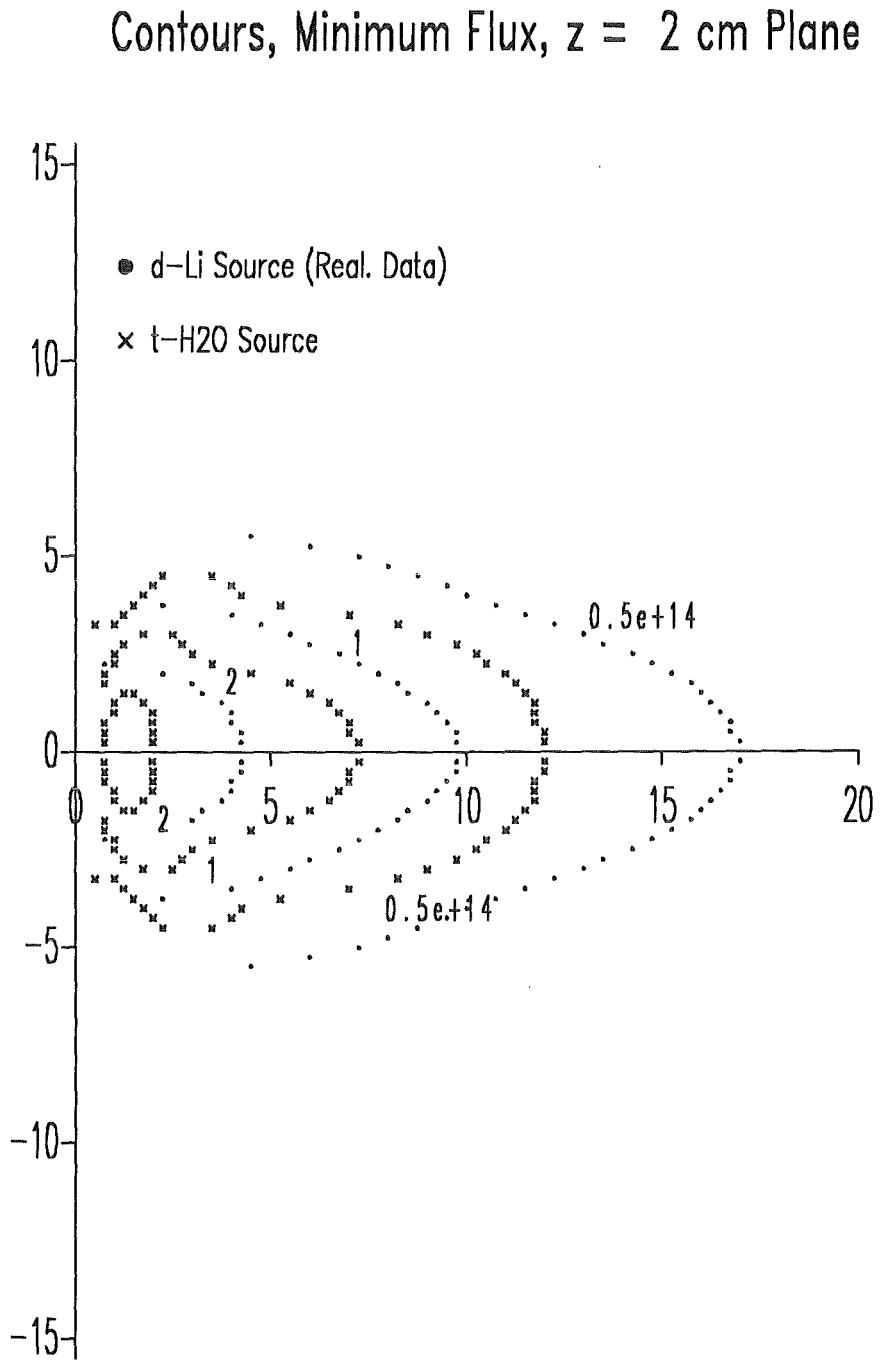

Single Source, 3.0 cm * 1.0 cm Beam

Contours, Minimum Flux, z = 3 cm Plane

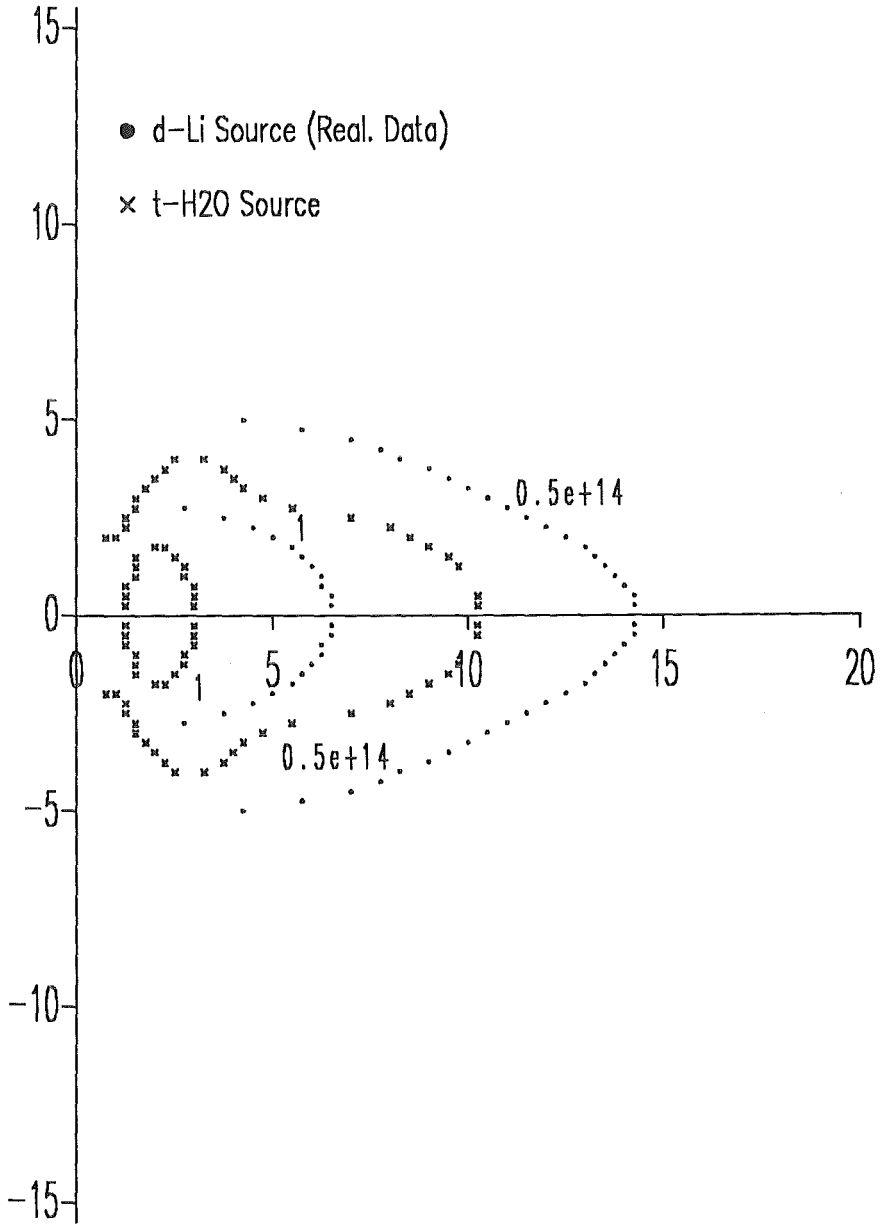

Single Source, 3.0 cm * 1.0 cm Beam

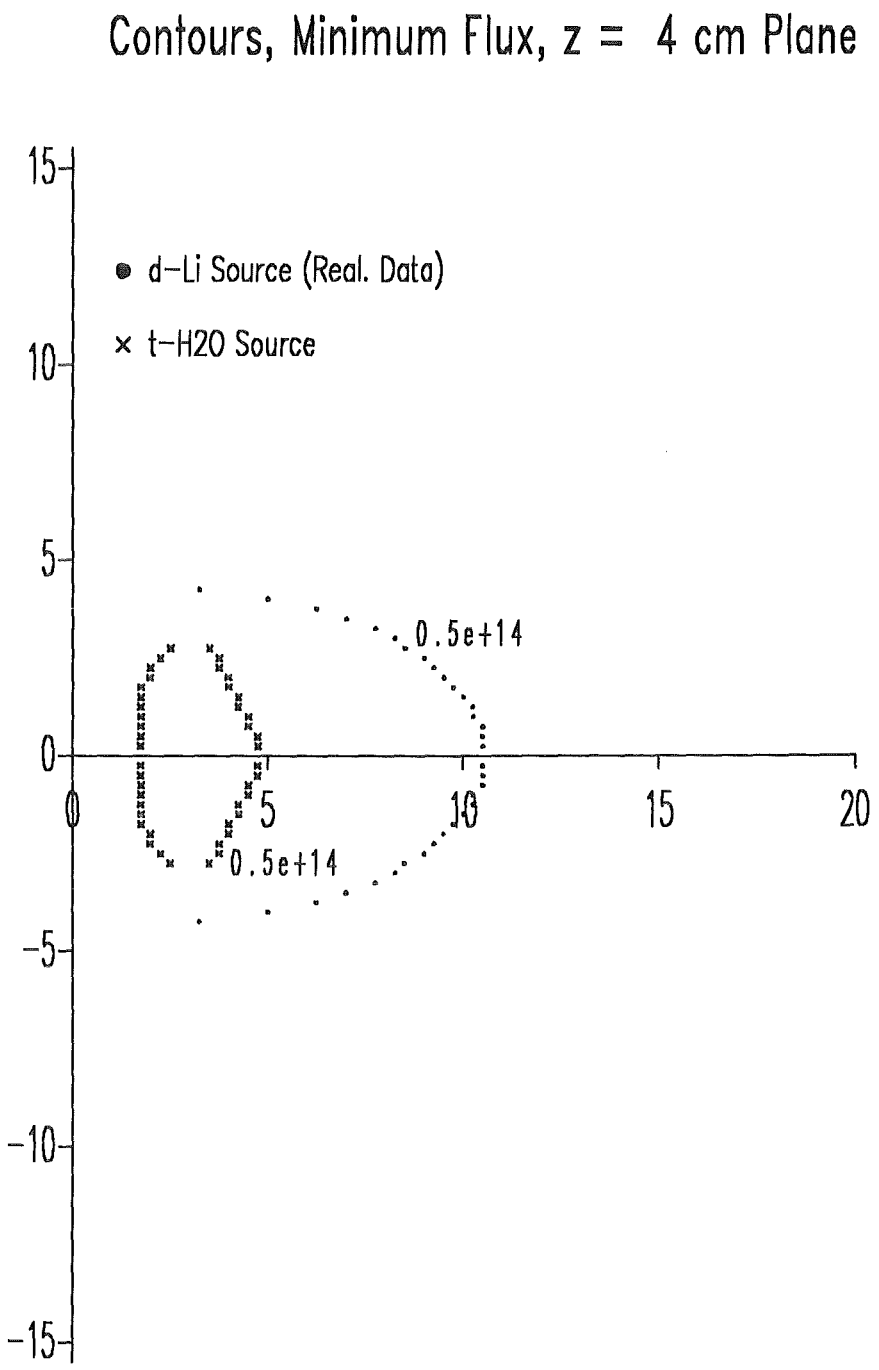

Single Source, 3.0 cm * 1.0 cm Beam

A.3 Comparative plots of neutron flux spectra (2-S)

Coordinates (cm)			Total flux (n/s/cm^2)		Fraction r (%)	
X	Y	Z	t-H	d-Li	t-H	d-li
0	0	0	$7.67 * 10^{13}$	$1.89 * 10^{14}$	1.0	6.3
2	0	0	$1.07 * 10^{14}$	$2.83 * 10^{14}$	1.0	6.7
4	0	0	$2.45 * 10^{14}$	$4.39 * 10^{14}$	0.7	9.0
6	0	0	$4.26 * 10^{14}$	$7.12 * 10^{14}$	0.9	15.1
8	0	0	$6.88 * 10^{14}$	$1.11 * 10^{15}$	1.3	24.8
10	0	0	$8.12 * 10^{14}$	$1.44 * 10^{15}$	2.7	31.28
12	0	0	$7.73 * 10^{14}$	$1.38 * 10^{15}$	2.9	33.2
14	0	0	$6.54 * 10^{14}$	$1.19 * 10^{15}$	3.1	34.3
16	0	0	$5.09 * 10^{14}$	$9.57 * 10^{14}$	3.4	34.7
18	0	0	$3.74 * 10^{14}$	$7.08 * 10^{14}$	3.4	34.2
20	0	0	$2.68 * 10^{14}$	$4.69 * 10^{14}$	2.6	32.2
22	0	0	$1.91 * 10^{14}$	$3.11 * 10^{14}$	1.6	29.4
24	0	0	$1.39 * 10^{14}$	$2.17 * 10^{14}$	1.0	27.0
26	0	0	$1.03 * 10^{14}$	$1.60 * 10^{14}$	1.0	25.1
2	2	0	$1.27 * 10^{14}$	$3.16 * 10^{14}$	1.0	6.7
4	2	0	$3.02 * 10^{14}$	$5.57 * 10^{14}$	0.7	8.8
6	2	0	$6.58 * 10^{14}$	$1.05 * 10^{15}$	0.9	18.4
8	2	0	$9.20 * 10^{14}$	$1.51 * 10^{15}$	1.9	27.3
10	2	0	$8.95 * 10^{14}$	$1.50 * 10^{15}$	2.1	30.2
12	2	0	$7.91 * 10^{14}$	$1.38 * 10^{15}$	2.7	32.5
14	2	0	$6.44 * 10^{14}$	$1.17 * 10^{15}$	3.1	33.8
16	2	0	$4.88 * 10^{14}$	$9.15 * 10^{14}$	3.4	34.1
18	2	0	$3.55 * 10^{14}$	$6.55 * 10^{14}$	3.1	33.3
20	2	0	$2.55 * 10^{14}$	$4.56 * 10^{14}$	2.6	31.8
22	2	0	$1.85 * 10^{14}$	$3.14 * 10^{14}$	2.0	29.8
24	2	0	$1.36 * 10^{14}$	$2.21 * 10^{14}$	1.5	27.6
26	2	0	$1.02 * 10^{14}$	$1.63 * 10^{14}$	1.1	25.5
4	4	0	$5.69 * 10^{14}$	$1.42 * 10^{15}$	1.0	7.7
6	4	0	$1.95 * 10^{15}$	$3.00 * 10^{15}$	1.4	23.2
8	4	0	$1.47 * 10^{15}$	$2.30 * 10^{15}$	1.5	26.0
10	4	0	$1.10 * 10^{15}$	$1.79 * 10^{15}$	1.73	28.4
12	4	0	$8.43 * 10^{14}$	$1.42 * 10^{15}$	2.2	30.8
14	4	0	$6.05 * 10^{14}$	$1.09 * 10^{15}$	3.0	32.2
16	4	0	$4.22 * 10^{14}$	$7.60 * 10^{14}$	2.8	31.8
18	4	0	$3.02 * 10^{14}$	$5.49 * 10^{14}$	2.6	31.2

Coordinates (cm)			Total flux ($n/s/cm^2$)		Fraction r (%)	
X	Y	Z	t-H	d-Li	t-H	d-li
20	4	0	$2.23 * 10^{14}$	$4.17 * 10^{14}$	2.92	31.0
22	4	0	$1.67 * 10^{14}$	$3.14 * 10^{14}$	2.8	30.2
24	4	0	$1.28 * 10^{14}$	$2.30 * 10^{14}$	2.3	28.8
26	4	0	$9.94 * 10^{13}$	$1.70 * 10^{14}$	1.8	26.9
6	6	0	$4.24 * 10^{15}$	$6.76 * 10^{15}$	0.9	15.1
8	6	0	$2.36 * 10^{15}$	$3.61 * 10^{15}$	1.3	22.0
10	6	0	$1.47 * 10^{15}$	$2.30 * 10^{15}$	1.5	26.3
12	6	0	$8.96 * 10^{14}$	$1.47 * 10^{15}$	1.9	28.8
14	6	0	$5.01 * 10^{14}$	$8.28 * 10^{14}$	1.7	27.5
16	6	0	$3.21 * 10^{14}$	$5.57 * 10^{14}$	2.1	27.4
18	6	0	$2.36 * 10^{14}$	$4.42 * 10^{14}$	2.8	28.8
20	6	0	$1.85 * 10^{14}$	$3.64 * 10^{14}$	3.3	29.9
22	6	0	$1.48 * 10^{14}$	$2.97 * 10^{14}$	3.4	30.3
24	6	0	$1.19 * 10^{14}$	$2.34 * 10^{14}$	3.1	29.8
26	6	0	$9.54 * 10^{13}$	$1.78 * 10^{14}$	2.6	28.8
8	8	0	$4.41 * 10^{15}$	$6.84 * 10^{15}$	0.9	15.2
10	8	0	$2.02 * 10^{15}$	$3.09 * 10^{15}$	1.4	23.4
12	8	0	$6.98 * 10^{14}$	$1.09 * 10^{15}$	1.0	21.5
14	8	0	$3.27 * 10^{14}$	$5.35 * 10^{14}$	1.0	19.6
16	8	0	$2.27 * 10^{14}$	$3.92 * 10^{14}$	1.7	22.6
18	8	0	$1.82 * 10^{14}$	$3.40 * 10^{14}$	2.5	26.3
20	8	0	$1.53 * 10^{14}$	$3.02 * 10^{14}$	3.2	28.9
22	8	0	$1.29 * 10^{14}$	$2.64 * 10^{14}$	3.7	30.3
24	8	0	$1.09 * 10^{14}$	$2.23 * 10^{14}$	3.7	30.7
26	8	0	$9.09 * 10^{13}$	$1.82 * 10^{14}$	3.3	30.3
10	10	0	$7.83 * 10^{14}$	$1.82 * 10^{15}$	0.9	8.8
12	10	0	$3.05 * 10^{14}$	$5.58 * 10^{14}$	0.8	11.1
14	10	0	$2.01 * 10^{14}$	$3.41 * 10^{14}$	0.8	14.8
16	10	0	$1.63 * 10^{14}$	$2.71 * 10^{14}$	1.2	19.2
18	10	0	$1.43 * 10^{14}$	$2.48 * 10^{14}$	2.0	24.0
20	10	0	$1.27 * 10^{14}$	$2.39 * 10^{14}$	2.7	27.6
22	10	0	$1.13 * 10^{14}$	$2.24 * 10^{14}$	3.5	29.9
24	10	0	$9.84 * 10^{13}$	$2.02 * 10^{14}$	4.0	31.2
12	12	0	$1.35 * 10^{14}$	$3.02 * 10^{14}$	1.0	9.6
14	12	0	$1.07 * 10^{14}$	$2.28 * 10^{14}$	1.0	12.8
16	12	0	$1.01 * 10^{14}$	$1.94 * 10^{14}$	1.0	17.1
18	12	0	$1.00 * 10^{14}$	$1.82 * 10^{14}$	1.5	21.8
20	12	0	$9.76 * 10^{13}$	$1.81 * 10^{14}$	2.4	26.0
22	12	0	$9.26 * 10^{13}$	$1.82 * 10^{14}$	3.1	29.0
0	0	1	$7.57 * 10^{13}$	$1.86 * 10^{14}$	1.0	6.3

Coordinates (cm)			Total flux ($n/s/cm^2$)		Fraction r (%)	
X	Y	Z	t-H	d-Li	t-H	d-li
2	0	1	$1.05 * 10^{14}$	$2.77 * 10^{14}$	1.0	6.7
4	0	1	$2.36 * 10^{14}$	$4.24 * 10^{14}$	0.7	8.9
6	0	1	$4.04 * 10^{14}$	$6.76 * 10^{14}$	0.9	14.6
8	0	1	$6.34 * 10^{14}$	$1.02 * 10^{15}$	1.2	23.7
10	0	1	$7.54 * 10^{14}$	$1.29 * 10^{15}$	2.2	29.9
12	0	1	$7.29 * 10^{14}$	$1.25 * 10^{15}$	2.4	32.1
14	0	1	$6.24 * 10^{14}$	$1.09 * 10^{15}$	2.6	33.4
16	0	1	$4.91 * 10^{14}$	$8.86 * 10^{14}$	2.9	33.9
18	0	1	$3.64 * 10^{14}$	$6.63 * 10^{14}$	3.0	33.5
20	0	1	$2.62 * 10^{14}$	$4.50 * 10^{14}$	2.3	31.7
22	0	1	$1.88 * 10^{14}$	$3.03 * 10^{14}$	1.5	29.1
24	0	1	$1.37 * 10^{14}$	$2.14 * 10^{14}$	1.0	26.8
26	0	1	$1.02 * 10^{14}$	$1.59 * 10^{14}$	1.0	24.9
2	2	1	$1.23 * 10^{14}$	$3.07 * 10^{14}$	1.0	6.7
4	2	1	$2.80 * 10^{14}$	$5.27 * 10^{14}$	0.7	8.6

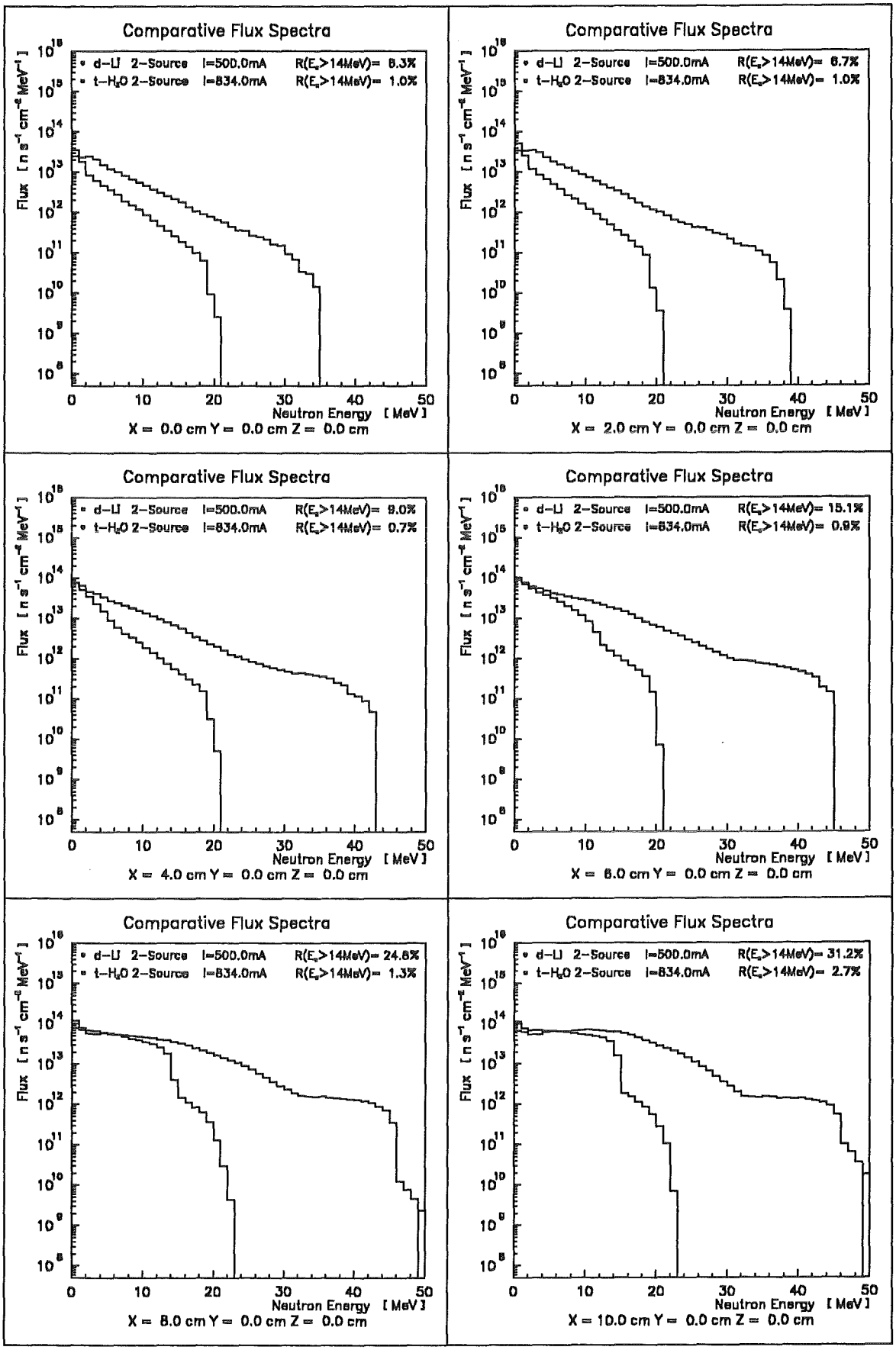
Comparative Flux Spectra
d-Li 2-Source I=500.0mA R(E>14MeV)= 8.3%
t-H2O 2-Source I=834.0mA R(E>14MeV)= 1.0%
Flux [n s-1 cm-2 MeV-1]
Neutron Energy [MeV]
X = 0.0 cm Y = 0.0 cm Z = 0.0 cm
Comparative Flux Spectra
d-Li 2-Source I=500.0mA R(E>14MeV)= 6.7%
t-H2O 2-Source I=834.0mA R(E>14MeV)= 1.0%
Flux [n s-1 cm-2 MeV-1]
Neutron Energy [MeV]
X = 2.0 cm Y = 0.0 cm Z = 0.0 cm
Comparative Flux Spectra
d-Li 2-Source I=500.0mA R(E>14MeV)= 9.0%
t-H2O 2-Source I=834.0mA R(E>14MeV)= 0.7%
Flux [n s-1 cm-2 MeV-1]
Neutron Energy [MeV]
X = 4.0 cm Y = 0.0 cm Z = 0.0 cm
Comparative Flux Spectra
d-Li 2-Source I=500.0mA R(E>14MeV)= 15.1%
t-H2O 2-Source I=834.0mA R(E>14MeV)= 0.9%
Flux [n s-1 cm-2 MeV-1]
Neutron Energy [MeV]
X = 6.0 cm Y = 0.0 cm Z = 0.0 cm
Comparative Flux Spectra
d-Li 2-Source I=500.0mA R(E>14MeV)= 24.8%
t-H2O 2-Source I=834.0mA R(E>14MeV)= 1.3%
Flux [n s-1 cm-2 MeV-1]
Neutron Energy [MeV]
X = 8.0 cm Y = 0.0 cm Z = 0.0 cm
Comparative Flux Spectra
d-Li 2-Source I=500.0mA R(E>14MeV)= 31.2%
t-H2O 2-Source I=834.0mA R(E>14MeV)= 2.7%
Flux [n s-1 cm-2 MeV-1]
Neutron Energy [MeV]
X = 10.0 cm Y = 0.0 cm Z = 0.0 cm

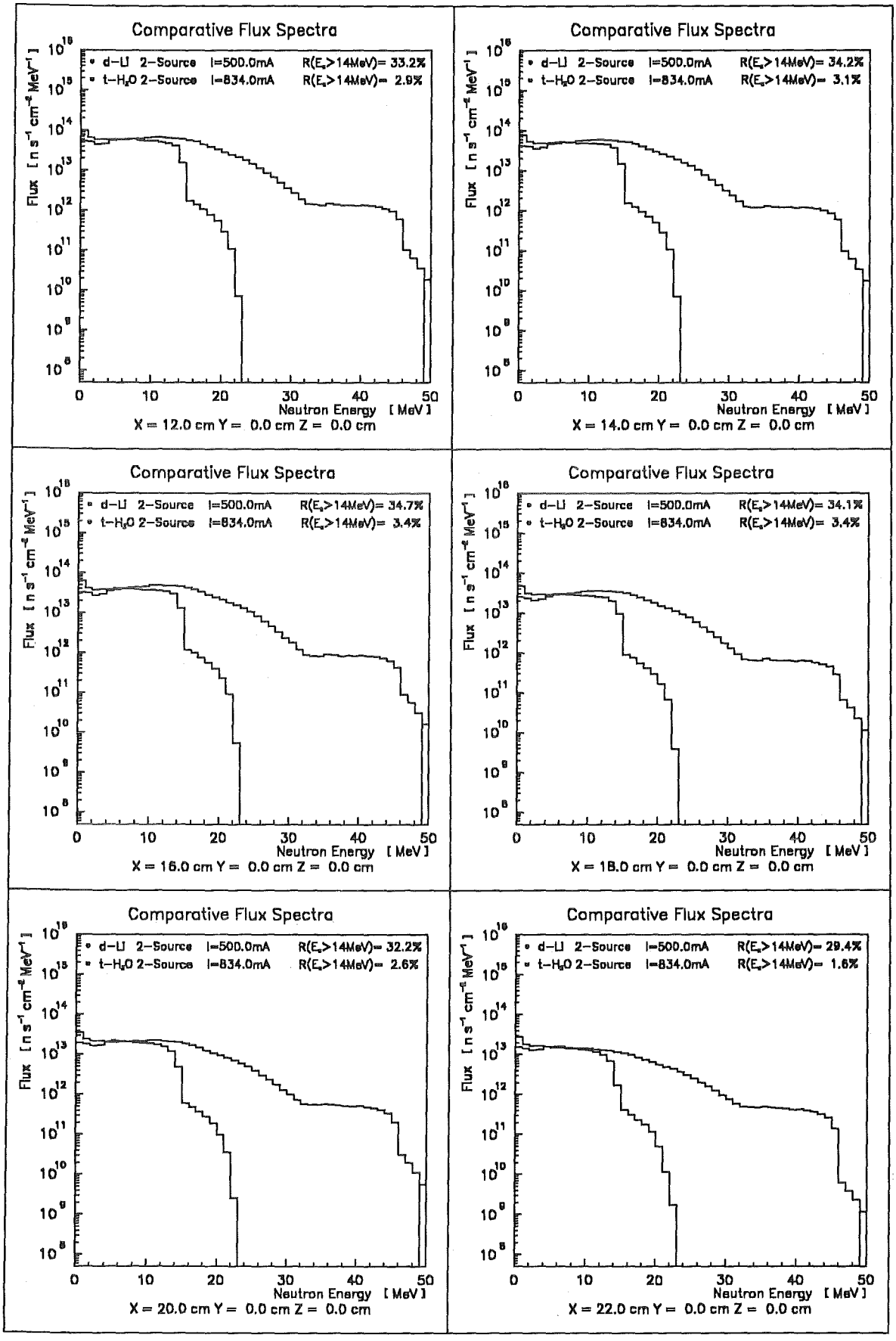
Comparative Flux Spectra
d-Li 2-Source I=500.0mA R(En>14MeV)= 33.2%
t-H2O 2-Source I=834.0mA R(En>14MeV)= 2.9%
Flux [n s-1 cm-2 MeV-1]
Neutron Energy [MeV]
X = 12.0 cm Y = 0.0 cm Z = 0.0 cm
Comparative Flux Spectra
d-Li 2-Source I=500.0mA R(En>14MeV)= 34.2%
t-H2O 2-Source I=834.0mA R(En>14MeV)= 3.1%
Flux [n s-1 cm-2 MeV-1]
Neutron Energy [MeV]
X = 14.0 cm Y = 0.0 cm Z = 0.0 cm
Comparative Flux Spectra
d-Li 2-Source I=500.0mA R(En>14MeV)= 34.7%
t-H2O 2-Source I=834.0mA R(En>14MeV)= 3.4%
Flux [n s-1 cm-2 MeV-1]
Neutron Energy [MeV]
X = 16.0 cm Y = 0.0 cm Z = 0.0 cm
Comparative Flux Spectra
d-Li 2-Source I=500.0mA R(En>14MeV)= 34.1%
t-H2O 2-Source I=834.0mA R(En>14MeV)= 3.4%
Flux [n s-1 cm-2 MeV-1]
Neutron Energy [MeV]
X = 18.0 cm Y = 0.0 cm Z = 0.0 cm
Comparative Flux Spectra
d-Li 2-Source I=500.0mA R(En>14MeV)= 32.2%
t-H2O 2-Source I=834.0mA R(En>14MeV)= 2.6%
Flux [n s-1 cm-2 MeV-1]
Neutron Energy [MeV]
X = 20.0 cm Y = 0.0 cm Z = 0.0 cm
Comparative Flux Spectra
d-Li 2-Source I=500.0mA R(En>14MeV)= 29.4%
t-H2O 2-Source I=834.0mA R(En>14MeV)= 1.6%
Flux [n s-1 cm-2 MeV-1]
Neutron Energy [MeV]
X = 22.0 cm Y = 0.0 cm Z = 0.0 cm

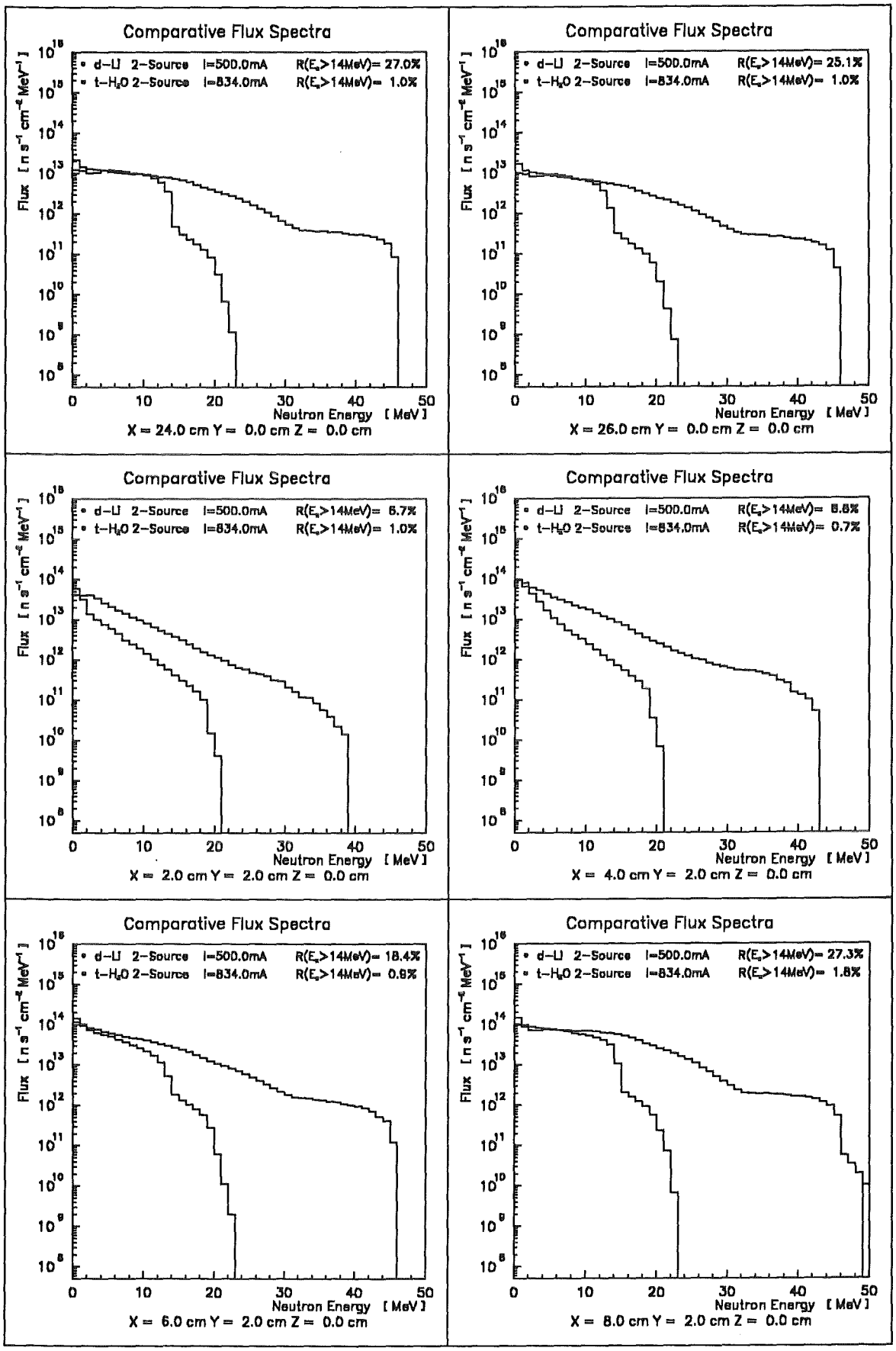
Comparative Flux Spectra
d-Li 2-Source I=500.0mA R(E>14MeV)= 27.0%
t-H2O 2-Source I=834.0mA R(E>14MeV)= 1.0%
Flux [n s-1 cm-2 MeV-1]
Neutron Energy [MeV]
X = 24.0 cm Y = 0.0 cm Z = 0.0 cm
Comparative Flux Spectra
d-Li 2-Source I=500.0mA R(E>14MeV)= 25.1%
t-H2O 2-Source I=834.0mA R(E>14MeV)= 1.0%
Flux [n s-1 cm-2 MeV-1]
Neutron Energy [MeV]
X = 26.0 cm Y = 0.0 cm Z = 0.0 cm
Comparative Flux Spectra
d-Li 2-Source I=500.0mA R(E>14MeV)= 6.7%
t-H2O 2-Source I=834.0mA R(E>14MeV)= 1.0%
Flux [n s-1 cm-2 MeV-1]
Neutron Energy [MeV]
X = 2.0 cm Y = 2.0 cm Z = 0.0 cm
Comparative Flux Spectra
d-Li 2-Source I=500.0mA R(E>14MeV)= 8.8%
t-H2O 2-Source I=834.0mA R(E>14MeV)= 0.7%
Flux [n s-1 cm-2 MeV-1]
Neutron Energy [MeV]
X = 4.0 cm Y = 2.0 cm Z = 0.0 cm
Comparative Flux Spectra
d-Li 2-Source I=500.0mA R(E>14MeV)= 18.4%
t-H2O 2-Source I=834.0mA R(E>14MeV)= 0.8%
Flux [n s-1 cm-2 MeV-1]
Neutron Energy [MeV]
X = 6.0 cm Y = 2.0 cm Z = 0.0 cm
Comparative Flux Spectra
d-Li 2-Source I=500.0mA R(E>14MeV)= 27.3%
t-H2O 2-Source I=834.0mA R(E>14MeV)= 1.8%
Flux [n s-1 cm-2 MeV-1]
Neutron Energy [MeV]
X = 8.0 cm Y = 2.0 cm Z = 0.0 cm

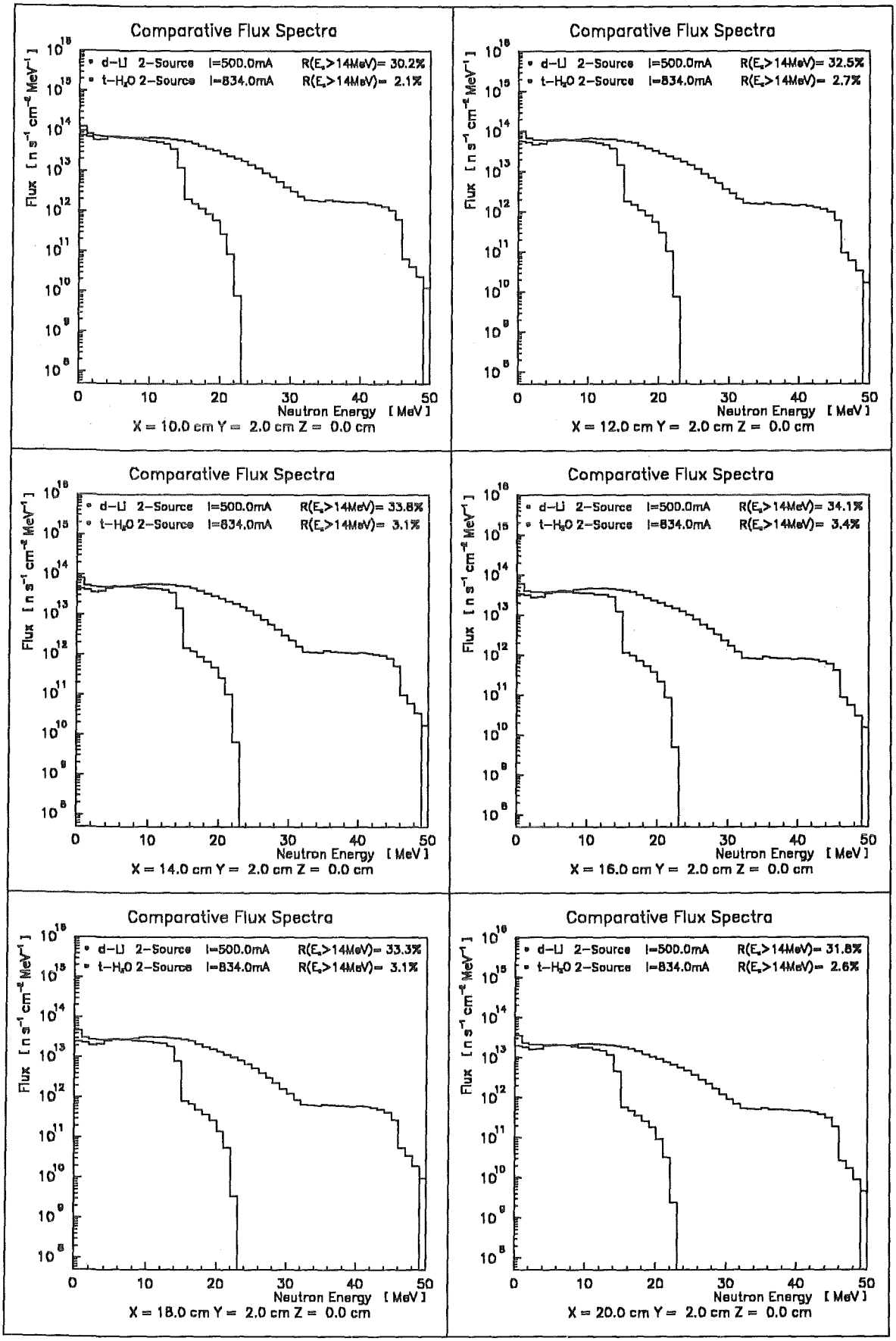
Comparative Flux Spectra
d-Li 2-Source I=500.0mA R(E>14MeV)= 30.2%
t-H2O 2-Source I=834.0mA R(E>14MeV)= 2.1%
Flux [n s-1 cm-2 MeV-1]
Neutron Energy [MeV]
X = 10.0 cm Y = 2.0 cm Z = 0.0 cm
Comparative Flux Spectra
d-Li 2-Source I=500.0mA R(E>14MeV)= 32.5%
t-H2O 2-Source I=834.0mA R(E>14MeV)= 2.7%
Flux [n s-1 cm-2 MeV-1]
Neutron Energy [MeV]
X = 12.0 cm Y = 2.0 cm Z = 0.0 cm
Comparative Flux Spectra
d-Li 2-Source I=500.0mA R(E>14MeV)= 33.8%
t-H2O 2-Source I=834.0mA R(E>14MeV)= 3.1%
Flux [n s-1 cm-2 MeV-1]
Neutron Energy [MeV]
X = 14.0 cm Y = 2.0 cm Z = 0.0 cm
Comparative Flux Spectra
d-Li 2-Source I=500.0mA R(E>14MeV)= 34.1%
t-H2O 2-Source I=834.0mA R(E>14MeV)= 3.4%
Flux [n s-1 cm-2 MeV-1]
Neutron Energy [MeV]
X = 16.0 cm Y = 2.0 cm Z = 0.0 cm
Comparative Flux Spectra
d-Li 2-Source I=500.0mA R(E>14MeV)= 33.3%
t-H2O 2-Source I=834.0mA R(E>14MeV)= 3.1%
Flux [n s-1 cm-2 MeV-1]
Neutron Energy [MeV]
X = 18.0 cm Y = 2.0 cm Z = 0.0 cm
Comparative Flux Spectra
d-Li 2-Source I=500.0mA R(E>14MeV)= 31.8%
t-H2O 2-Source I=834.0mA R(E>14MeV)= 2.6%
Flux [n s-1 cm-2 MeV-1]
Neutron Energy [MeV]
X = 20.0 cm Y = 2.0 cm Z = 0.0 cm

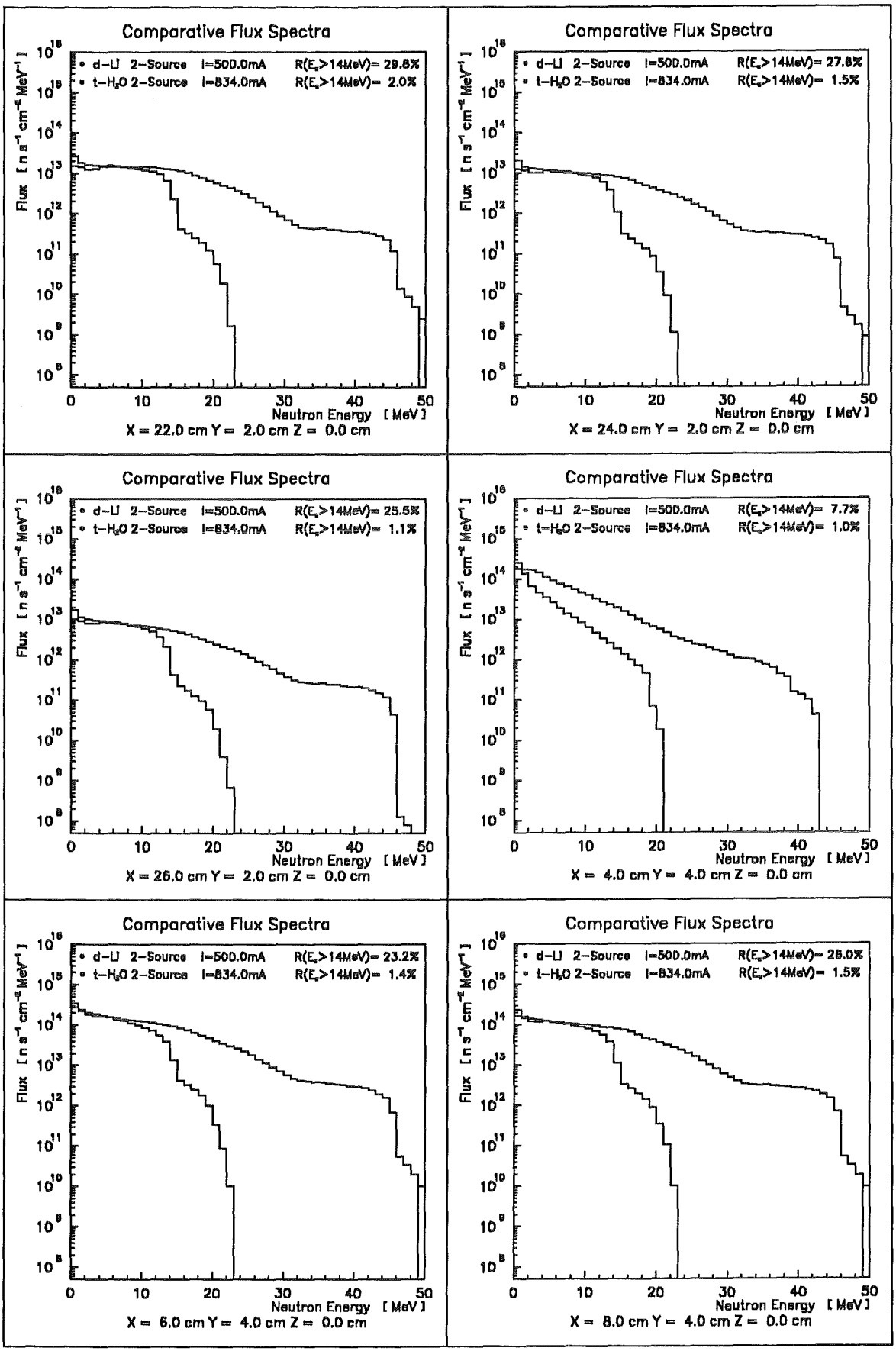
Comparative Flux Spectra
d-Li 2-Source I=500.0mA R(E>14MeV)= 29.8%
t-H2O 2-Source I=834.0mA R(E>14MeV)= 2.0%
Flux [n s-1 cm-2 MeV-1]
Neutron Energy [MeV]
X = 22.0 cm Y = 2.0 cm Z = 0.0 cm
Comparative Flux Spectra
d-Li 2-Source I=500.0mA R(E>14MeV)= 27.6%
t-H2O 2-Source I=834.0mA R(E>14MeV)= 1.5%
Flux [n s-1 cm-2 MeV-1]
Neutron Energy [MeV]
X = 24.0 cm Y = 2.0 cm Z = 0.0 cm
Comparative Flux Spectra
d-Li 2-Source I=500.0mA R(E>14MeV)= 25.5%
t-H2O 2-Source I=834.0mA R(E>14MeV)= 1.1%
Flux [n s-1 cm-2 MeV-1]
Neutron Energy [MeV]
X = 26.0 cm Y = 2.0 cm Z = 0.0 cm
Comparative Flux Spectra
d-Li 2-Source I=500.0mA R(E>14MeV)= 7.7%
t-H2O 2-Source I=834.0mA R(E>14MeV)= 1.0%
Flux [n s-1 cm-2 MeV-1]
Neutron Energy [MeV]
X = 4.0 cm Y = 4.0 cm Z = 0.0 cm
Comparative Flux Spectra
d-Li 2-Source I=500.0mA R(E>14MeV)= 23.2%
t-H2O 2-Source I=834.0mA R(E>14MeV)= 1.4%
Flux [n s-1 cm-2 MeV-1]
Neutron Energy [MeV]
X = 6.0 cm Y = 4.0 cm Z = 0.0 cm
Comparative Flux Spectra
d-Li 2-Source I=500.0mA R(E>14MeV)= 26.0%
t-H2O 2-Source I=834.0mA R(E>14MeV)= 1.5%
Flux [n s-1 cm-2 MeV-1]
Neutron Energy [MeV]
X = 8.0 cm Y = 4.0 cm Z = 0.0 cm

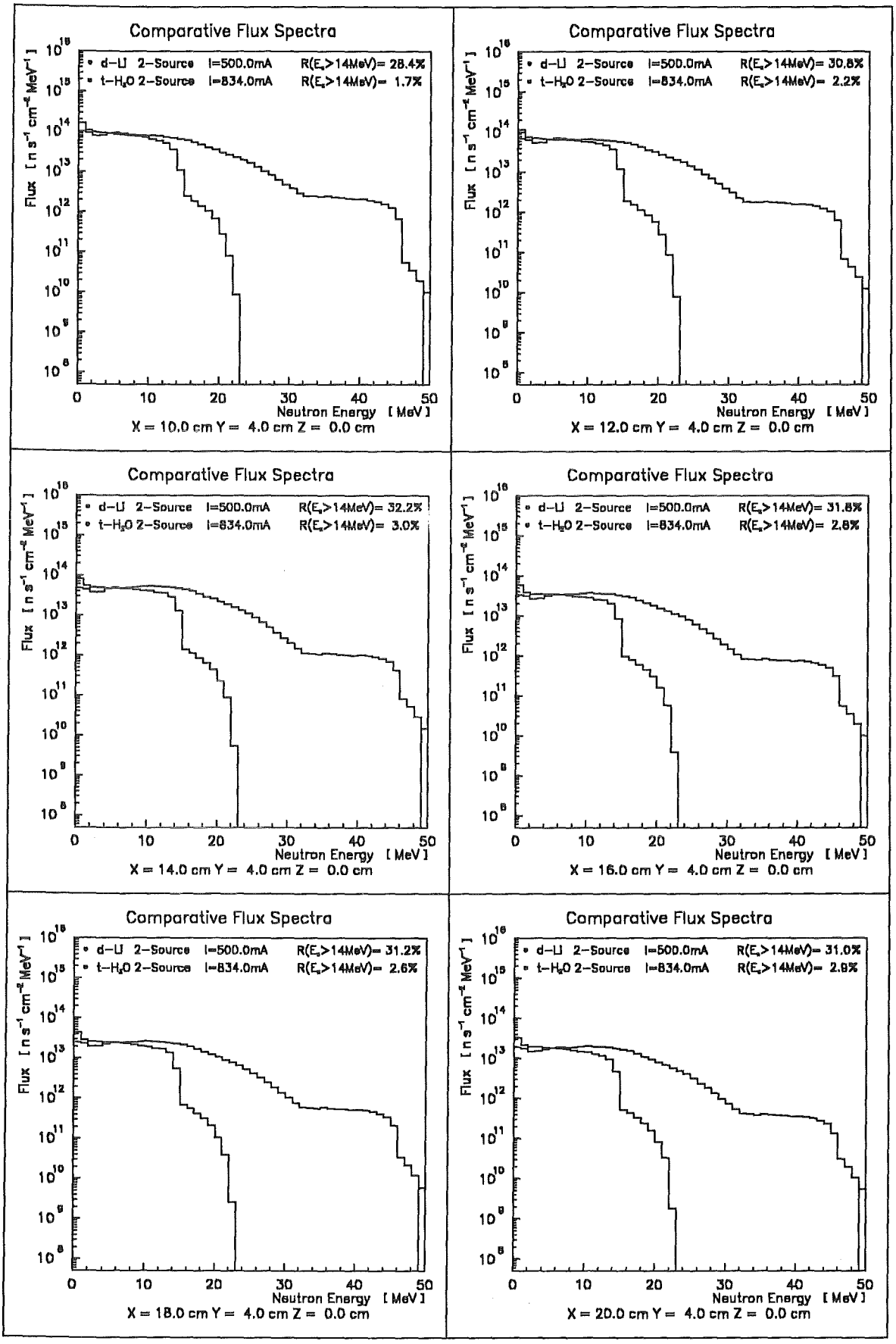
Comparative Flux Spectra
d-Li 2-Source I=500.0mA R(E>14MeV)= 28.4%
t-H2O 2-Source I=834.0mA R(E>14MeV)= 1.7%
Flux [n s-1 cm-2 MeV-1]
Neutron Energy [MeV]
X = 10.0 cm Y = 4.0 cm Z = 0.0 cm
Comparative Flux Spectra
d-Li 2-Source I=500.0mA R(E>14MeV)= 30.8%
t-H2O 2-Source I=834.0mA R(E>14MeV)= 2.2%
Flux [n s-1 cm-2 MeV-1]
Neutron Energy [MeV]
X = 12.0 cm Y = 4.0 cm Z = 0.0 cm
Comparative Flux Spectra
d-Li 2-Source I=500.0mA R(E>14MeV)= 32.2%
t-H2O 2-Source I=834.0mA R(E>14MeV)= 3.0%
Flux [n s-1 cm-2 MeV-1]
Neutron Energy [MeV]
X = 14.0 cm Y = 4.0 cm Z = 0.0 cm
Comparative Flux Spectra
d-Li 2-Source I=500.0mA R(E>14MeV)= 31.8%
t-H2O 2-Source I=834.0mA R(E>14MeV)= 2.8%
Flux [n s-1 cm-2 MeV-1]
Neutron Energy [MeV]
X = 16.0 cm Y = 4.0 cm Z = 0.0 cm
Comparative Flux Spectra
d-Li 2-Source I=500.0mA R(E>14MeV)= 31.2%
t-H2O 2-Source I=834.0mA R(E>14MeV)= 2.6%
Flux [n s-1 cm-2 MeV-1]
Neutron Energy [MeV]
X = 18.0 cm Y = 4.0 cm Z = 0.0 cm
Comparative Flux Spectra
d-Li 2-Source I=500.0mA R(E>14MeV)= 31.0%
t-H2O 2-Source I=834.0mA R(E>14MeV)= 2.8%
Flux [n s-1 cm-2 MeV-1]
Neutron Energy [MeV]
X = 20.0 cm Y = 4.0 cm Z = 0.0 cm

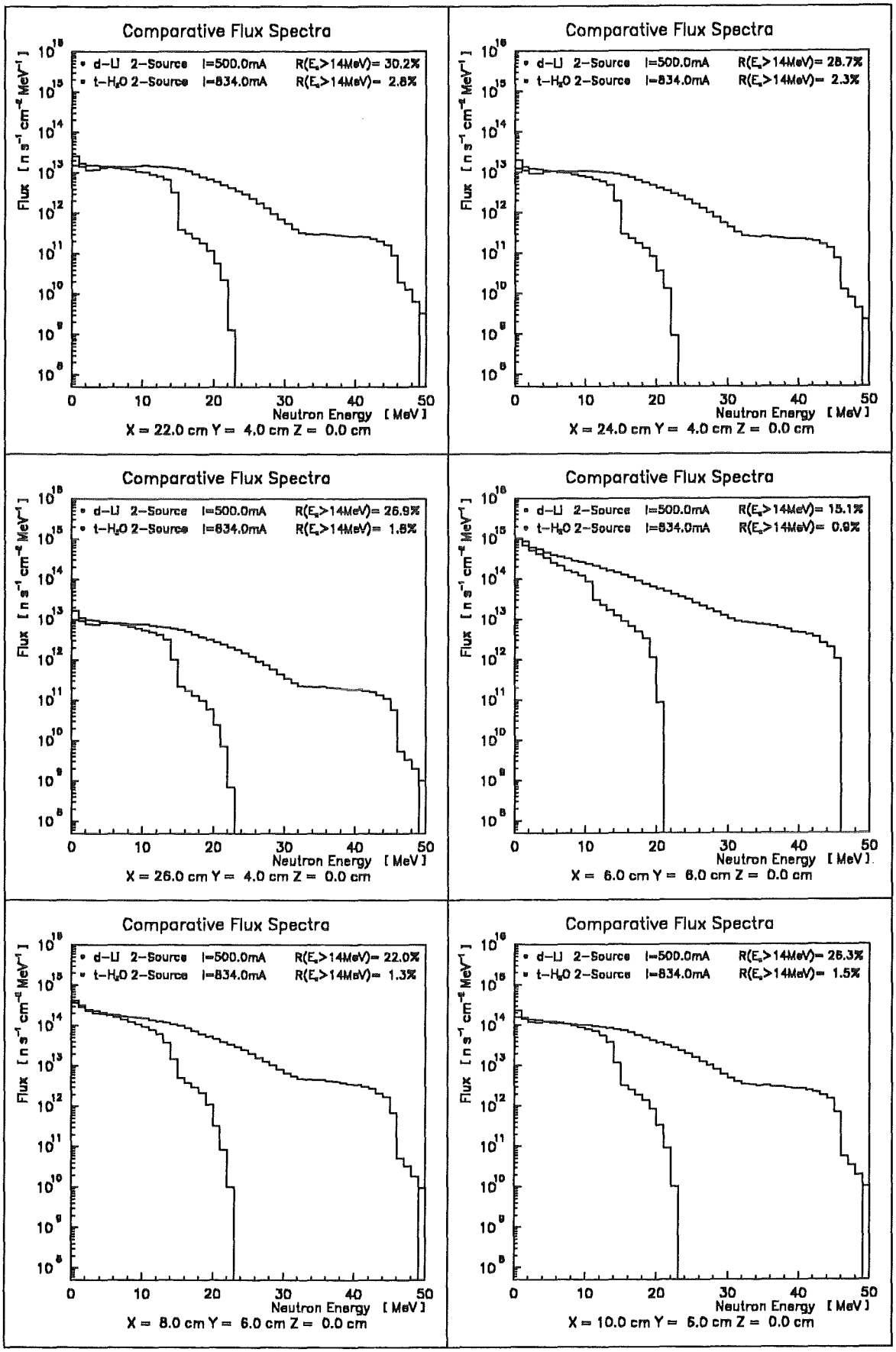
Comparative Flux Spectra
• d-Li 2-Source I=500.0mA R(E>14MeV)= 30.2%
• t-H2O 2-Source I=834.0mA R(E>14MeV)= 2.8%
Flux [n s-1 cm-2 MeV-1]
Neutron Energy [MeV]
X = 22.0 cm Y = 4.0 cm Z = 0.0 cm
Comparative Flux Spectra
• d-Li 2-Source I=500.0mA R(E>14MeV)= 28.7%
• t-H2O 2-Source I=834.0mA R(E>14MeV)= 2.3%
Flux [n s-1 cm-2 MeV-1]
Neutron Energy [MeV]
X = 24.0 cm Y = 4.0 cm Z = 0.0 cm
Comparative Flux Spectra
• d-Li 2-Source I=500.0mA R(E>14MeV)= 26.9%
• t-H2O 2-Source I=834.0mA R(E>14MeV)= 1.8%
Flux [n s-1 cm-2 MeV-1]
Neutron Energy [MeV]
X = 26.0 cm Y = 4.0 cm Z = 0.0 cm
Comparative Flux Spectra
• d-Li 2-Source I=500.0mA R(E>14MeV)= 15.1%
• t-H2O 2-Source I=834.0mA R(E>14MeV)= 0.9%
Flux [n s-1 cm-2 MeV-1]
Neutron Energy [MeV]
X = 6.0 cm Y = 6.0 cm Z = 0.0 cm
Comparative Flux Spectra
• d-Li 2-Source I=500.0mA R(E>14MeV)= 22.0%
• t-H2O 2-Source I=834.0mA R(E>14MeV)= 1.3%
Flux [n s-1 cm-2 MeV-1]
Neutron Energy [MeV]
X = 8.0 cm Y = 6.0 cm Z = 0.0 cm
Comparative Flux Spectra
• d-Li 2-Source I=500.0mA R(E>14MeV)= 26.3%
• t-H2O 2-Source I=834.0mA R(E>14MeV)= 1.5%
Flux [n s-1 cm-2 MeV-1]
Neutron Energy [MeV]
X = 10.0 cm Y = 6.0 cm Z = 0.0 cm

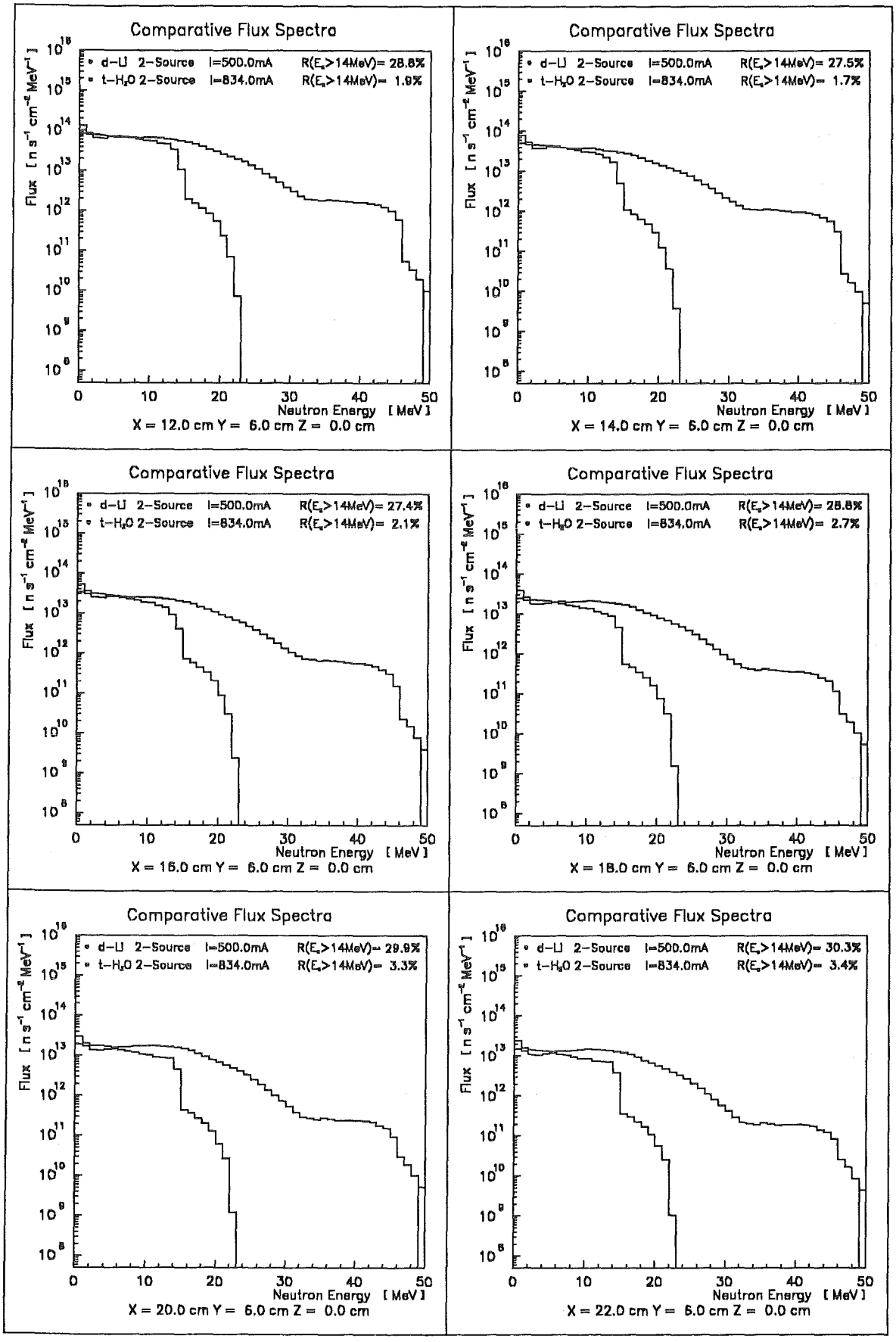
Comparative Flux Spectra
d-Li 2-Source I=500.0mA R(E>14MeV)= 28.8%
t-H2O 2-Source I=834.0mA R(E>14MeV)= 1.9%
Flux [n s-1 cm-2 MeV-1]
Neutron Energy [MeV]
X = 12.0 cm Y = 6.0 cm Z = 0.0 cm
Comparative Flux Spectra
d-Li 2-Source I=500.0mA R(E>14MeV)= 27.5%
t-H2O 2-Source I=834.0mA R(E>14MeV)= 1.7%
Flux [n s-1 cm-2 MeV-1]
Neutron Energy [MeV]
X = 14.0 cm Y = 6.0 cm Z = 0.0 cm
Comparative Flux Spectra
d-Li 2-Source I=500.0mA R(E>14MeV)= 27.4%
t-H2O 2-Source I=834.0mA R(E>14MeV)= 2.1%
Flux [n s-1 cm-2 MeV-1]
Neutron Energy [MeV]
X = 16.0 cm Y = 6.0 cm Z = 0.0 cm
Comparative Flux Spectra
d-Li 2-Source I=500.0mA R(E>14MeV)= 28.8%
t-H2O 2-Source I=834.0mA R(E>14MeV)= 2.7%
Flux [n s-1 cm-2 MeV-1]
Neutron Energy [MeV]
X = 18.0 cm Y = 6.0 cm Z = 0.0 cm
Comparative Flux Spectra
d-Li 2-Source I=500.0mA R(E>14MeV)= 29.9%
t-H2O 2-Source I=834.0mA R(E>14MeV)= 3.3%
Flux [n s-1 cm-2 MeV-1]
Neutron Energy [MeV]
X = 20.0 cm Y = 6.0 cm Z = 0.0 cm
Comparative Flux Spectra
d-Li 2-Source I=500.0mA R(E>14MeV)= 30.3%
t-H2O 2-Source I=834.0mA R(E>14MeV)= 3.4%
Flux [n s-1 cm-2 MeV-1]
Neutron Energy [MeV]
X = 22.0 cm Y = 6.0 cm Z = 0.0 cm

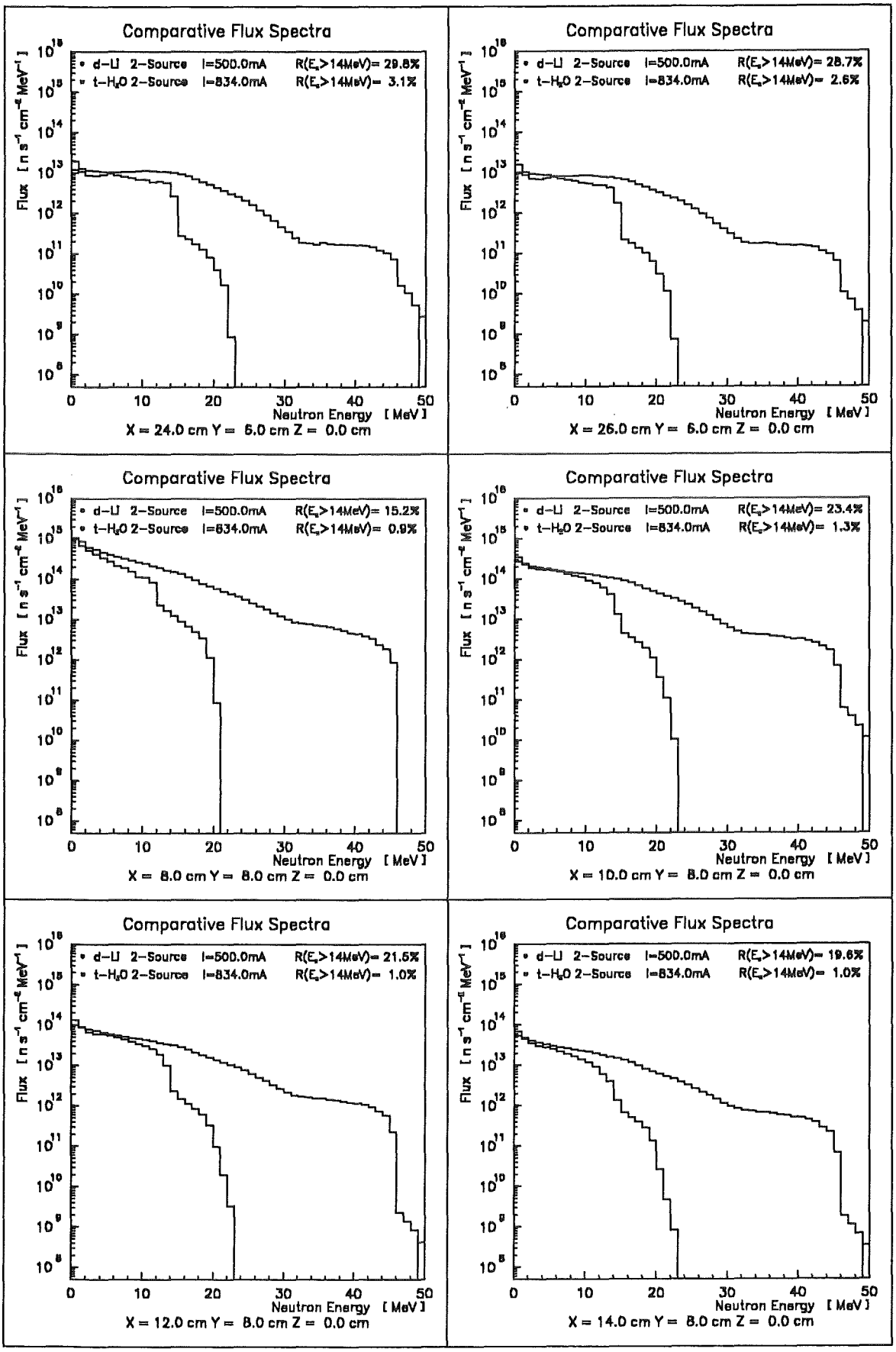
Comparative Flux Spectra
d-Li 2-Source I=500.0mA R(En>14MeV)= 29.8%
t-H2O 2-Source I=834.0mA R(En>14MeV)= 3.1%
Flux [n s-1 cm-2 MeV-1]
Neutron Energy [MeV]
X = 24.0 cm Y = 6.0 cm Z = 0.0 cm
Comparative Flux Spectra
d-Li 2-Source I=500.0mA R(En>14MeV)= 28.7%
t-H2O 2-Source I=834.0mA R(En>14MeV)= 2.6%
Flux [n s-1 cm-2 MeV-1]
Neutron Energy [MeV]
X = 26.0 cm Y = 6.0 cm Z = 0.0 cm
Comparative Flux Spectra
d-Li 2-Source I=500.0mA R(En>14MeV)= 15.2%
t-H2O 2-Source I=834.0mA R(En>14MeV)= 0.9%
Flux [n s-1 cm-2 MeV-1]
Neutron Energy [MeV]
X = 8.0 cm Y = 8.0 cm Z = 0.0 cm
Comparative Flux Spectra
d-Li 2-Source I=500.0mA R(En>14MeV)= 23.4%
t-H2O 2-Source I=834.0mA R(En>14MeV)= 1.3%
Flux [n s-1 cm-2 MeV-1]
Neutron Energy [MeV]
X = 10.0 cm Y = 8.0 cm Z = 0.0 cm
Comparative Flux Spectra
d-Li 2-Source I=500.0mA R(En>14MeV)= 21.5%
t-H2O 2-Source I=834.0mA R(En>14MeV)= 1.0%
Flux [n s-1 cm-2 MeV-1]
Neutron Energy [MeV]
X = 12.0 cm Y = 8.0 cm Z = 0.0 cm
Comparative Flux Spectra
d-Li 2-Source I=500.0mA R(En>14MeV)= 19.6%
t-H2O 2-Source I=834.0mA R(En>14MeV)= 1.0%
Flux [n s-1 cm-2 MeV-1]
Neutron Energy [MeV]
X = 14.0 cm Y = 8.0 cm Z = 0.0 cm

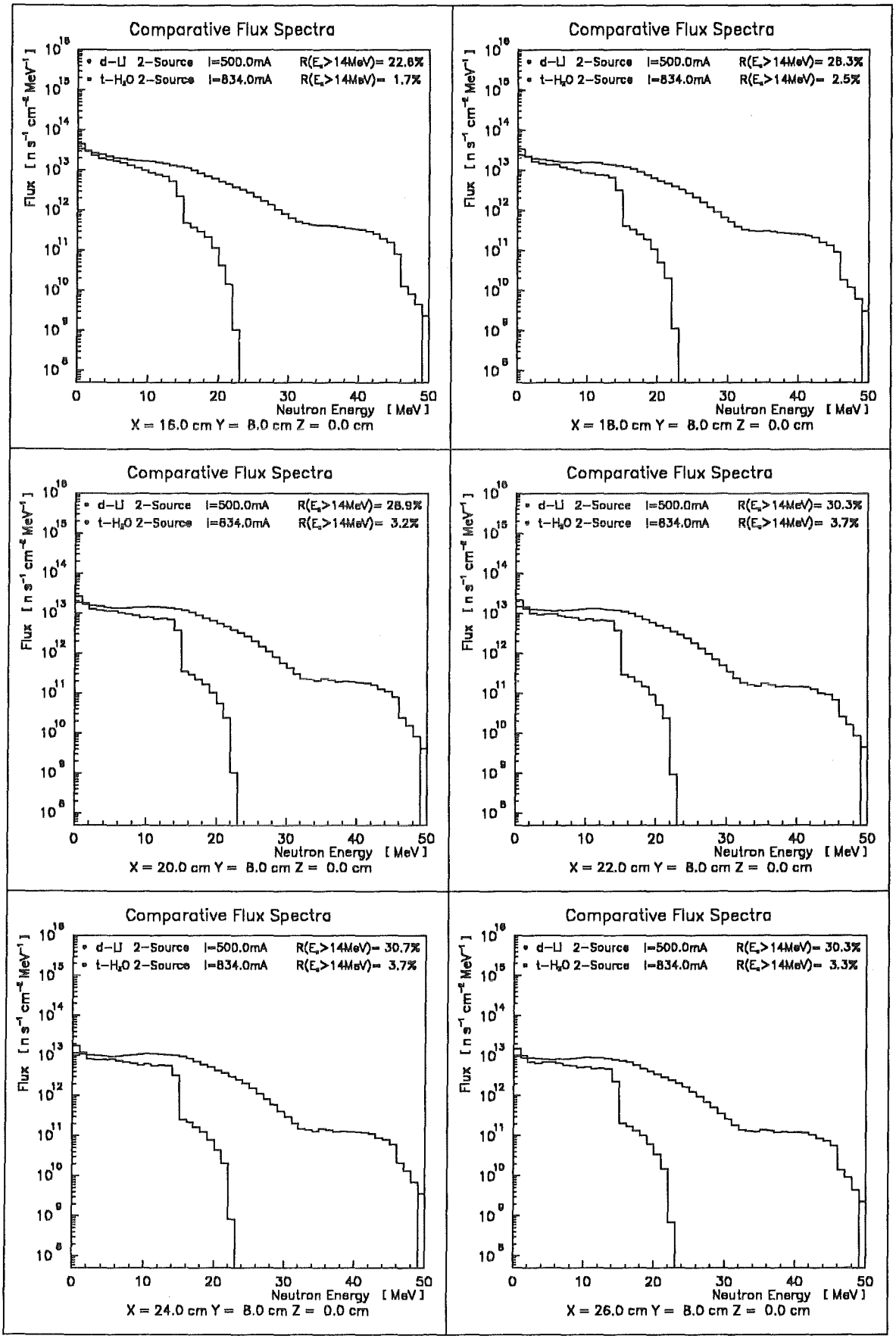
Comparative Flux Spectra
d-Li 2-Source I=500.0mA R(En>14MeV)= 22.6%
t-H2O 2-Source I=834.0mA R(En>14MeV)= 1.7%
Flux [n s-1 cm-2 MeV-1]
Neutron Energy [MeV]
X = 16.0 cm Y = 8.0 cm Z = 0.0 cm
Comparative Flux Spectra
d-Li 2-Source I=500.0mA R(En>14MeV)= 28.3%
t-H2O 2-Source I=834.0mA R(En>14MeV)= 2.5%
Flux [n s-1 cm-2 MeV-1]
Neutron Energy [MeV]
X = 18.0 cm Y = 8.0 cm Z = 0.0 cm
Comparative Flux Spectra
d-Li 2-Source I=500.0mA R(En>14MeV)= 28.9%
t-H2O 2-Source I=834.0mA R(En>14MeV)= 3.2%
Flux [n s-1 cm-2 MeV-1]
Neutron Energy [MeV]
X = 20.0 cm Y = 8.0 cm Z = 0.0 cm
Comparative Flux Spectra
d-Li 2-Source I=500.0mA R(En>14MeV)= 30.3%
t-H2O 2-Source I=834.0mA R(En>14MeV)= 3.7%
Flux [n s-1 cm-2 MeV-1]
Neutron Energy [MeV]
X = 22.0 cm Y = 8.0 cm Z = 0.0 cm
Comparative Flux Spectra
d-Li 2-Source I=500.0mA R(En>14MeV)= 30.7%
t-H2O 2-Source I=834.0mA R(En>14MeV)= 3.7%
Flux [n s-1 cm-2 MeV-1]
Neutron Energy [MeV]
X = 24.0 cm Y = 8.0 cm Z = 0.0 cm
Comparative Flux Spectra
d-Li 2-Source I=500.0mA R(En>14MeV)= 30.3%
t-H2O 2-Source I=834.0mA R(En>14MeV)= 3.3%
Flux [n s-1 cm-2 MeV-1]
Neutron Energy [MeV]
X = 26.0 cm Y = 8.0 cm Z = 0.0 cm

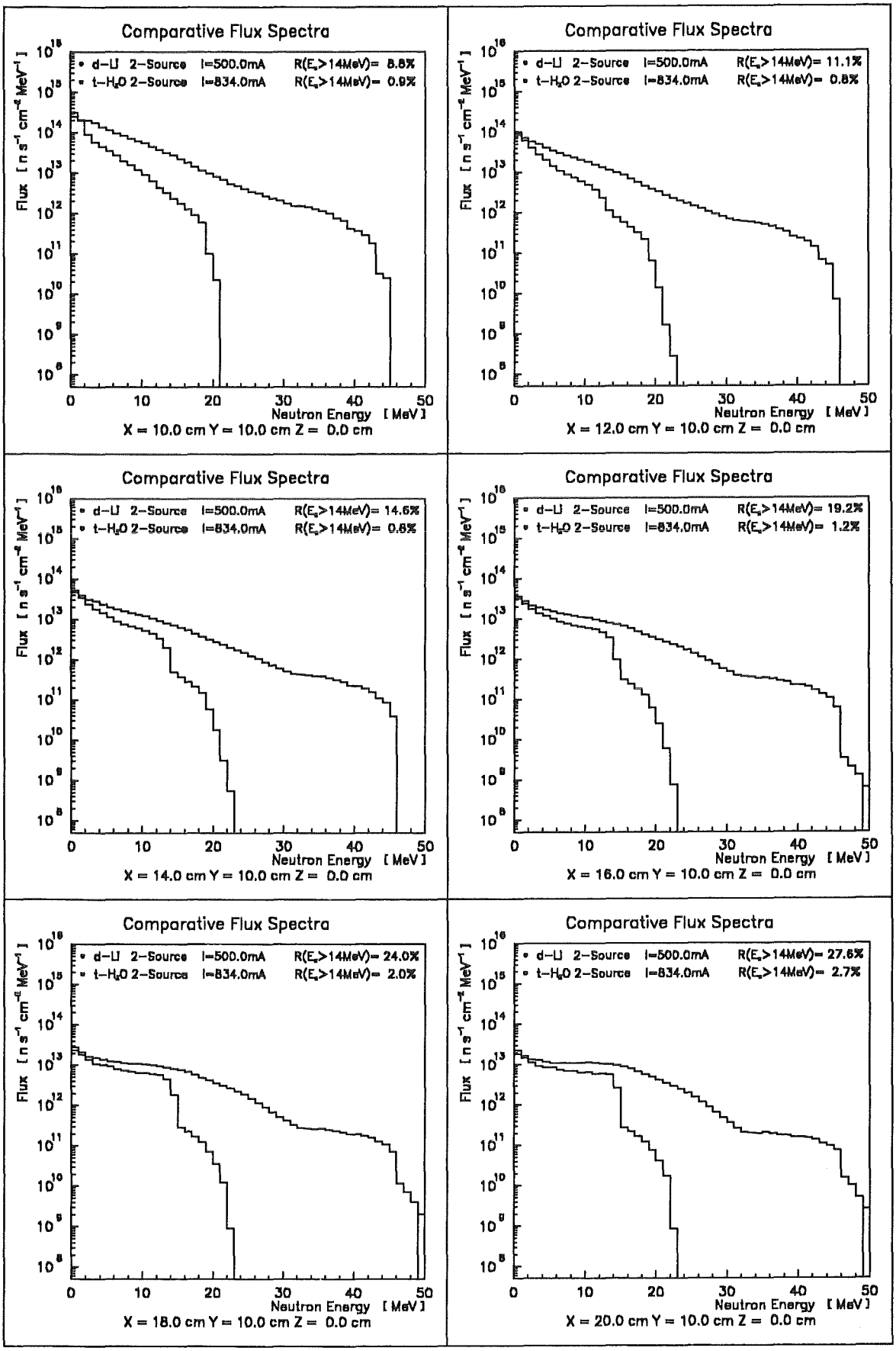
Comparative Flux Spectra
d-Li 2-Source I=500.0mA R(E_n>14MeV)= 8.8%
t-H2O 2-Source I=834.0mA R(E_n>14MeV)= 0.9%
Flux [n s-1 cm-2 MeV-1]
Neutron Energy [MeV]
X = 10.0 cm Y = 10.0 cm Z = 0.0 cm
Comparative Flux Spectra
d-Li 2-Source I=500.0mA R(E_n>14MeV)= 11.1%
t-H2O 2-Source I=834.0mA R(E_n>14MeV)= 0.8%
Flux [n s-1 cm-2 MeV-1]
Neutron Energy [MeV]
X = 12.0 cm Y = 10.0 cm Z = 0.0 cm
Comparative Flux Spectra
d-Li 2-Source I=500.0mA R(E_n>14MeV)= 14.6%
t-H2O 2-Source I=834.0mA R(E_n>14MeV)= 0.8%
Flux [n s-1 cm-2 MeV-1]
Neutron Energy [MeV]
X = 14.0 cm Y = 10.0 cm Z = 0.0 cm
Comparative Flux Spectra
d-Li 2-Source I=500.0mA R(E_n>14MeV)= 19.2%
t-H2O 2-Source I=834.0mA R(E_n>14MeV)= 1.2%
Flux [n s-1 cm-2 MeV-1]
Neutron Energy [MeV]
X = 16.0 cm Y = 10.0 cm Z = 0.0 cm
Comparative Flux Spectra
d-Li 2-Source I=500.0mA R(E_n>14MeV)= 24.0%
t-H2O 2-Source I=834.0mA R(E_n>14MeV)= 2.0%
Flux [n s-1 cm-2 MeV-1]
Neutron Energy [MeV]
X = 18.0 cm Y = 10.0 cm Z = 0.0 cm
Comparative Flux Spectra
d-Li 2-Source I=500.0mA R(E_n>14MeV)= 27.6%
t-H2O 2-Source I=834.0mA R(E_n>14MeV)= 2.7%
Flux [n s-1 cm-2 MeV-1]
Neutron Energy [MeV]
X = 20.0 cm Y = 10.0 cm Z = 0.0 cm

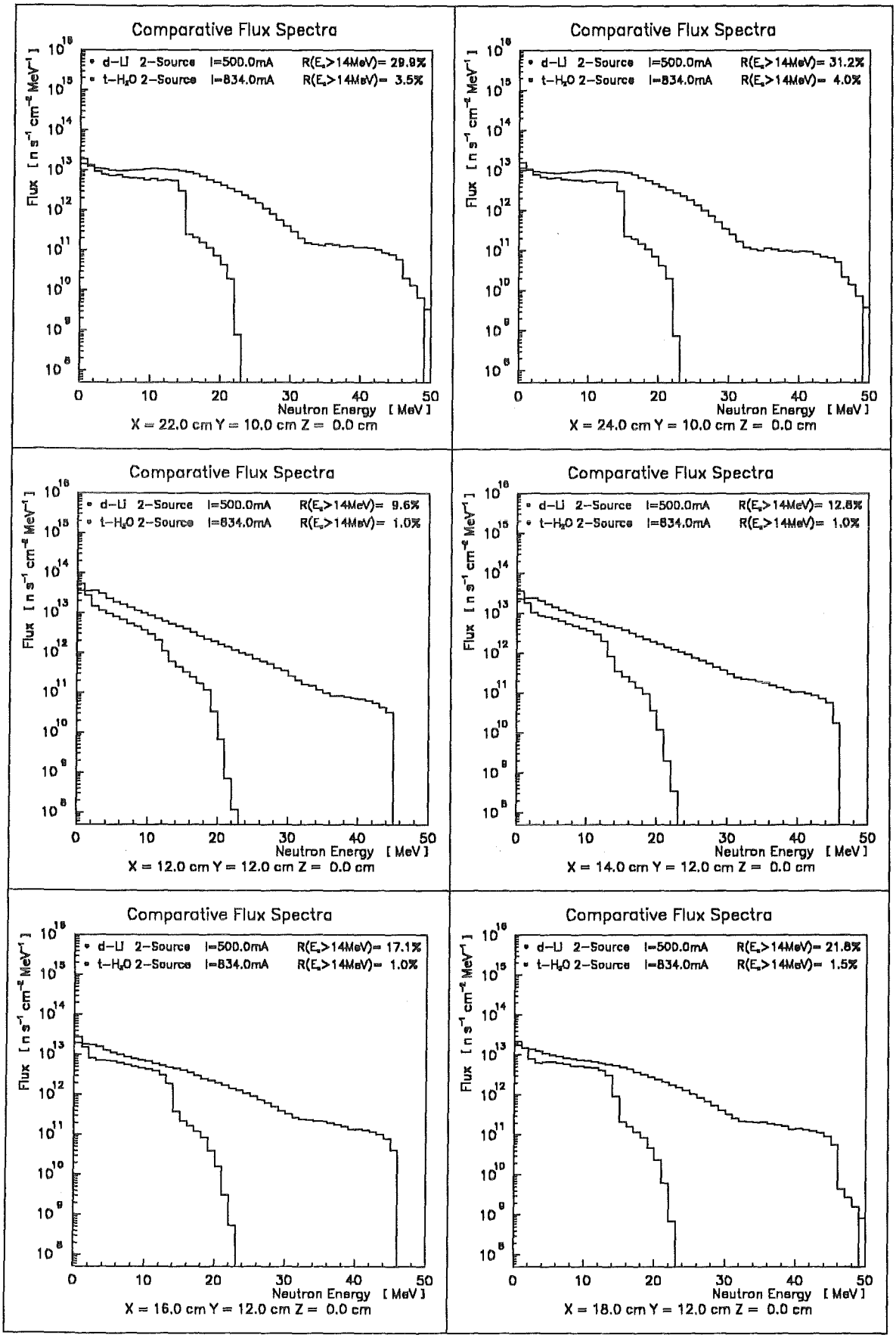
Comparative Flux Spectra
d-Li 2-Source I=500.0mA R(E>14MeV)= 29.8%
t-H2O 2-Source I=834.0mA R(E>14MeV)= 3.5%
Flux [n s-1 cm-2 MeV-1]
Neutron Energy [MeV]
X = 22.0 cm Y = 10.0 cm Z = 0.0 cm
Comparative Flux Spectra
d-Li 2-Source I=500.0mA R(E>14MeV)= 31.2%
t-H2O 2-Source I=834.0mA R(E>14MeV)= 4.0%
Flux [n s-1 cm-2 MeV-1]
Neutron Energy [MeV]
X = 24.0 cm Y = 10.0 cm Z = 0.0 cm
Comparative Flux Spectra
d-Li 2-Source I=500.0mA R(E>14MeV)= 9.6%
t-H2O 2-Source I=834.0mA R(E>14MeV)= 1.0%
Flux [n s-1 cm-2 MeV-1]
Neutron Energy [MeV]
X = 12.0 cm Y = 12.0 cm Z = 0.0 cm
Comparative Flux Spectra
d-Li 2-Source I=500.0mA R(E>14MeV)= 12.8%
t-H2O 2-Source I=834.0mA R(E>14MeV)= 1.0%
Flux [n s-1 cm-2 MeV-1]
Neutron Energy [MeV]
X = 14.0 cm Y = 12.0 cm Z = 0.0 cm
Comparative Flux Spectra
d-Li 2-Source I=500.0mA R(E>14MeV)= 17.1%
t-H2O 2-Source I=834.0mA R(E>14MeV)= 1.0%
Flux [n s-1 cm-2 MeV-1]
Neutron Energy [MeV]
X = 16.0 cm Y = 12.0 cm Z = 0.0 cm
Comparative Flux Spectra
d-Li 2-Source I=500.0mA R(E>14MeV)= 21.8%
t-H2O 2-Source I=834.0mA R(E>14MeV)= 1.5%
Flux [n s-1 cm-2 MeV-1]
Neutron Energy [MeV]
X = 18.0 cm Y = 12.0 cm Z = 0.0 cm

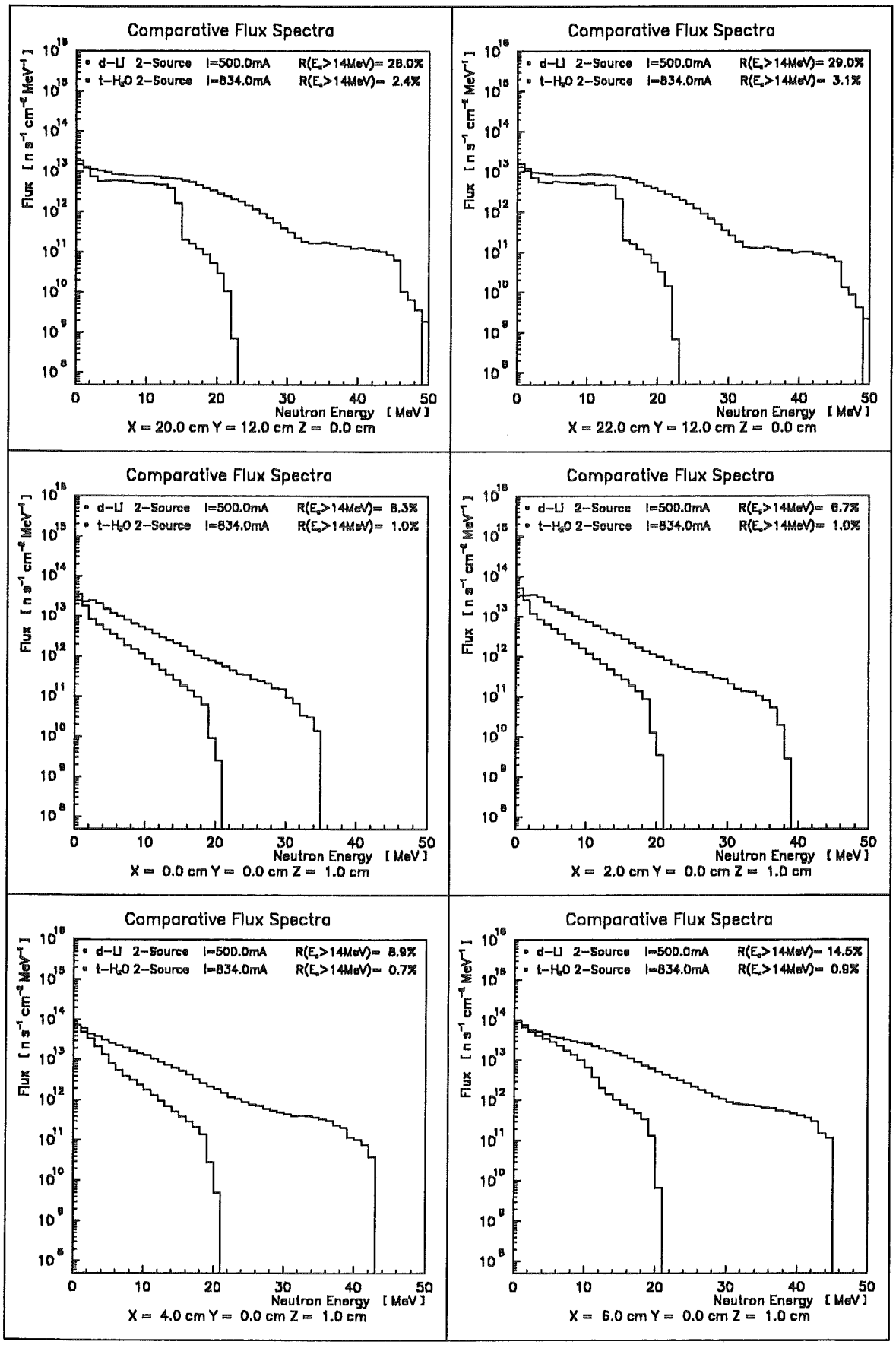
Comparative Flux Spectra
d-Li 2-Source I=500.0mA R(En>14MeV)= 28.0%
t-H2O 2-Source I=834.0mA R(En>14MeV)= 2.4%
Flux [n s-1 cm-2 MeV-1]
Neutron Energy [MeV]
X = 20.0 cm Y = 12.0 cm Z = 0.0 cm
Comparative Flux Spectra
d-Li 2-Source I=500.0mA R(En>14MeV)= 29.0%
t-H2O 2-Source I=834.0mA R(En>14MeV)= 3.1%
Flux [n s-1 cm-2 MeV-1]
Neutron Energy [MeV]
X = 22.0 cm Y = 12.0 cm Z = 0.0 cm
Comparative Flux Spectra
d-Li 2-Source I=500.0mA R(En>14MeV)= 6.3%
t-H2O 2-Source I=834.0mA R(En>14MeV)= 1.0%
Flux [n s-1 cm-2 MeV-1]
Neutron Energy [MeV]
X = 0.0 cm Y = 0.0 cm Z = 1.0 cm
Comparative Flux Spectra
d-Li 2-Source I=500.0mA R(En>14MeV)= 6.7%
t-H2O 2-Source I=834.0mA R(En>14MeV)= 1.0%
Flux [n s-1 cm-2 MeV-1]
Neutron Energy [MeV]
X = 2.0 cm Y = 0.0 cm Z = 1.0 cm
Comparative Flux Spectra
d-Li 2-Source I=500.0mA R(En>14MeV)= 8.9%
t-H2O 2-Source I=834.0mA R(En>14MeV)= 0.7%
Flux [n s-1 cm-2 MeV-1]
Neutron Energy [MeV]
X = 4.0 cm Y = 0.0 cm Z = 1.0 cm
Comparative Flux Spectra
d-Li 2-Source I=500.0mA R(En>14MeV)= 14.5%
t-H2O 2-Source I=834.0mA R(En>14MeV)= 0.9%
Flux [n s-1 cm-2 MeV-1]
Neutron Energy [MeV]
X = 6.0 cm Y = 0.0 cm Z = 1.0 cm

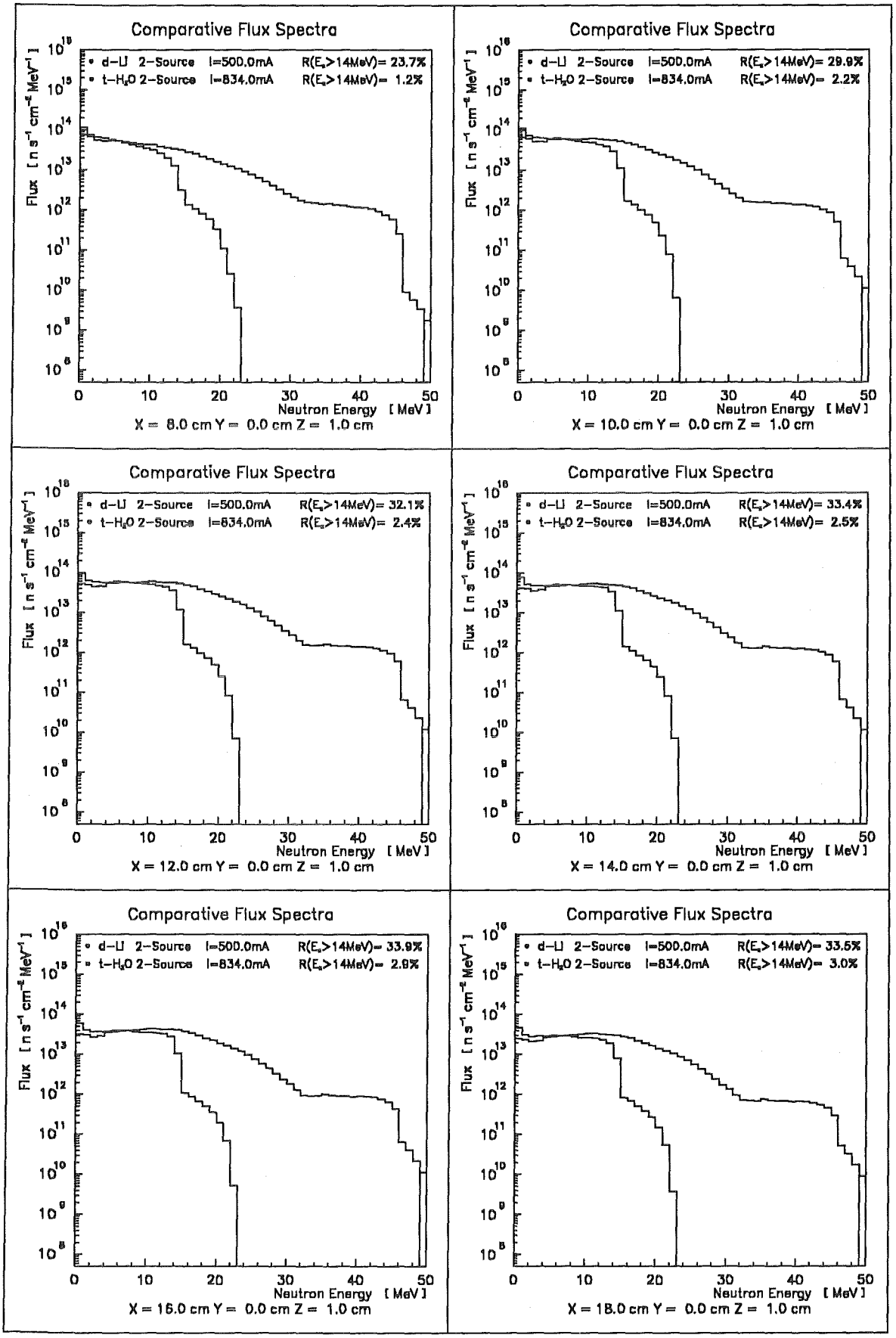
Comparative Flux Spectra
d-Li 2-Source I=500.0mA R(En>14MeV)= 23.7%
t-H2O 2-Source I=834.0mA R(En>14MeV)= 1.2%
Flux [n s-1 cm-2 MeV-1]
Neutron Energy [MeV]
X = 8.0 cm Y = 0.0 cm Z = 1.0 cm
Comparative Flux Spectra
d-Li 2-Source I=500.0mA R(En>14MeV)= 29.9%
t-H2O 2-Source I=834.0mA R(En>14MeV)= 2.2%
Flux [n s-1 cm-2 MeV-1]
Neutron Energy [MeV]
X = 10.0 cm Y = 0.0 cm Z = 1.0 cm
Comparative Flux Spectra
d-Li 2-Source I=500.0mA R(En>14MeV)= 32.1%
t-H2O 2-Source I=834.0mA R(En>14MeV)= 2.4%
Flux [n s-1 cm-2 MeV-1]
Neutron Energy [MeV]
X = 12.0 cm Y = 0.0 cm Z = 1.0 cm
Comparative Flux Spectra
d-Li 2-Source I=500.0mA R(En>14MeV)= 33.4%
t-H2O 2-Source I=834.0mA R(En>14MeV)= 2.5%
Flux [n s-1 cm-2 MeV-1]
Neutron Energy [MeV]
X = 14.0 cm Y = 0.0 cm Z = 1.0 cm
Comparative Flux Spectra
d-Li 2-Source I=500.0mA R(En>14MeV)= 33.8%
t-H2O 2-Source I=834.0mA R(En>14MeV)= 2.9%
Flux [n s-1 cm-2 MeV-1]
Neutron Energy [MeV]
X = 16.0 cm Y = 0.0 cm Z = 1.0 cm
Comparative Flux Spectra
d-Li 2-Source I=500.0mA R(En>14MeV)= 33.5%
t-H2O 2-Source I=834.0mA R(En>14MeV)= 3.0%
Flux [n s-1 cm-2 MeV-1]
Neutron Energy [MeV]
X = 18.0 cm Y = 0.0 cm Z = 1.0 cm

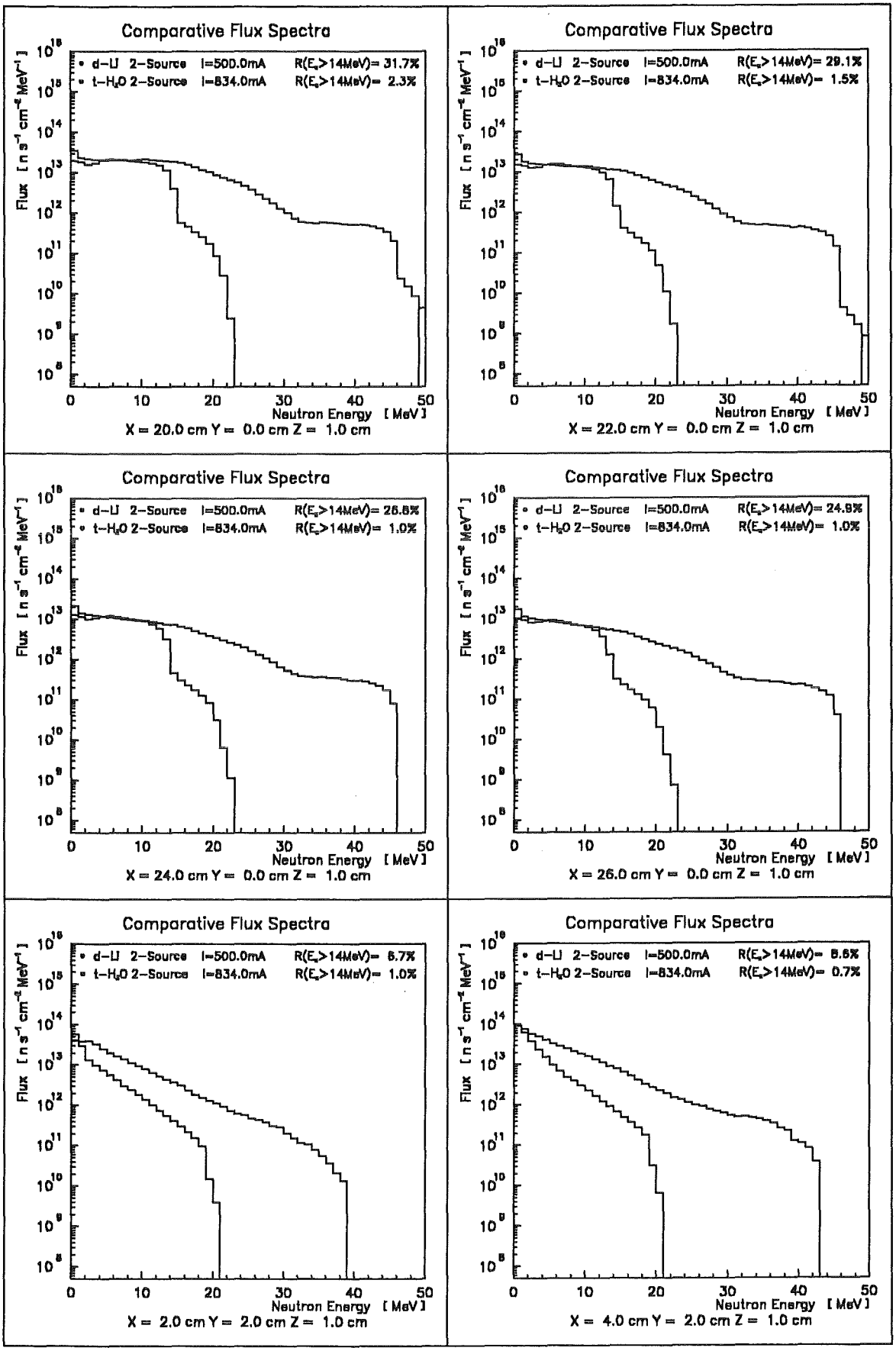
Comparative Flux Spectra
d-Li 2-Source I=500.0mA R(E>14MeV)= 31.7%
t-H2O 2-Source I=834.0mA R(E>14MeV)= 2.3%
Flux [n s-1 cm-2 MeV-1]
Neutron Energy [MeV]
X = 20.0 cm Y = 0.0 cm Z = 1.0 cm
Comparative Flux Spectra
d-Li 2-Source I=500.0mA R(E>14MeV)= 29.1%
t-H2O 2-Source I=834.0mA R(E>14MeV)= 1.5%
Flux [n s-1 cm-2 MeV-1]
Neutron Energy [MeV]
X = 22.0 cm Y = 0.0 cm Z = 1.0 cm
Comparative Flux Spectra
d-Li 2-Source I=500.0mA R(E>14MeV)= 26.8%
t-H2O 2-Source I=834.0mA R(E>14MeV)= 1.0%
Flux [n s-1 cm-2 MeV-1]
Neutron Energy [MeV]
X = 24.0 cm Y = 0.0 cm Z = 1.0 cm
Comparative Flux Spectra
d-Li 2-Source I=500.0mA R(E>14MeV)= 24.9%
t-H2O 2-Source I=834.0mA R(E>14MeV)= 1.0%
Flux [n s-1 cm-2 MeV-1]
Neutron Energy [MeV]
X = 26.0 cm Y = 0.0 cm Z = 1.0 cm
Comparative Flux Spectra
d-Li 2-Source I=500.0mA R(E>14MeV)= 6.7%
t-H2O 2-Source I=834.0mA R(E>14MeV)= 1.0%
Flux [n s-1 cm-2 MeV-1]
Neutron Energy [MeV]
X = 2.0 cm Y = 2.0 cm Z = 1.0 cm
Comparative Flux Spectra
d-Li 2-Source I=500.0mA R(E>14MeV)= 8.6%
t-H2O 2-Source I=834.0mA R(E>14MeV)= 0.7%
Flux [n s-1 cm-2 MeV-1]
Neutron Energy [MeV]
X = 4.0 cm Y = 2.0 cm Z = 1.0 cm

A.4 Comparative minimum flux contours (2-S)

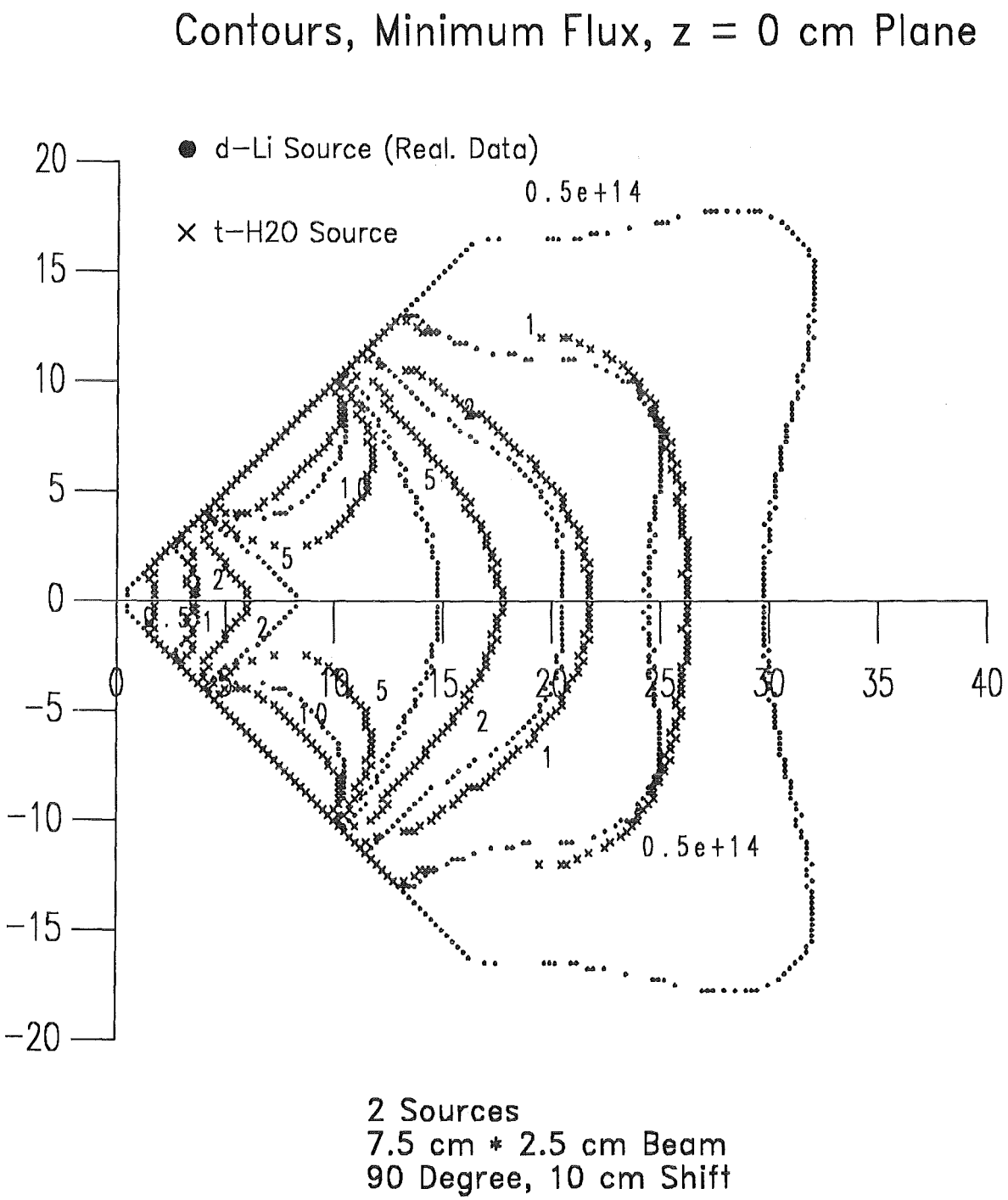

Contours, Minimum Flux, z = 1 cm Plane

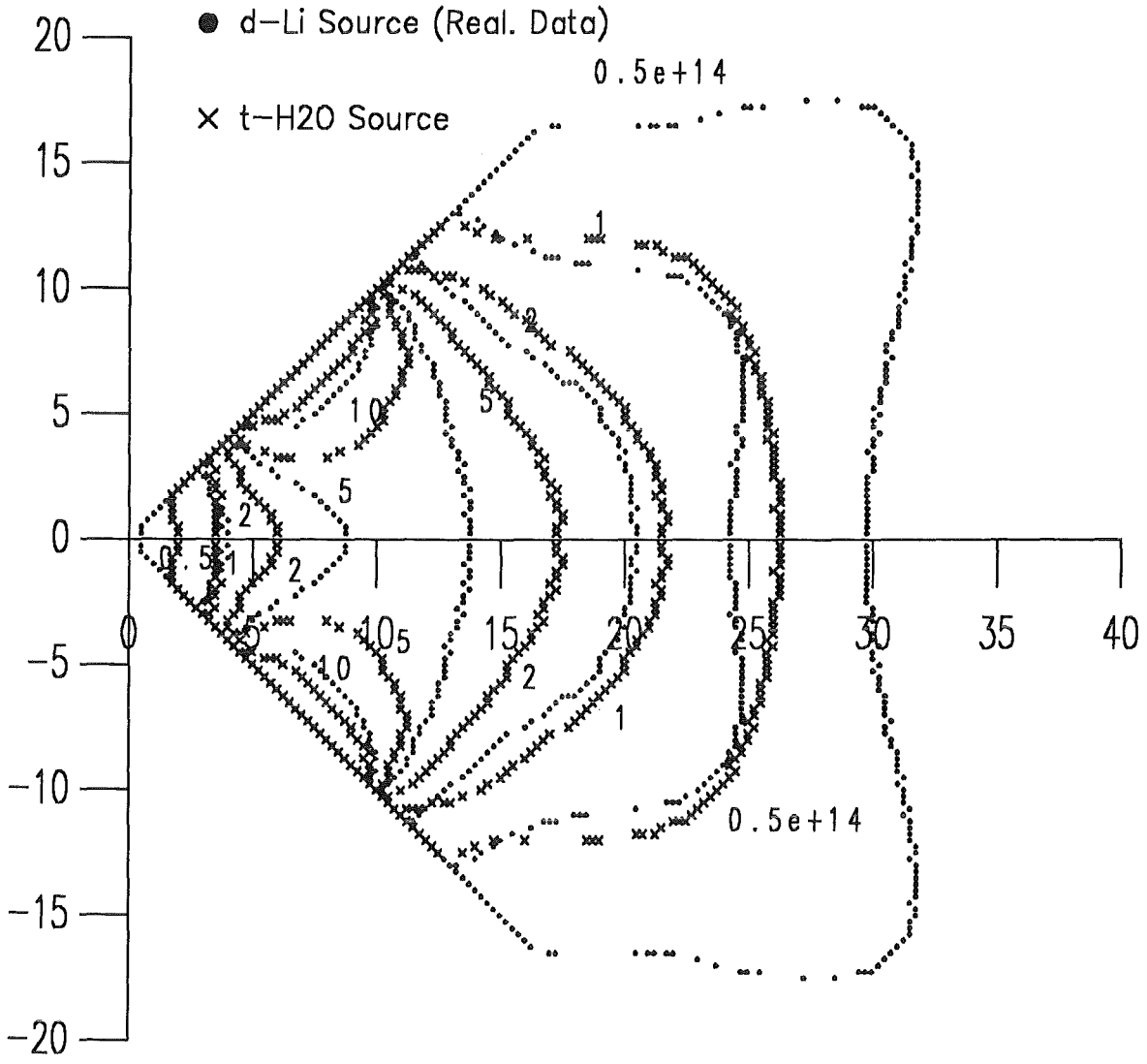

2 Sources
7.5 cm * 2.5 cm Beam
90 Degree, 10 cm Shift

Contours, Minimum Flux, z = 2 cm Plane

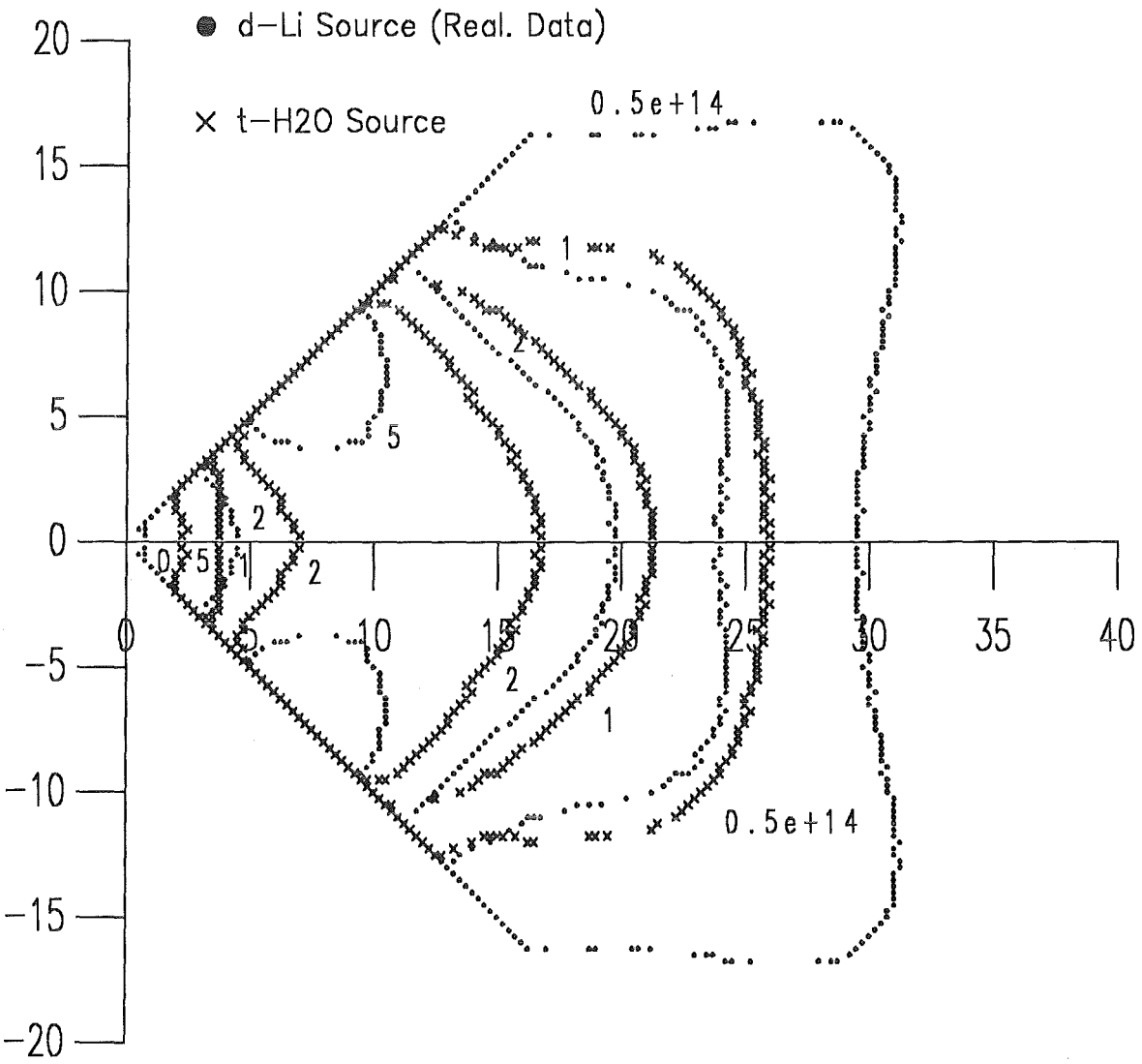

2 Sources
7.5 cm * 2.5 cm Beam
90 Degree, 10 cm Shift

Contours, Minimum Flux, z = 3 cm Plane

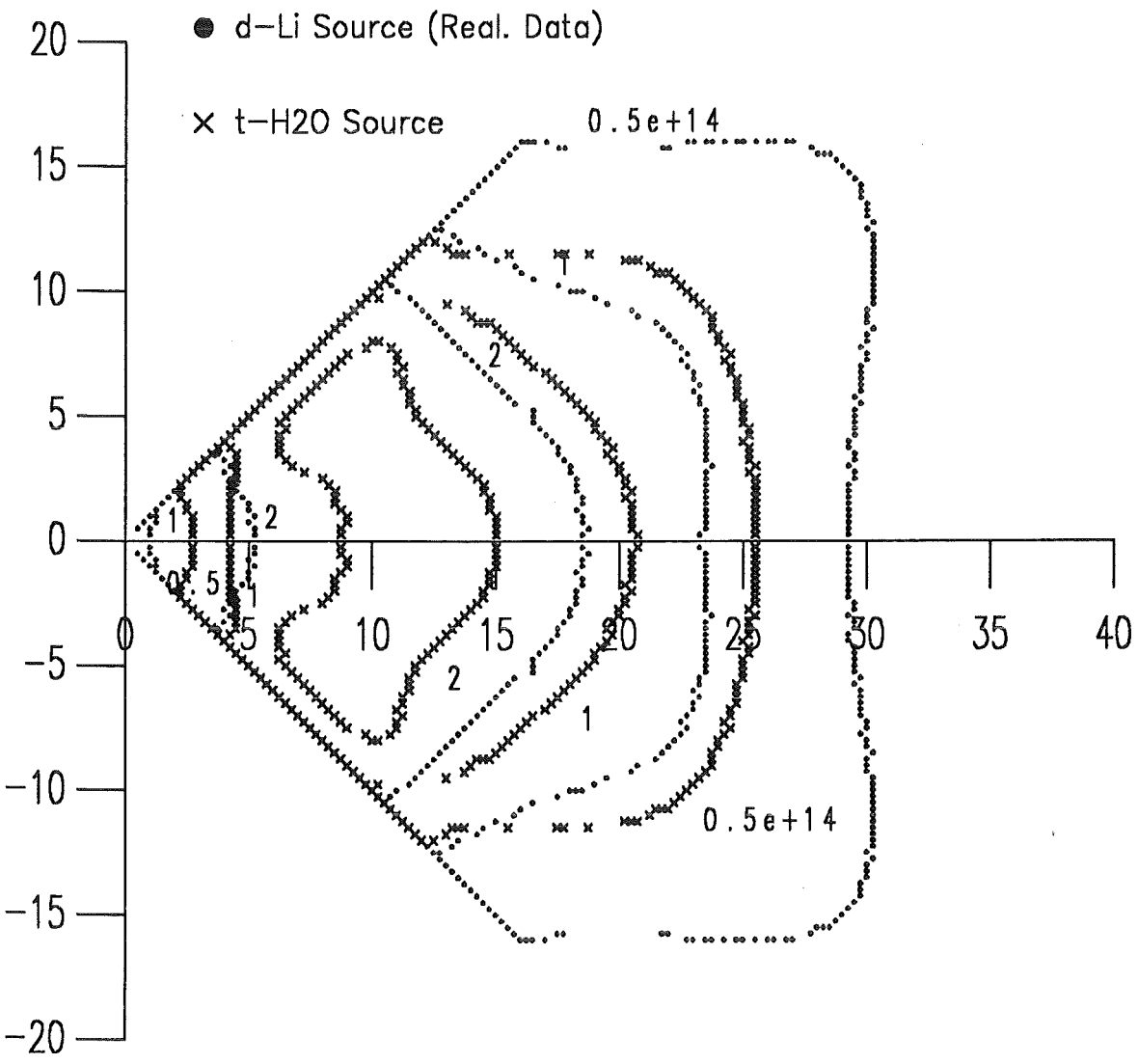

2 Sources
7.5 cm * 2.5 cm Beam
90 Degree, 10 cm Shift

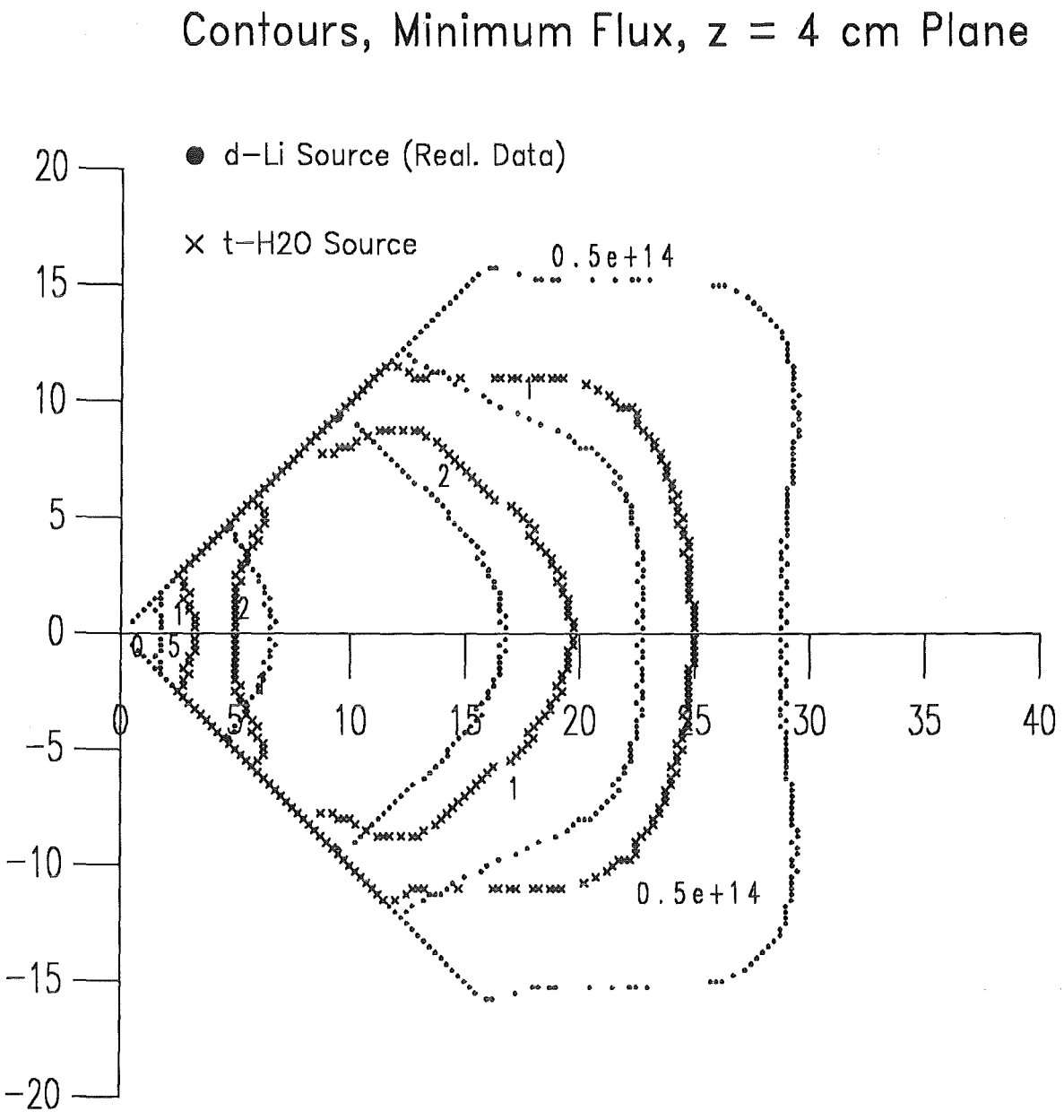

2 Sources
7.5 cm * 2.5 cm Beam
90 Degree, 10 cm Shift

Contours, Minimum Flux, z = 5 cm Plane

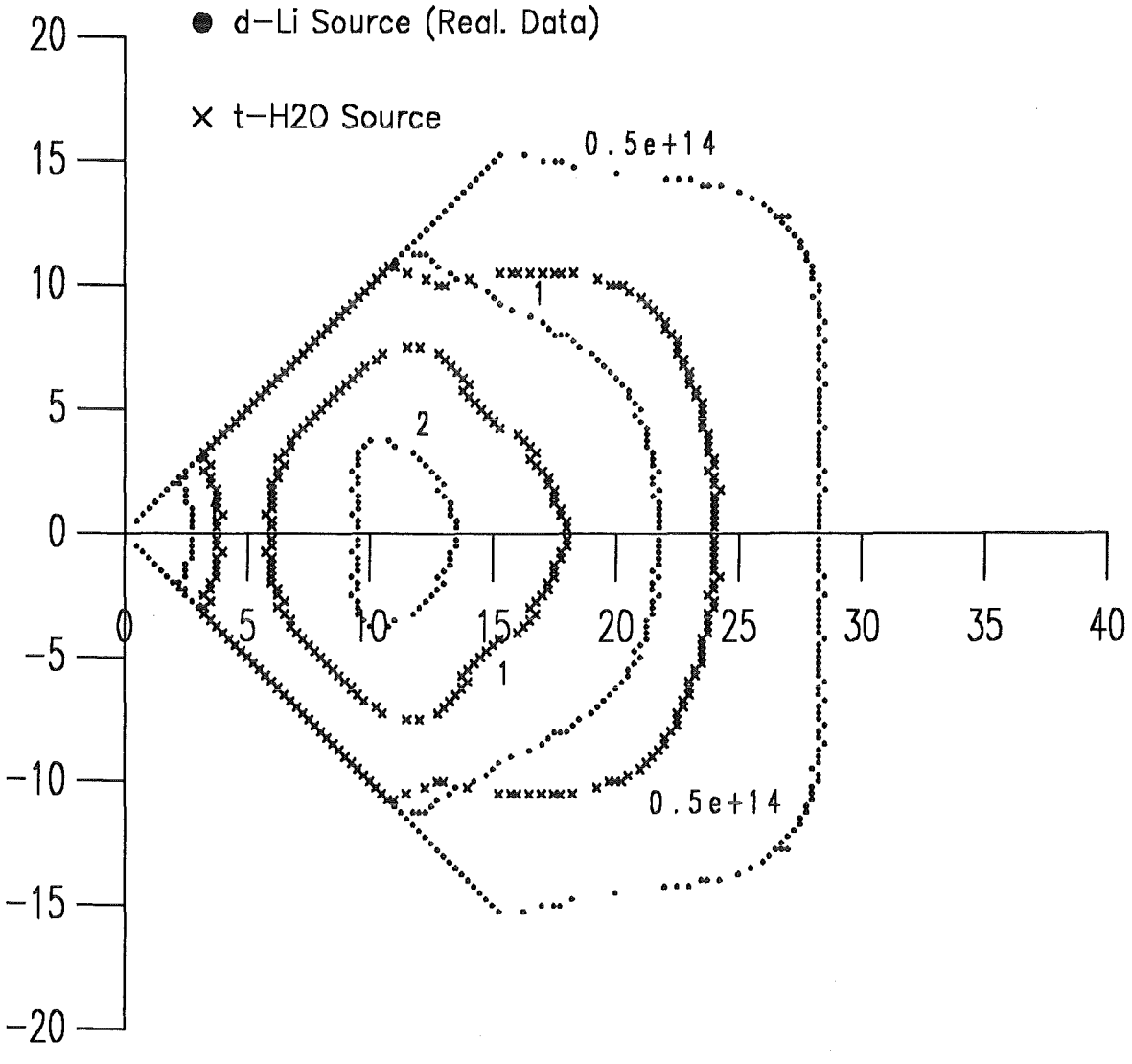

2 Sources
7.5 cm * 2.5 cm Beam
90 Degree, 10 cm Shift

Contours, Minimum Flux, z = 6 cm Plane

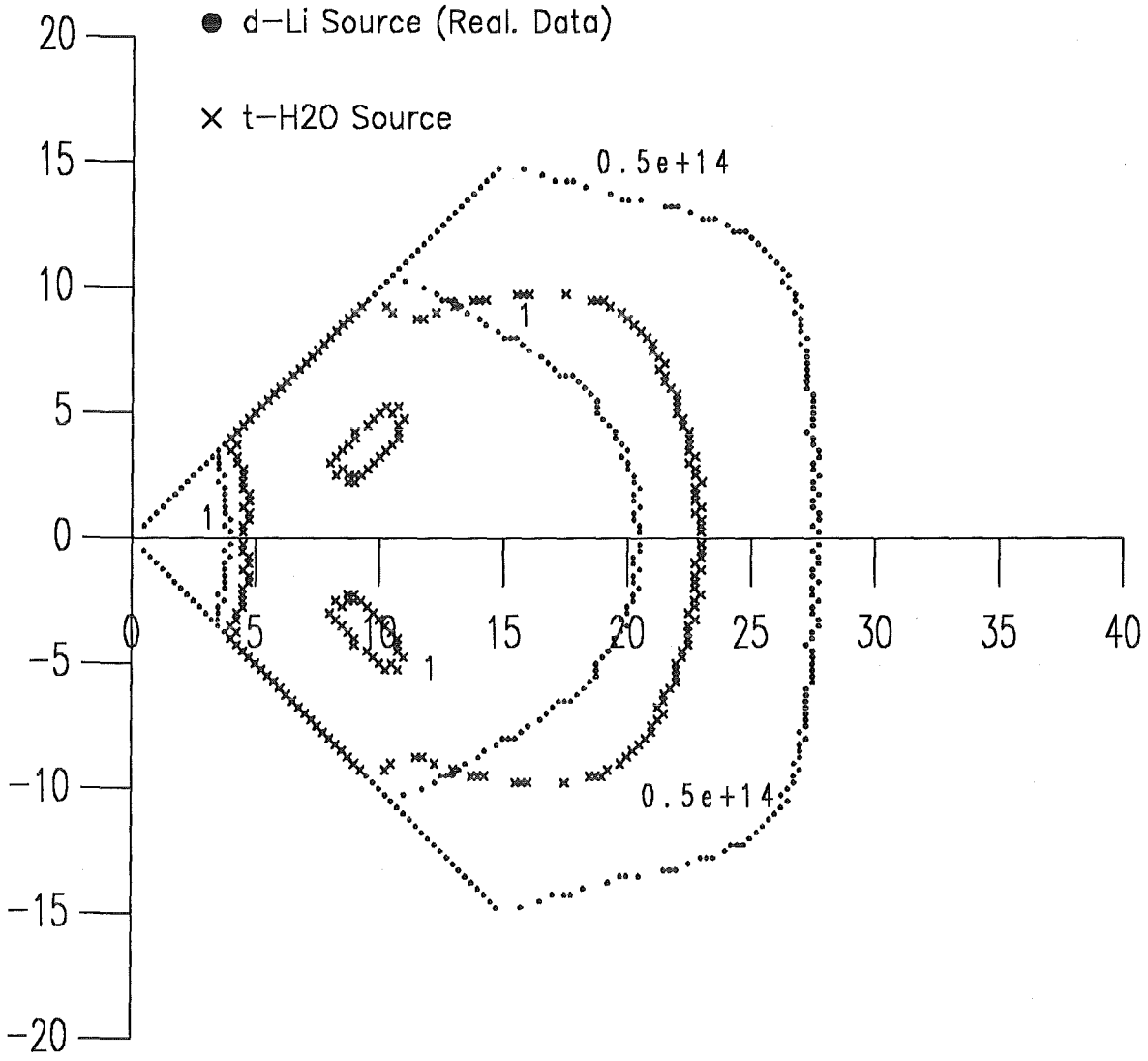

2 Sources
7.5 cm * 2.5 cm Beam
90 Degree, 10 cm Shift

Contours, Minimum Flux, z = 7 cm Plane

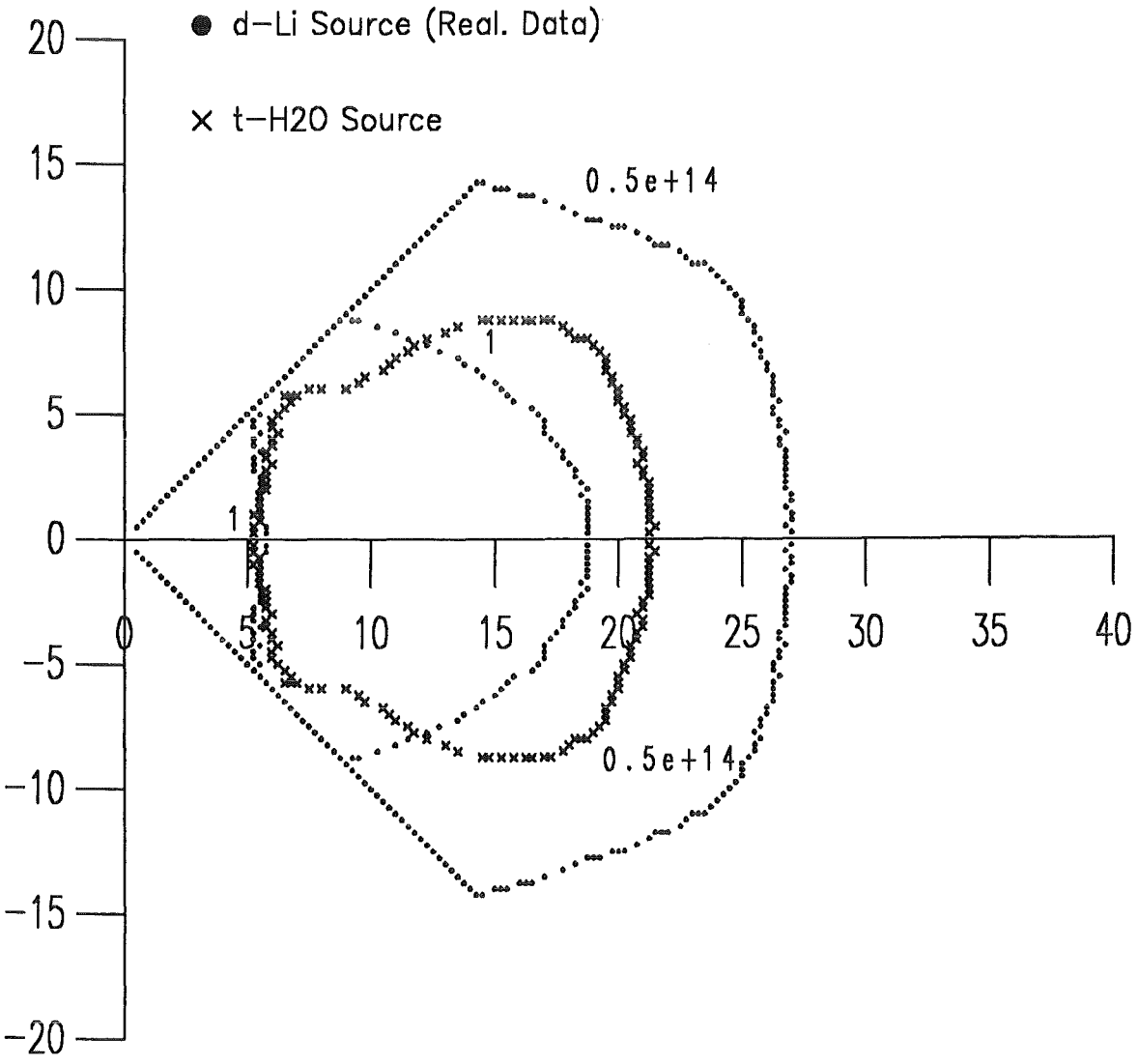

2 Sources
7.5 cm * 2.5 cm Beam
90 Degree, 10 cm Shift

Contours, Minimum Flux, z = 8 cm Plane

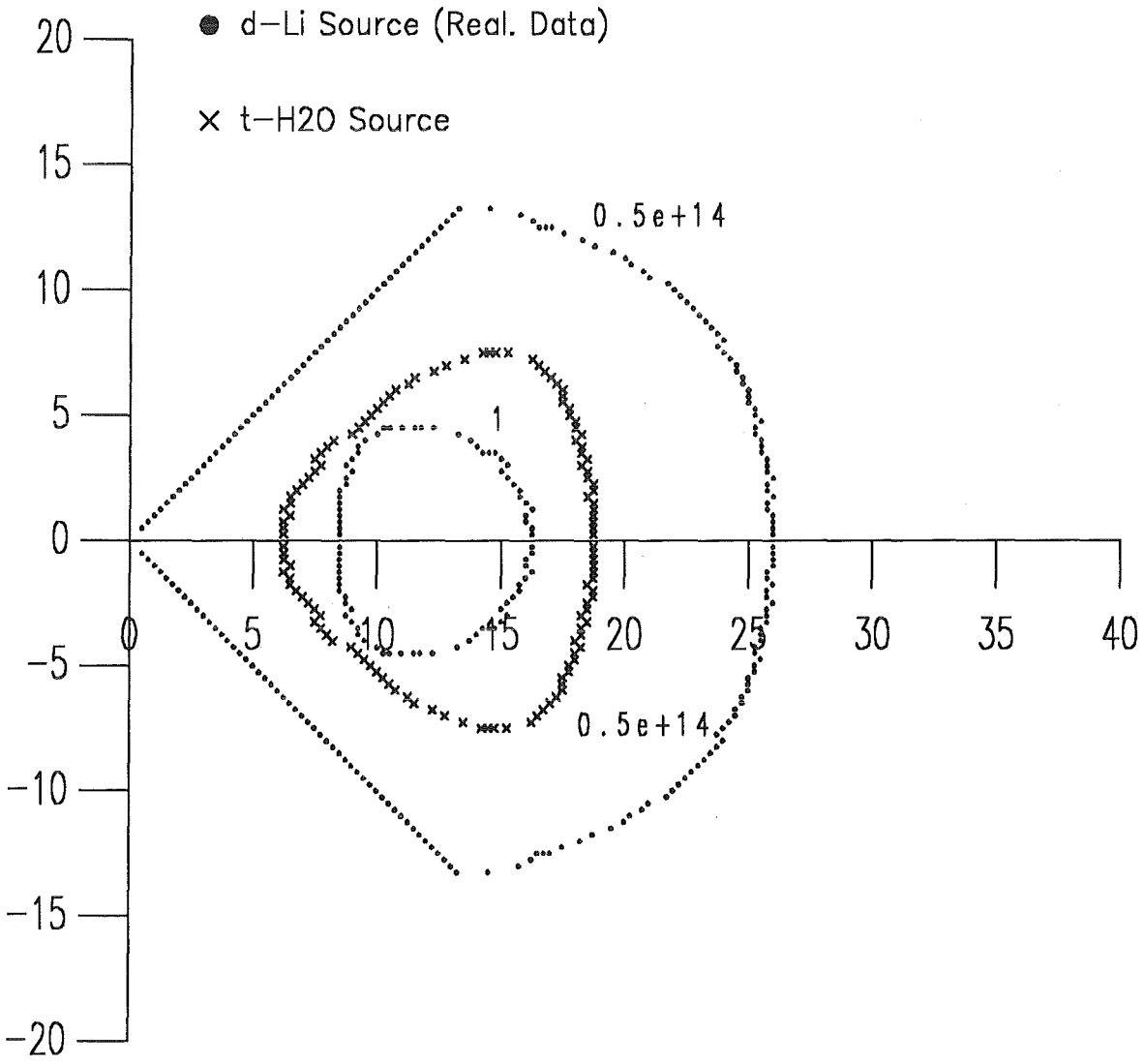

2 Sources
7.5 cm * 2.5 cm Beam
90 Degree, 10 cm Shift

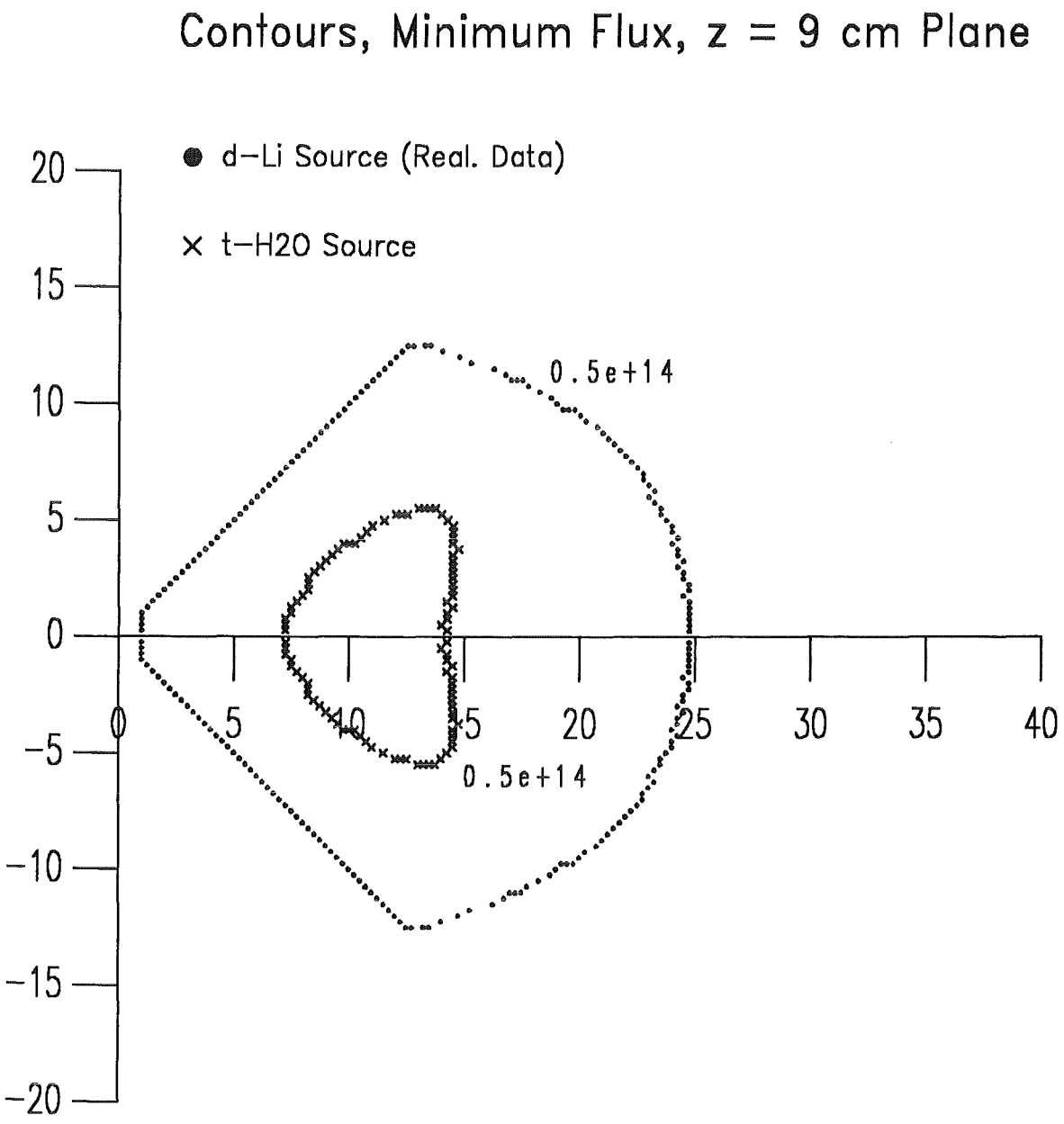

2 Sources
7.5 cm * 2.5 cm Beam
90 Degree, 10 cm Shift

Contours, Minimum Flux, z = 10 cm Plane

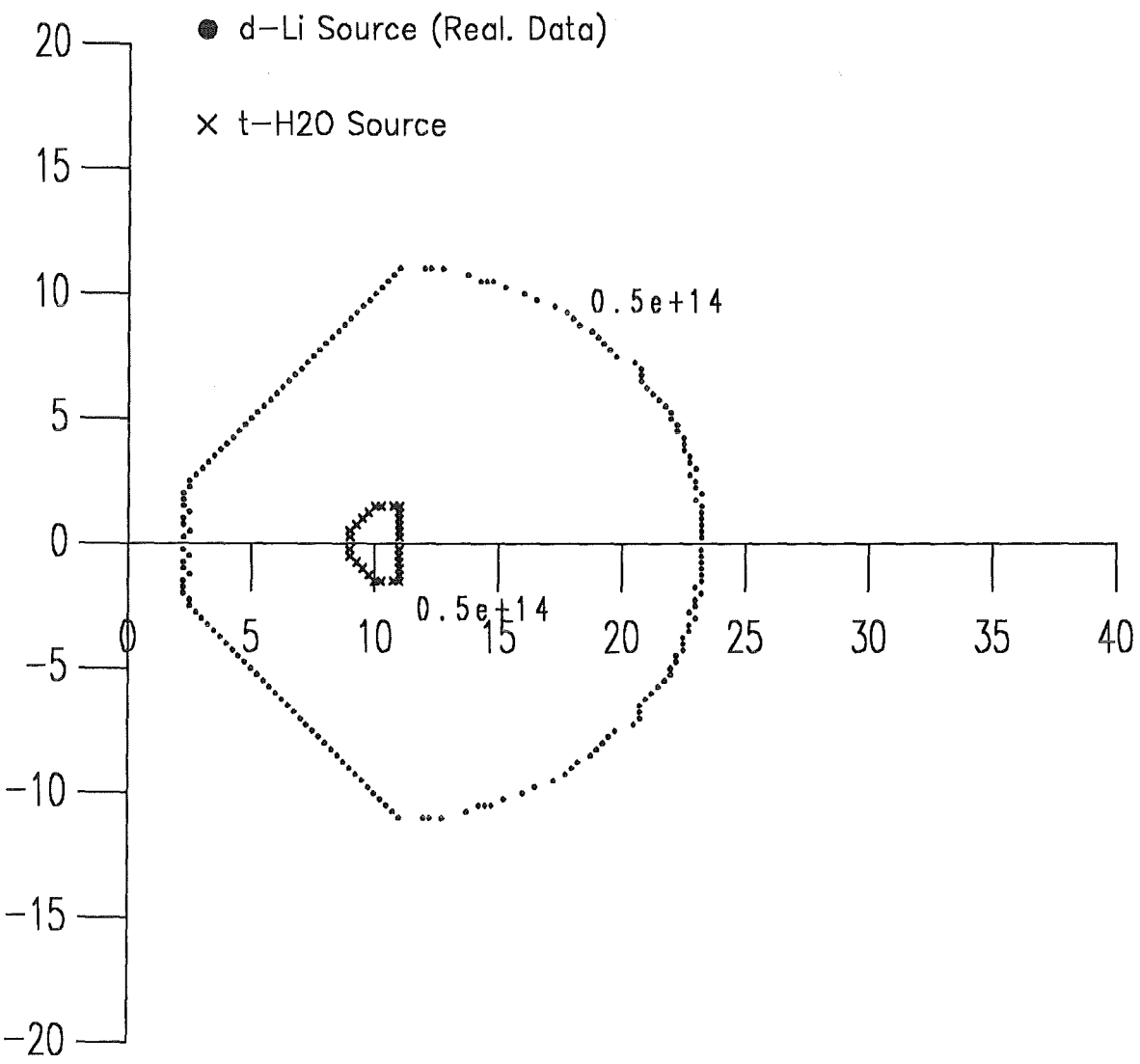

2 Sources
7.5 cm * 2.5 cm Beam
90 Degree, 10 cm Shift

References

[1] S. Cierjacks: *High-Intensity 14-MeV Cutoff Neutron Producting by the* $^1H(t,n)^3He$ *Source Reaction*, Journal of Fusion Energy, Vol. 8, Nos. 3/4, 1989

[2] S. Cierjacks, Y. Hino and M. Drosg: *Proposal for a High-Intensity 14-MeV Cutoff Neutron Source Based on the* $^1H(t,n)^3He$ *Source Reaction*, Nuclear Science and Engineering **106** ,183-191 (1990)

[3] S. Cierjacks and Y. Hino: *Differential Flux and Spectrum Calculations for a Novel High-Intensity 14-MeV Cutoff Neutron Source Based on the* $^1H(t,n)^3He$ *Source Reaction*, Acta Physica Hungarica **69** (3-4), pp. 285-308 (1991)

[4] S. Cierjacks: *The Intense* $t-H_2O$ *Neutron Source*, IEA Workshop on Intense Neutron Sources, Karlsruhe, September 21-23, 1992, Kernforschungszentrum Karlsruhe, to be published

[5] M.J. Saltmarsh: *The High Intensity d-Li Source*, IEA Workshop on Intense Neutron Sources, Karlsruhe, September 21-23, 1992, Kernforschungszentrum Karlsruhe, to be published

[6] D.L. Johnson, F.M. Mann, J.W. Watson, F.P. Brady, J.L. Ullmann, J.L. Romero, C.M. Castaneda, C.I.Zanelli and W.G.Wyckoff: *"Thick Target Neutron Yields and Spectra from the Li(d,xn) Reaction at 35 MeV", Symposium Neutron Cross Sections from 10 to 50 MeV*, Upton, New York, May 3-5, 1980, Report BNL-NCS-51245, p. 99, Brookhaven National Laboratory (1980)

[7] L.R. Greenwood and R.K. Smither: *SPECTER: Neutron Damage Calculations for Material Irradiations*, Report ANL/FPP/TM-197, January 1985

[8] M. Drosg and O. Schwerer: *Production of Monoenergetic Neutrons between 0.1 and 23 MeV* , Handbook of Nuclear Activation Data, IAEA Report Series No. 273, Vienna, 1987, p. 83

[9] M. Drosg and D.M. Drake: *Fast Neutron Yield from 20-MeV Tritons on Water, Part A: Triton Interaction with Light Water*, Nucl. Instr. and Meth. 73(1993) 387-391, Section B

[10] F.M. Mann: *Double Differential Cross Sections of the Li(d,xn) Reaction*, Private Communication

[11] H-BOOK, User Guide, Version 4, Cern Computer Center, Program Library Y250

[12] H-PLOT, User Guide, Version 5, Cern Computer Center, Program Library Y251

[13] HIGZ, High Level Interface to Graphics and Zebra, Cern Computer Center, Program Library Q120

[14] GKS Graphisches Kernsystem Benutzerhandbuch, 4. Auflage, Nov. 1990, HDI, KfK Karlsruhe

[15] GDDM, PGF Interactive Chart Utility, IBM, Program Number GDDM-PGF 5668-812, Version 2 Release 1

[16] A. Möslang: KfK-Bericht, April 1990, unpublished

[17] G.R. Odette and D.R. Doiron: *Neutron-energy dependent defect production cross sections for fission and fusion applications*, Nuclear Technology, Vol. 29, June 1976, p. 346-368

[18] A.Yu. Konobeyev, Yu.A. Korovin and V.N. Sosnin: *Neutron displacement cross sections for structural materials below 800 MeV*, Journal of Nuclear Materials 186(1992), 117-130

[19] L.R. Greenwood, ANL: *REAC computer code and Transmutation data available by F.M. Mann, Westinghouse Hanford Company, Richland*, Private Communication

[20] *ENDF/B-V Gas Production File (533), Brookhaven National Laboratory*

[21] M. Drosg: *Double Differential Cross Sections of the H(t,n) and differential yields of the O(t,xn) Reaction*, Private Communication

[22] M. Drosg: *IAEA, Vienna, DROSG-87 Computer Code, V 3.10*

[23] L.R. Greenwood, ANL: *Extended damage energy cross sections*, Private Communication

[24] L.J. Backer, et al.: *Cullham Report CLM-R-254 (1985).*

[25] D.G. Doran, F.M. Mann and L.R. Greenwood: *Damage parameters for candidate fusion materials test facilities*, Journal of Nuclear Materials 174(1990), 125-134

[26] D.G. Doran and S. Cierjacks *Some Comparisons of d-Li and* $t - H_2O$ *Conceptual Neutron Sources*, IEA Working Group on Neutron Sources

[27] D.G. Doran: *Summary of IEA Neutron Source Working Group Activities*, IEA Workshop on Intense Neutron Sources, Karlsruhe, September 21-23, 1992, Kernforschungszentrum Karlsruhe, to be published

[28] L.R. Greenwood: *Neutron Source Characterization and Radiation Damage Calculations for Material Studies*, Journal of Nuclear Materials 108 & 109(1982), 21-27